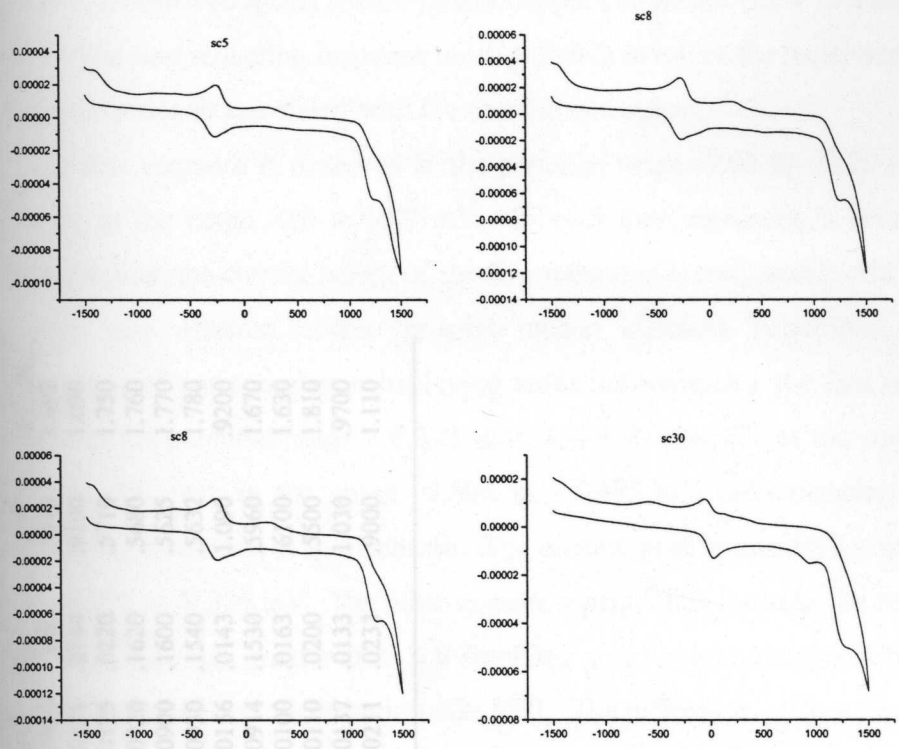

Fig 3.6 Cyclic voltammograms of representative Cu complexes of N-N-S donors (**1, 3, 5, 8, 11, 12.**)

The solvent was of AR grade and purified by using standard methods. The supporting electrolyte, (TEAFB) was dried *in vacuo* for 1 h at 80°C and stored in an evacuated desiccator. The profiles of cyclic voltammograms representative complexes are shown in Fig 3.6 (y axis- ampere, and x axis- milli volt). The parameters obtained from the electrochemical studies are presented in Table 3.6.

The electrochemical behaviour of the complexes was carried out in the range from +1.5 to -1.5 V .In the positive range, +1 to 0 V, the oxidation process Cu(III)/Cu(II) could be observed. Cyclic scanning between 0 and -1.5V permits study of the copper reduction centered process and ligand reductions [63]. The electrochemical response in the total range studied showed a pattern that could be considered as some of the individual responses. All complexes gave similar cyclic voltammograms. The number of electron involved in the reaction has been found to

Table.3.6
Cyclic voltammetric data of Cu(II) complexes with N-N-S donors

Compound	Epa (mv)	Epc(mv)	Ep(Epa-Epc)	E^0(Epa+Epc) / 2	i pa*	Ipc*	i pa/ipc	ipc /ipa
CuL4MCl	-405	-334	71	-370	. 0930	. 158	.5910	1.692
CuL4MBr	-398	-339	59	-369	. 0131	.0144	.9100	1.090
CuL4MI	-390	-320	70	-335	. 0125	.0220	.5710	1.750
CuL4MAc.H_2O	-364	-292	72	-328	. 0920	.1620	.5680	1.760
CuL4MNO_3	-393	-322	71	-358	. 0900	.1600	.5625	1.770
CuL4MNCS	-388	-324	64	-356	. 0930	.1540	.5632	1.780
CuL4MN_3	-383	-329	54	-356	. 0156	.0143	1.090	.9200
CuHL4MSO_4	-396	-329	67	-362	. 0914	.1530	.5960	1.670
CuL4MH_2OClO_4	-364	-295	69	-330	. 0100	.0163	.6100	1.630
CuL4PCl	-375	-304	71	-340	. 0110	.0200	.5500	1.810
CuL4PBr	-304	-250	54	-277	. 0137	.0133	1.030	.9700
CuL4PAc.H_2O	-322	-261	61	-292	. 0211	.0233	.9000	1.110

The reported data corresponds to a scan rate of 200 mV/ s

be one. It is reported [64] that square planar copper complexes show two reduction responses. The first reduction response most probably involves the metal centre and the second reduction is associated with the coordinated ligand.

The first response is observed in the potential range -0.06 to - 0.29 mV and second one, in the range -0.6 to -0.7 mV. In each case, assuming a monomeric species in solution, the current height of the first reduction is comparable with that of the known one electron redox process under identical conditions. The voltammograms of our complexes displaying reduction responses, the first response is observed in the potential range – 0.292 to -0.334 mV. The CV of the complexes shows an anodic peak in the range -0.304 to - 0.405 mV corresponding to one electron oxidation reaction at Pt electrode. The counter peak is also well resolved in the range -0.292 to -0.339 mV. The peak-to-peak separation is found in the range (54 - 72) mV and (I_{pa} / I_{pc}) greater than 0.9 implying quasi reversible electrochemical behavior or heterogeneous electron transfer [65]. The difference, $Ep = (E_{pa} - E_{pc})$ exceeds the Nerstian requirement of 59/n mV which support quasireversible character of electron transfer.

The changes in ^{4}N substituent are not affecting the E^0 values appreciably and comparable to other Cu(II) / Cu(I) couples. An anodic peak at + 0.696 mV associated with the cathodic peak at + 0. 699 mV to + 0. 785 mV is due to a quasi reversible one electron transfer of Cu(III) / Cu(II) redox couple [66]. The ΔE value fall in the range 54 to72 mV for different scan rates also support the above conclusions. The quasireversibility associated with the reduction based on the E^0 value, probably arise from the relaxation process involved in the stereochemical changes from planar copper(II) to tetrahedral copper(I). The change from the Cu(II) to Cu(III) state (d^8, low spin) involves a drastic reduction of the metal ion radius. In addition this process does not involve changes in the geometries of the copper(II) complexes in solution. The oxidation values agree with that, because complexes with more positive values are more difficult in stabilizing the copper(III) oxidation state [67]. On the other hand the values of the reduction potential fall in the range -0.400 mV to -0.520 mV

indicating difficulty in reducing the copper(II) ion in these favorable fittings of the copper(II) / Cu(I) ion

A study of the experimental data inferred that the reduction of copper(II) is quasireversible. In this type of electron transfer, process the current is controlled by a mixture of diffusion and charge transfer kinetics and can be identified by the following criteria [68]. 1) $\Delta E = E_a - E_c$ is greater than 59 mV and increases with increasing V. and 2) The ratio I_a / I_c is equal to unity only for x=0.59 (x is the charge transfer coefficient). The cathodic peak current function values were found to be independent of scan rate. Repeated scans as well as different scan rates showed that dissociation does not take place in these complexes.

It is reported that the formal electrode potential of the copper(II) / copper(I) couple is *ca* -0.44 V for chloro complex and *ca*-0.39 V for the more easily reduced bromo complexes [68]. The values that we got were consistent with the earlier reports. The lower copper(II) / copper(I) reduction potentials for the bromo complexes suggests greater distortion towards tetrahedral geometry in agreement with their lower wave number values for the d-d band. The potential of the first response for chloride containing complexes is higher than that observed for the complexes containing acetate. It has been observed that with increase in the basicity of the coordinating atom, the metal ligand sigma bond strength increases and a result the metal centered reduction potential decreases. The basicity of the acetate is much higher than that of chloride.

It is reported [69] that the copper(II) / copper(I) redox process are influenced by coordination number, stereochemistry and the hard/soft character of the ligand donor atoms. However due to inherent difficulties in relating coordination number and stereochemistry of the species present in the solution redox process are generally described in terms of the nature of the ligand present. The potential reduction of the Cu(II) / Cu(I) process is related to the potential SOD mimetic activity [70]. Patterson and Holm have shown that softer ligands tend to produce more positive E_0 values, while hard acids give rise to negative E_0 value. The observed values for the

complexes of thiosemicarbazones indicate considerable "hard acid "character comparable to ligand like ethylene diamine, (E_0, - 0.35) which is likely to be due to the pyridyl and azomethine nitrogen donors and solvent coordination. The two series bromo ligand, exhibit lower potentials in agreement with previous observations. The irreversible peak at + 1.200 V might correspond to the reduction of the conjugated portion of the thiosemicarbazones moiety and its value ranges between +1.200 to +1.285 V which is comparable with the values observed for many thiosemicarbazones ligands. This reduction is followed by three peaks which are due to coupled chemical oxidation process all are irreversible and may represent three different electronic configurations resulting from addition of electron to the thiosemicarbazone ligands. Potential site for the additional electron density on the ligand are π*orbital of the pyridyl ring and the two C=N bond of the thiosemicarbazones moieties as well as nonbonding d orbital of sulphur. The oxidation peak at + 0.45 mV and its counter part at + 0.22 mV might correspond to oxidation of the chloro ligand. This process occurs after complete ligand reduction (it is not observed in the initial positive scan). Analogous peaks are present in the scans of all bromo complexes consistent with oxidation and reduction of the bromo ligand [71].

A comparison of the electrochemical information with the powder spectra shows that the reduction potential increases with increase in $g_{\|}$. Since $g_{\|}$ increases with the size of the thiosemicarbazones moiety hence weaker sigma bonding occurs with ligand bulkiness. These results in the increased electron density being retained on the ligand and therefore higher reduction potentials for the bulkier ligands [72]. The electrochemical behaviours of other polyatomic anions were not clearly observed in our studies.

3.5 Antimicrobial activity

Wide variety of chemicals called antimicrobial agents is available for controlling the growth of microbes. Chemotherapeutic agents include antibiotics, disinfectants and antiseptics. Disinfectants are chemicals used on inanimate objects to lower the level of microbes present on the objects. Antiseptics are chemicals used on living tissues to decrease the number of microbes present in that tissue. Disinfectants and antiseptics affect bacteria in many ways. Those that result in bacterial death are called bactericidal agents and those causing temporary inhibition of growth are bacteriostatic agents.

Metal complexes of some heterocyclic thiosemicarbazones have recently screened for their potential biological activity. The majority of such studies have dealt with pyridine derivatives, and more specifically, 2-acetylpyrididine. Recently the structural and biological studies of copper(II) complexes with thiosemicarbazones were comprehensively reviewed by West *et al* [73]. The exact mechanism by which copper complexes exert their antimicrobial activity is not clear due to the large number of potential sites of action within the cell and the difficulties associated with monitoring and unequivocally assigning a reaction to a particular step. In some cases lowering of denticity of the thiosemicarbazones leads to a decrease of activity but the literature reports [74] examples of biologically significant bidentate thiosemicarbazones.

Copper complexes of thiosemicarbazones are drugs widely used to control of several infections. There are some hypotheses that explain the mechanism of action. One idea suggests that a metal ion, like copper could be a drug-carrier to the binding site. Copper in biological systems is mainly coordinated to nitrogen donor, like histidine residues [75]. To mimic this environment, we used thiosemicarbazones derived from 2-acetylpyridine such as HL4M and HL4P to get a model that enhance the understanding of the thiosemicarbazone coordination chemistry.

The synthesized N-N-S ligands and their Cu(II) complexes were tested for their antimicrobial activity. The growth inhibitory activity of these ligands and their twelve Cu(II) complexes are reported in Table 3.7.

The effectiveness of an antimicrobial agent in sensitivity testing is based on the area of zone of inhibition. When the test substances are introduced on to a lawn of bacterial culture by either disc diffusion or well method, if the bacteria are sensitive, there develops a zone of no growth around the disc. This is referred to as zone of inhibition. The diameter of the zone is measured to the nearest millimeter (mm). Test substances that produce a zone of inhibition of diameter 9 mm or more are regarded as positive, *i.e.* having microbial activity; while in those cases where the diameter is less than 9 mm, the bacteria are resistant to the sample tested and the sample is said to have no antibacterial activity.

3.5.1 Test organisms

Based on stain test bacteria may be of two types-Gram positive and Gram negative. The Gram stain, the most useful staining procedure employed in bacteriology, is a differential stain. By using this procedure, it is possible to divide bacteria in to two groups- Gram-positive and Gram negative. The Gram stain requires four different solutions; a basic dye, a mordant, a decolorizing agent, and a counter stain. The first three terms have their usual meanings. The counter stain is a basic dye of different colour from the initial one. The first step in Gram stain involves, staining the cell intensely with a basic dye; this is followed by a treatment of these stained cells with a mordant. The cells are then treated with a decolorizing agent, such as alcohol. The cells that retain the basic dye following depolarization are called Gram positive, and those that decolourised are Gram negative [76].

The microorganisms used as test organisms were bacteria isolated from clinical samples. Two Gram positive bacteria and nine-Gram negative bacteria were used as test organisms.

Followings were the bacteria that we used for our studies.

1) *Staphylococcus aureus*, 2) *Bacillus sp* **(Gram positive)**

3) *Escherichia coli*, 4) *Pseudomonas sp*, 5) *Klebsiella sp*, 6) *Proteus sp*, 7) *Salmonella typhi*, 8) *Salmonella Para typhi*, 9) *Shigella sp*, 10) *Vibrio cholerae.O1 and* .11) *Vibrio parahahaemolyticus*. **(Gram negative)**

3.5.2 Sample preparation

The compounds were separately dissolved in DMF to a concentration of 0.1% and then diluted with same solvent such that the concentration per disc would be 0.5 µg.

Preparation of discs

Discs of 4 mm diameter were cut out of Whatman No.1 filter paper and autoclaved at 15 psi for 15 minutes under aseptic conditions. Test samples (5 µL) were dispensed on to the discs under aseptic conditions. The discs were dried at 30°C and stored in sterile vials until further use.

Media

Unless otherwise specified, the medium used for growing the cultures was nutrient agar.

3.5.3. Procedure

Two methods were used for studying the antimicrobial activities of the test materials.

Disc diffusion method

It is used for screening the antimicrobial property of the test samples. When a filter paper disc impregnated with a chemical is placed on agar, the chemical will diffuse from the filter paper in to the agar. The diffusion will place the chemical in the agar only around the disc. The solubility of the chemical and its molecular size will determine the size of the area of chemical infiltration around the disc if it is susceptible to the chemical. The area of no growth is known as 'zone of inhibition' [77]. A loopful of an overnight slant culture of the test organism was inoculated to 5 µL of sterile physiological saline to make a uniform suspension. This suspension culture was surface spread on nutrient agar plate by swabbing with a sterile cotton swab to get a uniform lawn culture.

The discs with test samples prepared as mentioned above, were placed on the swabbed surfaces of the plates (4 discs per plate), (Fig 3.7) using sterile forceps. The

plates were incubated at 37°C for 24 hours and then checked for zones of inhibition around the discs. The zone diameters were measured in millimeters (mm). The testing was repeated **five times** simultaneously to check for consistency in the results.

Agar diffusion method

The agar diffusion test is not used to determine weather a chemical is bactericidal or bacteriostatic. It is used to quantify the antibacterial activity in terms of MIC. Minimum inhibitory concentration (MIC) is the lowest concentration of the antimicrobial agent at which it can inhibit the growth of the test microorganism after incubation. The MIC of the test samples which showed a positive antimicrobial property was made by this method and results are presented in Table 3.8. In agar diffusion method, one species of bacteria is uniformly swabbed on to a nutrient agar plate. Chemicals are placed on paper discs. The discs are added to the surface of the agar. During incubation, the chemicals diffuse from the disc containing the agent in to the surrounding agar. An effective agent will inhibit bacterial growth, and measurements are made to quantify the size of zone of inhibition around the disc. The relative effectiveness of a compound is determined by comparing the diameter of the zone of inhibition with values in standard tables.

Nutrient agar plates were prepared as before. Wells of diameter 4 mm were cut in the inoculated plates using a well borer 5 μL, 4 μL, 3 μL, 2 μL, and 1 μL of each of the test samples were dispensed directly in the wells. The plates were incubated at 37^0C for 24 h and checked for zones of inhibition around the wells. The MIC for each sample was determined and the results are tabulated in Table 3.8

Investigations on copper(II) complexes of thiosemicarbazones point to a redox mechanism involving thiols as the main cause of the biological activity of these compounds [108]. It was observed that the ligand HL4M was almost inactive against Gram positive and moderatively active against two Gram negative bacteria, whereas ligand HL4P was very high or moderatively active against two Gram positive and three-Gram negative bacteria at the studied doses. We found that the concentration had only little significance on microbial activity.

Staphylococcus aureus

Bacillus sp.

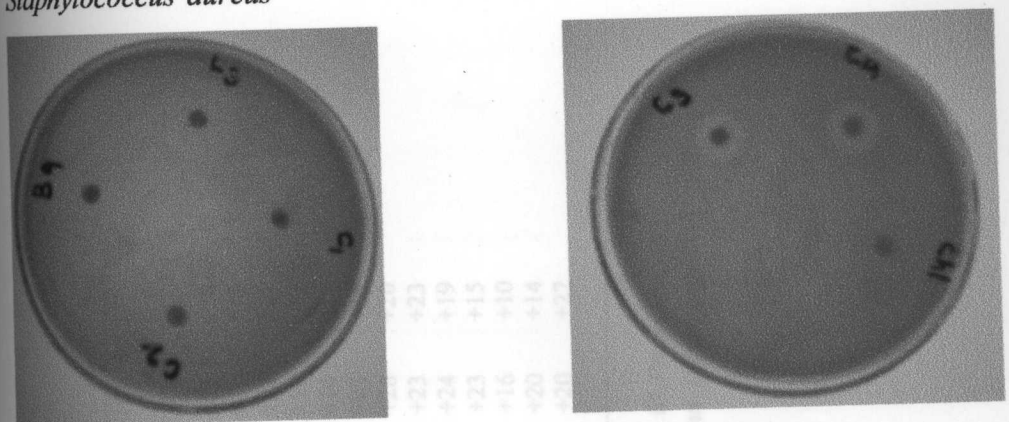

Vibrio cholerae.O1

Vibrio parahahaemolyticus aureus

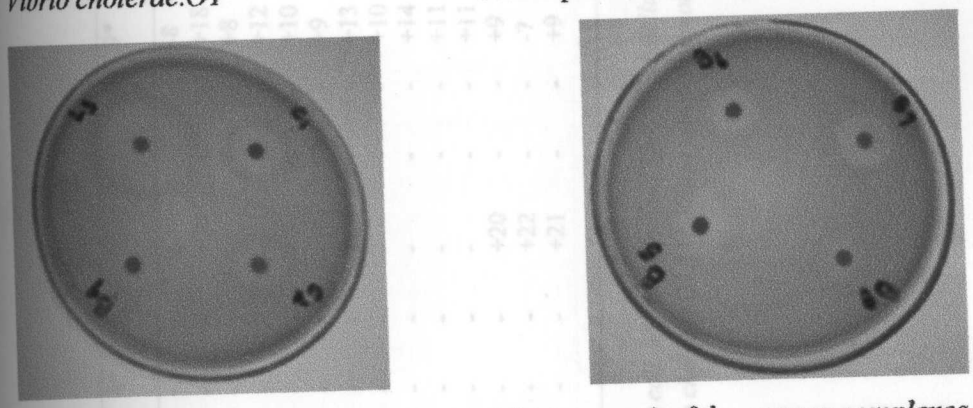

Fig 3.7 Antimicrobial studies (inhibition zone) of the copper complexes

The chelation induces significant changes in the cytotoxicity of the ligand. It exhibited moderate activity against two Gram negative bacteria, *Vibrio cholera O1* and *Vibrio parahaemolyticus* but its copper(II) complexes exhibited two to three fold antibacterial activity against two Gram-positive and three of Gram negative bacteria. In general when tested against Gram-positive and Gram-negative bacteria, complexes were found to possess a higher activity than that of the ligand itself. All the copper complexes of HL4M show moderate to very high activity against most of the organisms. The ligand and its copper complexes were equally inactive against *E.coli*, *Pseudomonas sp Klebsiella sp*, *Salmonella typhi* and *Salmonella paratyphi*. Though

Table.3.7
Microbial studies of N-N-S donors and their Cu(II) complexes

Compound	Con/Disc .µg	1*	2*	3*	4*	5*	6*	7*	8*	9*	10*	11*
HL4M	.5	-	-6	-	-	-	-	-	-	-8	+14	+12
HL4P	.5	+22	+21	-	-	-	+20	-	-	+18	+23	+20
CuL4MCl	.5	+10	+11	-	-	-	-	-	-	+8	+14	+13
CuL4MBr	.5	+16	+13	-	-	-	-	-	-	+12	+22	+21
CuL4MI	.5	+15	+15	-	-	-	-	-	-	+10	+18	+12
$CuL4MAc.H_2O$	.5	+13	+14	-	-	-	-	-	-	+9	+16	+14
$CuL4MNO_3$	.5	+18	+14	-	-	-	-	-	-	+13	+23	+19
CuL4MNCS	.5	+14	+11	-	-	-	-	-	-	+10	+28	+20
$CuL4MN_3$	.5	+20	+20	-	-	-	-	-	-	+14	+23	+23
$CuHL4MSO_4$	.5	+16	+12	-	-	-	-	-	-	+11	+24	+19
$CuL4MH_2OClO_4$	.5	+15	+11	-	-	-	-	-	-	+11	+23	+15
CuL4PCl	.5	+12	+10	-	-	-	+20	-	-	+9	+16	+10
CuL4PBr	.5	+18	+13	-6	-	-	+22	-	-	-7	+20	+14
$CuL4PAc.H_2O$	.5	+14	+10	-6	-	-	+21	-	-	+9	+20	+22

.

1* *Staphylococcus aureus*, 2* *Bacillus sp* **(gram positive)**3*. *Escherichia coli*, 4* *Pseudomonas sp*, 5* *Klebsiella sp*. 6* *Proteus sp.*
7* *Salmonella typhi*, 8* *Salmonella Para typhi*,.9* *Shigella sp*, 10* *Vibrio cholerae*.O1.11* *Vibrio parahahaemolyticus.* **(gram negative)**

Table 3.8
MIC Study of N-N-S donors and their Cu (II) complexes.

Code	1*	2*	3*	4*	5*	6*	7*	8*	9*	10*	11*
HL4M	-	2	-	-	-	-	-	-	-	4	4
HL4P	1	1	-	-	-	1	-	-	1	1	1
CuL4MCl	3	2	-	-	-	-	-	-	2	1	2
CuL4MBr	1	3	-	-	-	-	-	-	1	1	1
CuL4MI	1	1	-	-	-	-	-	-	5	1	1
$CuL4MAc.H_2O$	3	5	-	-	-	-	-	-	1	1	1
$CuL4MNO_3$	1	1	-	-	-	-	-	-	5	1	1
CuL4MNCS	1	1	-	-	-	-	-	-	4	1	1
$CuL4MN_3$	1	2	-	-	-	-	-	-	5	1	1
$CuHL4MSO_4$	1	1	-	-	-	-	-	-	5	1	1
$CuL4MH_2OClO_4$	1	1	-	-	-	-	-	-	5	1	1
CuL4PCl	3	2	-	-	-	-	-	-	5	1	2
CuL4PBr	1	1	-	-	-	-	-	-	4	1	1
$CuL4PAc.H_2O$	1	3	-	-	-	-	-	-	5	1	2

1* *Staphylococcus aureus*, 2* *Bacillus sp* **(gram positive)**3*. *Escherichia coli*, 4* Pseudomonas sp, 5* *Klebsiella sp.* 6* *Proteus sp.*
7* *Salmonella typhi*, 8* *Salmonella Para typhi*,.9* *Shigella sp,* 10* *Vibrio cholerae*.O1.11* *Vibrio parahahaemolyticus*. **(gram negative)**

the ligand is very active against *Proteus sp* it was found that upon complexation activity, decreased considerably. Among the copper(II) complexes of HL4M, the most active against *Vibrio cholera O1* was the nitrato complex and for *Vibrio parahaemolyticus*, *Staphylococcus aureus*, and *Bacillus sp* the thiocyanato complex was the most active. The copper complexes of HL4P were found to have equal or higher activity at the studied concentration against the two classes of bacteria. The bromo and acetato complexes were found to have higher activity than chloro analogue. It is thought to be due to more distortion from planarity and higher covalency of metal ligand bond [78]. A possible mechanism for the poor activity of the compounds studied may be their inability to chelate metals essential for the metabolism of microorganisms and or to form hydrogen bonds with the active centers of cell structures, resulting in an interference with the normal cell cycle [79].

The MIC of copper complexes of HL4M is found to be far less than uncomplexed thiosemicarbazones for *Vibrio cholera O.1*, *Vibrioparahaemolyticus*, *Shigella sp, Staphylococcus aureus*, and *Bacillus sp* indicating that complexes were very effective in destroying such microorganism even at very low concentration. Similar trend was observed in the case of copper(II) complexes of HL4P but for *Shigella sp* the most active was found to the uncomplexed ligand itself. We also noticed that the MIC of these complexes was less than some of the commercially available antimicrobial agents. In organic solvents, these complexes are better antimicrobial agents than commercially available antibiotics. From the data available, it is found that Cu(II) complexes of HL4M have more bactericidal activity than Cu(II) complexes of HL4P.

3.6 Concluding remarks

According to the procedure reported elsewhere, we prepared two N-N-S donor ligands and synthesized twelve Cu(II) complexes having square planar or square pyramidal geometry. They were characterized by various physico chemical methods. The ligands were coordinated as monoanionic tridentate manner in most of the complexes. The structures of the complexes were scrutinized by UV-Visible, IR and EPR spectral methods. The results were consistent with a square planar geometry. The EPR spectra of all complexes in the frozen state were simulated to get spin Hamiltonian and bonding parameters and observed that EPR symmetry and molecular symmetry were different in complexes. The electrochemical behaviour of the complexes were studied by cyclic voltammetry and observed quasireversible one electron transfer. Detailed picture of the reduction of ligands were not obtained. The biological activity of ligands and complexes were screened against both Gram positive and Gram negative bacteria and found most of them were more active against Gram negative bacteria particularly *Vibrio cholera O1* and *Vibrio parahaemolyticus*. We successfully isolated two complexes having antibacterial activity equal or more than commercial antibiotics against *Vibrio cholera O.1*. We observed that antibacterial activity of complexes increases with increase in, $g_{\|}$ value, covalency of M-L bond and distortion from planarity.

Reference

1 A.W.Addison,:K. D. Karlinand J. Zubieta, *Copper Coordination Chemistry: Biochemical and Inorganic Perspectives,AdeninePress*, NewYork,1983,**1**,109.

2 M. Michel. J. M. Campbell. *Coord. Chem. Rev.* 1975, **15**, 270.

3 G. Wilkinson, *Comprehensive coordination chemistry, Pergamon Press. Oxford* 1987. Vol **6.**

4 J. Costamanga, J. Vargas, R. Latorse. A. Alvarado, G. Mena., *Coord. Chem. Rev.* 1992, **119**, 67.

5 B. Singh, H. Misra, *J. Indian Chem.Soc. 1986*, **63**, *692.*

6 R. R. Joshi, K. N. Ganesh. *Biol.Chem*. 1989, **264**, 15435.

7 C. R. K.. Rao and P. S. Zacharias, *Polyhedron* 1997 **16**, 1201.

8 R. Shukla, S. Mandal, P. K. Bharadwaj, *Polyhedron* **1993 12**, 83.

9 B. Singh,B. P. Yadava and R. C. Aggrawal, *Indian .J. Chem*.,. 1984, **23** A 441.

10 I. M. Procter, B. J. Hathaway, P.. Nicholas, *J. A Chem.Soc*, 1968, **1678,** 236.

11 R. B. Martin, Y. M. Mariam, H.Sigel, *Metal ions in Biological Systems. Marcel Dekker.* New York, 1987. Vo. **121**, 57.

12 K. C. Agrawal, B. A.Booth, R. I.Michadd, E. C. Moore, *Biochem.Pharm*, 1974, **23** 2421.

13 F. M Petring, and W. Collins, *J. of. General Microbiolog.*1982, **128**, 1349.

14 D. X.West,S. B. Padhye, P. B. Sonawane, *Structure and Bonding,* 199*1* **76**, 4.

15 E. Cartnel and G. W. A. Fowles, *Valency and Molecular Stucture,* Butterworths Scientific Piublications,Ltd., London.1956.

16 M. J. M.Campbell, R. Grzeskowiak and M. Goldstein, *Spectrochim.Acta*,Part A 1968, **25**,1149.

17 M. R. P Kurup.,Ph.D. Thesis,Dept. of Chemistry, University of Delhi,1987.

18 P. Bindu, M. R. P. Kurup.T. R. Satyakeerty, *Polyhedron*, 1999, **18**, 321-331.

19 I. Garcia, E. Bermejo, A. K. El-Sawaf, A. Castiñeiras and D. X. West, *Polyhedron*, 2002, **21**,729.

20 S. V. Deshpande and T. S. Srivastava.; *Polyhedron*, 1983, **2**, 767.

21 F. Szczepura, K. K. Eilts, A. K. Hermetet, L. J. Ackerman. J. K. Swearingen and D. X. West, *J. Mol. Struct.*, 2002, **607**, 101.

22 W. Kaminsky, J. P. Jasinski, R. Woudenberg, K. I. Goldberg and D. X. West, *J. Mol. Struct.*, 2002, **608**, 135.

23 D. X. West, S.B. Padhye, P.S. Sonawane, *Structure and Bonding* 1991, **76**, 1 and references therein.

24 E. W. Ainscough, A. M Brodie, J D. Ranford and J M. Waters, *Dalton Trans* 1991, **23**, 2125.

25 S. Mandal, P .K.Bharadwaj, *Polyhedron* 1992, **11**, 1037.

26 V.. Sakaguchi and A. W.Addison, *J.Chem. Soc., Dalton Trans.*, 1979, **45**, 600.

27 K. H Reddy, M. R Reddy and K. M Raju. *Ind. J. Chem.*, 1999, **38**A, 299.

28 K. Nakamoto, *Infrared and Raman Spectra of Inorganic and Coordination Compounds,* Wlley Interscience, New York,1978, **2**, 345.

29 A. M.Bond, and R. L. Martin, *Coord. Chrem. Rev*,1984, **54**, 23.

30 R. Osterberg. *Coord.Chem.Rev*.1974.**12**.309.

31 M. Mohan, .P. Sharma, M. Kumar, N. L. Jha, *Inorg.Chem Acta* 1986,**4**, 125.

32 D. K. Demertzi, A. Domopoulou, A.; Demetzis, J Valdez-Martinez, S. Hernadez-Ortega, G E Perez, D. X. West, M. Salberg, G. Bain, P.D. Bloom, *Polyhedron*, 1996, **15**, 2587.

33 B. N. Figgis and J. Lewis, .*Modern Coordination Chemistry*, .Interscience, New York, 1960, **2,** 400.

34 M. Akbar Ali and A. E. Liberta, *Coord.Chem.Rev,* 1993, **123**, 49.

35 B. Singh, B. P. Yadava and R.C.Agrawal, *Indian J. Chem.*,1984, **23A** .441.

36 M. C.Jain, A. K. Srivastava, and P. C. Jain.,*Inorg.Chim.Acta*,1977, **23**,199.

37 A. E. Landers and D. J. Phillips, *Inorg.Chim.Acta*. 1983, **74,** 43 and reference therein.

38 A. B. P. Lever "*Inorganic Electronic Spectroscopy*", Elsevier, Amsterdam, 1968.

39 W. J. Geary, *Coord. Chem. Rev*; 1971, **7**, 81.

40 K. M. Ibrahim and M. M. Bekheit,*Transition Met.Chem*., 1988, **13,** 230.

41 R. N. Pathak and L. K. Mishra, *J.Indian Chem*.Soc, 1988, **65**,119.

42 Y. K. Bhoon, *IndianJ.Chem*, 1983, **22**A, 430.

43 A. K. El-Sawaf, D.X. West, F. A. El-Saied, R. M. El-Bahnasawy. *Inorg. Met.-Org. Chem.* 1997, **27**.3459.

44 A. Ali and Tarafdar, *Chem. Rev*, 1993, **93**, 2295.

45 The author acknowledges with thanks for EPR simulation programme, provided by Prof. M. V. Rajasekharan, University of Hydrabad. Hydrabad.

46 F. E. Mabbs, *Some aspects of the electron paramagnetic resonance spectroscopy of d-Transition metal compounds.* Chemistry Department, University of Manchester, Manchester.1991, M**13**. 9.

47 P. Bindu, M. R. P. Kurup, *Transition Met. Chem*., 1997, 22, 578.

48 B. J. Hathaway and D. E. Billing, *Coord.Chem.Rev*., 1970 **5**, 149.

49 C. R. K.Rao and P. S .Zacharias, *Polyhedron* 1997, **16**, 1201.

50 S. Abdul Samath, M. Raman N. Raman K.T. Jeyasubramanian and S.K. Ramalingam, *Transition Met. Chem.* 1992.**17** 13.

51 K. Jeyasubramanian, S. Abdul Samath, S. Tambidurai R. Murugesan and S. K. Ramalingam, *Transition Met. Chem.* 1995, **20,** 76.

52 R. Murugesan and S. Subramanian, *Mol. Phys.* 1984, **52,** 129.

53 V. M. Massacesi and A. W. Addison. *J. Chem. Soc, Dalton Trans*, 1979. **32**, 600.

54 D. Kevilson and R. Neiman, *The J.of Chemical Physics,*.1961, Vol.**35**, 1.

55 G. Gemperle, G. Aebli, A. Schweiger, and R. R. Ernst, *J. Magn. Reson.* 1990, ***88,*** 241.

56 J. R. Pilbrow, T. D. Smith and A. D. Toy, *Aus.J.Chem*, 1970, **23**, 2287.

57 B. J. Hathaway "*Essay in Chemistry*" Edited by Bradley J.N. and Gilled R.D Acad. Press, 1971, **2,** 61.

58 K. D, Karlin and J. Zubieta, *Copper Coordination Chemistry*, Biological and Inorganic Perspectives, Adenine Press, NY, 1983.

59 B. J. Hathaway and D.E.Billing, *Coord. Chem. Rev*, 1970, 5, 143.

60 Y. Nakao,W. Mori, T. Sakurai and A.Nakahara.*Inorg.Chim.Acta*.1981, **55**, 103.

61 A. D. Rebecca and P. R Cao, *Inorganica Chimica Acta* 1998, **275,** 552-526.

62. M. Bond, and R. L. Martin, *Coord. Chem.Rev.*1984, **54**, 23.

63 J. F Llopis, F. Colom, *Encyclopedia of Electrochemistry of the Elements*, New York, 1976; Vol. **6**, p 224–226.

64 J Wang, *Analytical Electrochemistry*, John Wiley & Sons, 2000, Chapter **2,** 94A.

65 J .Heinze, *Cyclovoltammetrie – die Spektroskopie des Elektrochemiker*s, Angew. Chem, 2000, **2**, 456.

66 J. J. Van Benschoten, J. Y Lewis, W. R Heineman, D. A. Roston, P. T. Kissinger, *J. Chem. Educ.* 1983**, 60**, 772.

67 S. Dutta, P. Basu, A. Chakravorthy, *Inorg. Chem.*, 1991, **30**, 4031.

68 P. T. Kissinger, D. A. Roston, J. J. Van Benschoten, J. Y. Lewis and W. R. Heineman, *J. Chem. Ed.* 1983 **60**, 772.

69 V. Eisner, A. J. Bard, H. Lund, *Encyclopedia of Electrochemistry of the elements*, Marcel Dekker, NY, 1979, Vol.**13**, p338.

70 Q. Wang, A. Geiger, R. Frias, T. D.; Golden, *Chem. Educator* [Online] 2000, *5,* 58.

71 M. C. Granger, G. M. Swain, *J. Electrochem. Soc.* 1999, **146**, 4551.

72 C. M. Pharr, P. R. Griffiths, *Anal. Chem.* 1997, **69**, 4673.

73 R. F Boyd, *General microbiology* 1998, **2**nd edn, p. 441.

74 L. H. Hall, K. G.. Rajendran, D. X. West and A. E.Liberta, *Anticancer Drug*, 1993, **4**, .2.

75 B. J.Barnes, J. E. Rowell, K. A. Shaffer S. E. Cho, D. X. West and A. M .Stark, *Pharmazie*, 2001, **56(8),** 648.

76 S. E. J. Rigby, M. C. W. Evans and P Heathcote, *Biochemistry* 1996, *35*, 6651.

77 J. S. Wolfson, D. C. Hooper, M. N. Swartz, In: J.S. Wolfson, D.C. Hooper (Ed.),*American Society for Microbiology*, Washington, D. C., 1989, **21**,655.

78 Y. Teitz, D. Ronen, A. Vansover, T. Stematsky, J. L. Riggs, *Antiviral Research* 1994, **24**, 305.

78 S. E. Livingstone, K. Veda,J. Mortia and J. Komano, *J. Antibiotics*, 1981, **34**,317.

Chapter

4

SPECTRAL, BIOLOGICAL AND CYCLIC VOLTAMMETRIC INVESTIGATIONS OF COPPER(II) COMPLEXES WITH O-N-S DONOR LIGANDS

4.1 Introduction

Copper is considered one of the most familiar metals in our life, and is one of the minerals considered to form the ultimate basis of life. Not only is it essential for life, it has been used by man for thousand years for objects ranging from copper bells to micro electronics. It also plays numerous physiological roles in all organisms and is used to in the treatment of wide variety of metabolic disorders.

Copper is an important essential mineral present in the blood stream which is vital for infant growth, host defense mechanism, bone strength and red and white cell maturation, iron transport, iron transport cholesterol and glucose metabolism, myocardial contractility and brain development. Deficiency of copper can lead to a number of potentially fatal conditions such as the expression of menkes syndrome, occipital horn syndrome, mycrocytic anemia and neutropenia, bone disorders such as osteoporosis in children with radiological abnormalities. Copper deficiency has even been linked to some forms of cardiovascular disease and sudden infant death syndrome. Copper deficiency in children is often misdiagnosed as scurvy [1]

In recent years considerable interest has developed in the coordination chemistry of copper(II) with Schiff base as models of physical and chemicals behavior of biological copper systems. An interesting report [2] gives the electronic states of biologically important complexes, which help in understanding various properties such as stabilities reactions and structures. There has been continuing interest in the magnetic properties of copper(II) complexes. The report [3] gives an analysis of the use magnetochemical and spectroscopic investigations to estimate molecular and electronic structure.

The importance of thiosemicarbazones is extensively dealt in the Chapter1. Applications of thiosemicarbazones in industry, medicine and analytical determination of various metals ions are largely dealt in Chapter 2.

This chapter describes the syntheses of copper complexes with monoanionic O-N-S donor ligands (H_2SAP and H_2APP), various spectral investigations to characterize and explore their structures, redox behaviors and antimicrobial studies of such compounds.

4.2 Experimental

4.2.1. Materials

Details of the preparation and characterization of various ligands are given in Chapter 2. The solvents were of AR grade and purified by standard methods. Various copper(II) salts were purified by standard methods. Copper(II) perchlorate hexahydrate was obtained by treating GR copper(II) carbonate with 1:1 perchloric acid followed by evaporation and recrystallisation.

4.2.2 Synthesis of complexes

The Cu(II) complexes having general formula [Cu(HSAP)X], [Cu(HAPP)X], (HSAP and HAPP are monoanions of salicylaldehyde-^{4}N-pyrrolidine and 2-

hydroxyacetophenone-^{4}N-pyrrolidine thiosemicarbazones respectively and X is a mono or poly atomic anion) were prepared by adding 2 mmol of the appropriate ligand in hot methanol (25 mL) at a slightly higher pH (≈.6) than neutral to a hot and filtered solution of 2 mmol of appropriate Cu(II) salt in hot methanol (30 mL) with constant stirring. The mixture was heated at reflux for 3 h and volume is reduced to half. Crystalline complexes separated out on cooling were collected by filtration, thoroughly washed with hot water, methanol and then ether and dried *in vacuo* over P_4O_{10}.

Azido and thiocyanato complexes were prepared from the corresponding chloride complexes. A solution of 2 mmol of chloro complex in 100 mL of refluxing propionitrile was treated with a solution of 2.55 mmol of sodium azide / KCNS in 30 mL of propiononitrile. The solution was heated at reflux for 30 minutes and chilled. On cooling micro crystals of the compound in decent yield crystallized out. The compound was filtered off, washed with hot water, .methanol and ether and dried *in vacuo* over P_4O_{10}.

The complexes synthesized with the O-N-S donor ligands are the following.
Cu(HSAP)Cl,**13** ;Cu(HSAP)Br.3H_2O, **14**; Cu(HSAP)I.5H_2O, **15**;
CuHSAP.H_2OClO_4,**16**; Cu(HSAP)OAc, **17**; Cu(HSAP)N_3.H_2O, **18**;
Cu(HSAP)NCS,**19**;Cu(HSAP)NO_3.2H_2O,**20;** Cu(HAPP)H_2O.ClO_4, **21**;
Cu(HAPP)Cl,**22**;Cu(HAPP)Br.H_2O,**23**;Cu(HAPP)NO_3.H_2O,**24**; Cu(HAPP)NCS, **25**.

4.3 Measurements

Details of the analytical methods and other characterization techniques are given in Chapter 2.

4.4 Results and discussion

The yields, colours, elemental analyses, stoichiometries, magnetic susceptibilities and conductivities of Cu(II) complexes of O-N-S donors are listed in Table 4.1. The O-N-S donors are pale yellow in colour but their copper complexes are either green or

brown colour. Analytical results reveal the presence of one copper atom, one molecule of monoanionic thiosemicarbazones and one monatomic or polyatomic anion. The complexes are almost insoluble in most of the common polar and nonpolar solvents. They are however soluble in dimethylformamide in which conductivity measurements were made and showing the complexes to be nonconductors. But compounds **16** and **21** had unusually higher conductivities indicating their electrolytic nature.

4.4.1 Magnetic susceptibilities

The room temperature magnetic moments of copper(II) complexes in the polycrystalline state fall in the range 1.78 - 1.88 B.M, which are very close to spin only value of 1.73 B.M, for systems with only one unpaired electron. It also indicates that they are certainly magnetically dilute and therefore the possibility of spin- spin coupling is ruled out [4]

4.4.2 Vibrational spectra

The most significant IR bands useful for determining the ligand mode of coordination in copper(II) complexes of O-N-S donors are listed in Table 4.2 along with their tentative assignments. The most important bands of the ligands were assigned according to published data.

The IR spectra of the complexes are compared with that of the free ligand to determine the changes that might have taken place during complexation. The bands at 1634 and 1600 cm^{-1} are characteristic of the azomethine nitrogen atom present in H_2SAP and H_2APP respectively. On coordination the azomethine nitrogen, $\nu[^7C=^1N]$ shifts to lower wave numbers by 21-34 cm^{-1}. The appearance of a new medium sharp peak at *ca* 1496-1546 cm^{-1} is due to stretching vibration of the newly formed $^2N=^9C$ bond as a result of enolisation of thiosemicarbazones moiety. The bonding due to imine nitrogen is further confirmed by the presence of a new band at 428-457 cm^{-1} assignable to ν(Cu-N) for these complexes. The increase in $\nu(^1N-^2N)$ in the spectra of complexes is due to the increase in double bond character offsetting the loss of

Table 4.1
Analytical data, conductivity, magnetic moments, colours and yield of complexes of Cu(II) with O-N-S donor ligands

Compound	Emp.formula [b]	Colours	μ [c] (BM)	ΛM [d]	Analytical data, observed (calculated) %			
					C	H	N	Cu
Cu(HSAP)Cl, **13**	$C_{12}H_{14}ClCuN_3OS$	Brown	1.79	29	41.48 (41.50)	4.24 (4.06)	11.91 (12.10)	18.19 (18.30)
Cu(HSAP)Br.3H_2O, **14**	$C_{12}H_{20}BrCuN_3O_4S$	Brown	1.87	20	32.21 (32.33)	4.44 (4.52)	9.21 (9.43)	14.21 (14.25)
Cu(HSAP)I.5H_2O, **15**	$C_{12}H_{24}CuIN_3O_6S$	Brown	1.88	14	27.64 (27.25)	4.21 (4.57)	7.98 (7.05)	12.11 (12.02)
CuHSAP.H_2OClO_4, **16**	$C_{12}H_{16}ClCuN_3O_6S$	Green	1.95	34	33.88 (33.57)	3.83 (3.76)	9.80 (9.79)	14.69 (14.80)
Cu(HSAP)OAc, **17**	$C_{14}H_{18}CuN_3O_3S$	Green	1.75	22	45.11 (45.21)	4.66 (4.88)	11.13 (11.30)	17.14 (17.00)
Cu(HSAP)N3.H_2O. **18**	$C_{12}H_{15}CuN_6O_2S$	Green	1.84	9	39.01 (38.88)	4.12 (4.08)	22.44 (22.68)	17.20 (17.13)
Cu(HSAP)NCS, **19**	$C_{13}H_{14}CuN_4OS_2$	Green	1.87	17	42.00 (42.20)	4.21 (3.81)	15.36 (15.14)	17.26 (17.18)
Cu(HSAP)NO3.2H_2O, **20**	$C_{12}H_{17}CuN_4O_6S$	Brown	1.96	16	35.16 (35.25)	4.26 (4.19)	14.09 (13.70)	15.61 (15.54)
Cu(HAPP)$H_2O.ClO_4$, **21**	$C_{13}H_{18}ClCuN_3O_6S$	Green	1.86	37	35.36 (35.22)	4.11 (4.09)	10.02 (9.48)	14.36 (14.33)
Cu(HAPP)Cl, **22**	$C_{13}H_{16}ClCuN_3OS$	Green	1.78	26	43.19 (43.24)	4.40 (4.26)	11.74 (11.63)	17.71 (17.59)
Cu(HAPP)Br.H_2O, **23**	$C_{13}H_{18}BrCuN_3O_2S$	Green	1.84	18	37.06 (36.84)	3.98 (4.28)	10.07 (9.91)	15.12 (14.99)
Cu(HAPP)$NO_3.H_2O$, **24**	$C_{13}H_{19}N_4O_5SCu$	Brown	1.83	12	38.44 (38.47)	4.51 (4.47)	14.01 (13.80)	15.72 (15.65)
Cu(HAPP)NCS, **25**	$C_{14}H_{16}CuN_4OS_2$	Green	1.78	15	44.14 (43.79)	4.10 (4.20)	14.72 (14.59)	16.81 (16.55)

[a] In parentheses calculated values. [b] Emperical formula. [c] Magnetic moment [d] Molar conductivity, 10^{-3} M solution (DMF) at 298 K

electron density *via* donation of the metal is a another confirmation of the coordination of the donors through the azomethine nitrogen.

The ligand and the complexes show an intense peak at 3150 cm^{-1} that is characteristic of the (N-H) stretching, indicating the existence of free (N-H) group. The band in the region 2600-3800 cm^{-1} of the IR spectra of O-N-S donors suggests the presence of thioketo form in the solid state. The O-N-S donors show a strong and medium band in the region 1341 and 1357 cm^{-1} due to ν(C=S) stretching but no band due to ν(S-H) near 2570 $cm.^{-1}$. Coordination *via* the sulphur atom is indicated by a decrease in the frequency of the thioamide band by 11 to 48 $cm.^{-1}$. The thioamide (1V) band appears at *ca* 854 cm^{-1} and is shifted by approximately 30 cm^{-1} in the spectra of complexes, indicating coordination of the thione sulphur atom [5]. A substantial shift to lower energies of the above bands indicates thione sulphur coordination. This fact can be due to both a decrease in the double bond character of C=S bond and the change in the conformation along N-C bond on complexation. The presence of a new band (non-ligand band, weak to medium) in the 320-348 cm^{-1} range which is assignable to ν(Cu-S) is another indication of involvement of sulphur coordination.

In H_2SAP and H_2APP the ν(O-H) band appears at 3183 cm^{-1} and 3410 cm^{-1} respectively. The phenolic oxygen by loss of proton occupies the third coordination site, causing ν(C-O) to shift to lower wavenumbers by 50-80 cm^{-1}. The presence of a non-ligand band in the region 392-416 cm^{-1} is assigned to ν(Cu-O) further confirms phenolic oxygen coordination.

The fourth coordination position is taken by mono and polyatomic anion or water. The chloro complexes **13** and **22** show a sharp ν(Cu-Cl) band at 316 cm^{-1}, indicating terminal rather than bridging chlorine. The ν(Cu-Br) band for the complexes **14** and **23** is found at *ca* 233 cm^{-1} and 238 cm^{-1}. These values suggestive for terminally bonded bromine. The ratio ν(Cu-Br) / ν(Cu-Cl) is in the range 0 .73 to 0.76 for the solids and same results is consistent with usual values obtained for the

Table 4.2
Selected IR bands (cm^{-1}) with tentative assignments of Cu(II) complexes with O-N-S donor ligands

Compd [a]	ν(C-N)	ν(NC)	ν(N-N)	ν(C-S)	δ(C-S)	ν(C-O)	ν(Cu-O)	ν(Cu-S)	ν(Cu-N)	ν(Cu-X)	ν(N-H)
H_2SAP	1634 s	-----	1040 w,	1391 m	854 m	1290 s	-----	-----	-----	-----	3270 s
13	1613 s	1532 s	1073 m	1330 m	825 m	1202 s	392 s	320 m	430 m	315 s	3268 s
14	1607 s	1539 s	1070 m	1324 m	825 m	1202 s	396 s	336 m	432 m	233 m	3271 s
15	1600 s	1533 m	1074 m	1334 m	825 m	1204 s	393 m	335 m	430 m	----	3269 m
16	1607 s	1531 s	1076 m	1330 s	818 m	1229 s	395 s	332 m	446 m	400 m/w*	3270 s
17	1600 s	1532 s	1088 m	1357 m	825 m	1209 s	390 w, 397s	333 m	428 m	390 w	3266 m
18	1613 s	1530 m	1074 m	1317 m	825 m	1276 m	410 m	336 w	430 w	446 m	3268 m
19	1607 m, 2071 s	1546 s	1061 m	1317 m	825 m	1211 s	393 m	348 m	438, 429m	329 m	3266 m
20	1607 s	1519 m	1074 m	1377 m	845 m	1204 s	416 s	330 w	432 m	311 w	3271 m
H_2APP	1600 s	-------	1096 m	1379 m	856 m	1243 s	----	----	----	----	3333 s
21	1587 s	1530 m	1123 m	1313 m	819 m	1190 m	398 m	324 m	454 m	396 m	3329 s
22	1592 s	1533 s	1144 m	1316 m	824 w	1193 s	405 m	322 m	456 s	317 m	3338 w
23	1565 m	1528 s	1162 m	1309 m	824 m	1191 s	392 s	324 m	458 s	238 m	3334 w
24	1593 m	1496 s	1144 m	1313 m	838 m	1198 s	394 m	321 m	460 m	----	3329 s
25	1592 s, 2069 m	1531 s	1156 m	1324 m	836 w	1193 m	410 m	321 m	457 m	----	3335 s

s = strong; m = medium; w = weak; sh = shoulder
[a] = Compound

complexes of first row transition series [6]. As ν(Cu-I) is beyond the range of instrument, it is not assigned.

The thiocyanate complex **19** has a very strong band at 2071 cm^{-1}, a strong band at 825 and a sharp band at 485 cm^{-1} corresponding to ν(CN), ν(CS) and δ(NCS) modes of the NCS group respectively. For the compound **25** these bands appeared at 2069, 825 and 486 cm^{-1}. The δ(NCS) is not clearly observed because it is obscured partially by the ligand absorption in that region. These results are in consistent to a monodentate N bonded thiocyanate group. The ν(Cu-N) of the thiocyanato group for solids **19** and **25** is observed at 329 cm^{-1} and 334 cm^{-1} respectively. The results are in agreement with the reported value of 329 cm^{-1}.

The spectra of complexes **20** and **24** show bands corresponding to the nitrate anion coordinated to the copper. Since .nitrate group is displaced by the bromide ions from the KBr pellets and so measurements on nujol mull were required. The coordination mode of the nitrate group cannot be deduced unequivocally from IR data alone. But we found that nitrato complexes have two strong bands at 1268 and 1390 cm^{-1} corresponding to ν_1 and ν_4 of the nitrato group with a separation of 122 cm^{-1} indicating the presence of a terminally bonded monodentate nitrato group. A combination band $\nu_1+\nu_4$, considered as diagnostic for the monocordinate nitrato group has been observed at 1764 cm^{-1}. The absence of a split band in this region indicates that strong coordination of nitrate ions is unlikely. The ν_3 ν_5 and ν_6 could not be assigned due to the richness of the spectra of the complexes. The ν(Cu-N) of the nitrato solid is reported in the range 250-350 cm^{-1} and we identified a band at 311 cm^{1} in **20** and 314 cm^{-1} in **24**, for this mode and these are consistent with earlier reports

The acetate complex **17** has bands at 1618 and 1311 cm^{-1} corresponding to asymmetric and symmetric COO- stretching bands respectively, which are in agreement with the acetate group being monodentate [7]. The ν(Cu-O) of acetate at 390 $cm,^{-1}$ for the acetate solid is based on the assignment of Baldwin *et al.*.

The perchlorate complexes **16** and **21** show a single broad band *ca* 1120 cm^{-1} and a strong band at 620 cm,$^{-1}$ indicating the presence of ionic perchlorate. The band at 1120 cm^{-1} is assignable to $\nu_3(ClO_4)$ and an unsplit band at 620 cm^{-1} assignable to $\nu_4(ClO_4)$. Moreover, no bands assignable to ν_1(*ca* 930 cm^{-1}) or ν_2(*ca* 460 cm^{-1}) are observable in the spectra. This along with unsplit ν_3 and ν_4 bands show exclusive presence of non-coordinated perchlorate group having slight distortion from T_d symmetry due to lattice effects. A broad band in the range 3500-3100 cm^{-1} for compounds **16** and **21** suggests that water is coordinated to central metal atom. Moreover bands at 3317, 1627, 601, 423 cm^{-1} are attributable to ν(O-H) $\delta(OH_2)$, π $w(OH_2)$, and ν(Cu-O) of coordinated water. Accordingly, it appears that the water molecule occupies the fourth coordination position

The azide complex **18** shows a single broad band at 2046 cm^{-1} and a strong band at 1342 cm^{-1}. These are assigned to ν_a and ν_s. The broad band at 656 and 446 cm^{-1} are assigned to δ(N-N-N) and ν(Cu-N) bands. This suggests that Cu-N-N-N bond is linear. Azide derivatives can be explosive on strong heating. T.G measurements showed that compounds violently decomposes at 390 K. The spectra of **14**, **15**, **18**, **20**, **23** and **24** have strong and broad bands between 3500-3100 cm^{-1} of non coordinated water.

4.4.3 Electronic spectra

Owing to flexible stereochemistry of the copper(II) ions. the electronic reflectance spectra of copper(II) complexes (Fig 4.1) is probably the most easily determined. Single crystal electronic spectral technique thought to be good for copper(II) complexes has reduced to a dribble in view of the uncertainties associated with the assignment of these types of spectra, especially in low symmetry environment [8]. The significant electronic absorption bands in the spectra of complexes recorded in the solid sate and in dimethylformamide solution are presented in Table 4.3.

Thiosemicarbazones and their copper(II) complex have a ring $\pi \rightarrow \pi^*$ band at *ca* 255 nm and $n \rightarrow \pi^*$ band at 334 nm. The bands undergo a slight shift in energy on complexation. A second $n \rightarrow \pi^*$ band located below 317 nm in the spectra of the copper(II) complexes found at *ca* 317 nm. This band which involves transition

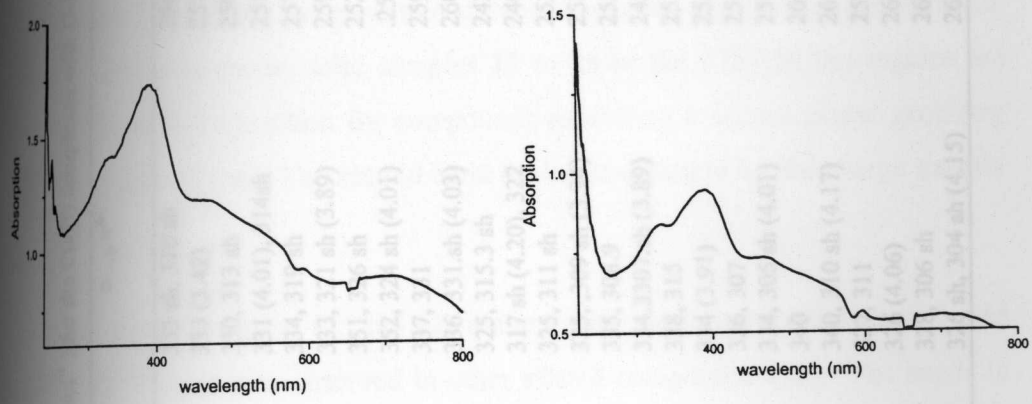

Fig 4.1 UV-Vis DRS of representative copper complexes

within the thiosemicarbazones moiety mainly C=N and C=S group, is of reduced intensity in the spectra of the complexes. Two ligand to metal charge transfer (CT) band are found at *ca* 385 nm and 402-417 nm. In accordance with earlier reports [9], we assigned higher energy intense absorption band to $S \rightarrow Cu(II)$ and lower energy band to $O \rightarrow Cu(II)$. It is found that compounds with anionic thiosemicarbazones, slight shift to lower energies occurs, suggesting the presence of lower π interaction between the Cu and S atoms. This fact would imply a C-S bond close to thiolate behavior in system containing anionic thiosemicarbazones. It is also reported that the position of this band is dependent on the steric requirements of the ^4N substituent, such that thiosemicarbazones with bulkier substituent show this band at somewhat higher energies [10]. Since the substituent at the ^4N position remained unaltered, we did not observe any change in the energy of this band. The solid-state spectrum of each complex has two d-d bands or a single broad band in the lower energy range. In solution, there is a single broad band found at essentially the same energy for each of

Table 4.3

Electronic spectral assignments. (nm).(Log ε in parenthesis, ε is expressed in l mol^{-1} cm^{-1}) for the Cu(II) complexes with O-N-S donor ligands

compd	mode	d-d	LMCT	$n \rightarrow \pi^*$	$\pi \rightarrow \pi^*$
13	Solid	673 sh, 577	402 sh,383 sh	335 sh, 310 sh	256 sh
	DMF	579 sh (2.94)	403 sh,390 sh (3.01)	333 (3.42)	257.4 sh (3.98)
14	Solid	667 s h, 570	402 sh, 360sh	330, 313 sh	250 sh
	DMF	573.sh (2.58)	403.sh, 364 sh (3.61)	331 (4.01), 314sh	251 sh (4.11)
15	Solid	652 sh, 560 sh	402, 351 sh	334, 319 sh	257, 252.5
	DMF	640 sh, 562 sh (2.49)	403, 352 sh (3.71)	333, 321 sh (3.89)	259 sh (4.03)
16	Solid	652, 567 sh	402, 391 sh	351, 326 sh	252, sh
	DMF	639, 568.sh (2.39)	405 w (3.94)	352, 324 sh (4.01)	.252 sh (4.11)
17	Solid	763, 550 sh	445, 423.5	337, 331	259 sh, 243
	DMF	604, 555.3 sh (2.91	450, ,426 (3.62)	336, 331.sh (4.03)	260 sh, 244 (4.21)
18	Solid	653, 645 sh	406, 400.	325, 315.3 sh	242, 248
	DMF	654.sh (3.01)	407, 404.sh (3.44)	317 sh (4.20), 322	240, 249.sh (4.32)
19	Solid	735, 600 sh	411,386 sh	325, 311 sh	252, 243 sh
	DMF	645, 601 sh (2.41)	413 sh,387.(3.25)	325, ,309 sh (3.94)	253 sh, 245 sh (4.20)
20	Solid	714, 644	410, 386	335, 308.9	252, 244
	DMF	657, 644 (2.89)	425, 387.(3.27)	334.3307.sh (3.89)	245, 253 sh (4.03)
21	Sold	724, 600	405, 390	338, 315	252
	DMF	658, 601.5 sh (3.03)	407, 392 (3.65)	334 (3.91)	255, 240 sh (4.31)
22	Solid	759, 629	400, 384	336, 307	257, 246
	DMF	658, 602 sh (3.030	403 sh (3.51), 391 sh (3.62)	334, 305 sh (4.01)	257 sh (4.21), 248 sh (4.31)
23	Solid	645, 596 sh	403, 373 sh	340	260, 231sh
	DMF	598 sh (2.89)	405 sh (3.71)	340, 310 sh (4.17)	267, 245 sh (4.37)
24	Solid	660, 580 sh	407, 381	327, 311	259, 244 sh
	DMF	666, 583.(2.74)	407.sh (3.91)	326 (4.06)	261 sh(4.12)
25	Solid	658, 567 sh	424, 414 sh	328, 306 sh	260, 245 sh
	DMF	660 sh (2.91)	430 sh (3.89)	326 sh, 304 sh (4.15)	261 sh, 246 sh (4.12)

the complexes and have approximately the same molar absorptivities. The small difference in the d-d band in dimethylformamide solution from those in the solid state is indicative of the coordination of the solvent. The electronic spectra of square planar copper(II) complexes of Schiff bases display a weak absorption band in the range 560 nm and 723 nm and the latter being seen as a very weak shoulder in the tail of the CT band have been assigned to d-d transition as reported by Ali and Tarafdar. The bands observed in the solid samples **13** to **25** in the 575-734 nm regions are characteristic of d-d transition for compounds exhibiting a square planar geometry with $d_{x^2-y^2}$ ground state. The second band is almost obscured by the charge transfer bands.

The absorption at *ca* 425 and 420 nm in the nitrate derivative can be attributed to LMCT O→Cu as was observed in other related compounds [11]. The bands in the 435-445 nm regions for complexes **18**, **19** and **25** are assigned to pseudo halide→Cu(II) LMCT transitions.

We noticed that peaks resulting from n→π*transitions are shifted to shorter wavelengths (blue shift) in DMF solution. This arises from increased solvation of the lone pair, which lowers the energy of the non bonding orbital. We also found a red shift for π→π* transitions. The attractive polarization forces between the solvent and the absorber, which lowers the energy level of the both excited and unexcited states, cause this. This effect is greater for the excited state and so the energy difference between the excited and unexcited states is slightly reduced-resulting in small red shift. This effect also influences n→π*transitions but is overshadowed by the blue shift resulting from solvation of lone pair. The absorption at *ca* 425-420 nm in the nitrato derivatives can be attributed to the O→Cu(II) LMCT, transition as was observed in other related compounds.

4.4.4 EPR spectra

The EPR spectra of polycrystalline sample at 298 K in dimethylformamide solution at 298 K and 77 K were recorded in the X band, using the 100-kHz field modulation; g factors are quoted relative to the standard marker TCNE. Spectral simulations were performed using computer programs described elsewhere [12]. The EPR parameters obtained for copper(II) complexes are presented in Tables.4.4, 4.5a. and 4.5b.

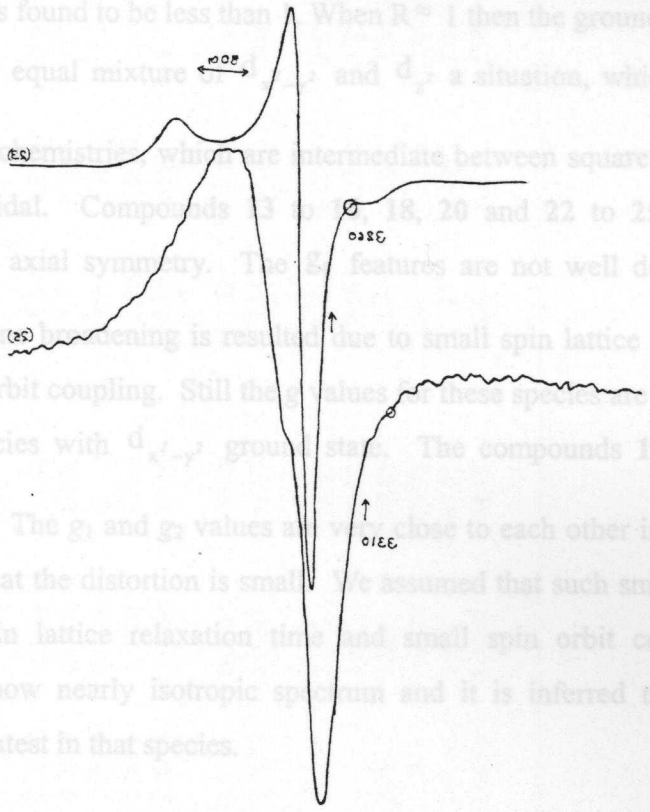

Fig 4.2 EPR spectra of copper complexes (17,19) in the polycrystalline state at 298 K

The appearance of the spectrum in the polycrystalline state is that of a single species containing one nitrogen in the coordination sphere of copper. Expect for **21**, which shows a broad signal due to enhanced spin lattice relaxation, all others show either a two line or three line spectra. The G values obtained for our complexes are in

the range 3.5 to 5 which indicate that the g values obtained in the polycrystalline sample are near to the molecular *g* values and hence the unit cell of the compounds contain magnetically equivalent sites. In rhombic with $g_1 < g_2 < g_3$, the value of R may be significant; if it is greater than one, a predominant d_{z^2} ground state is present and if it is less than one a predominant $d_{x^2-y^2}$ ground state present. In the new complexes showing three g values, the ground state orbital is therefore $d_{x^2-y^2}$ because R value is found to be less than 1. When $R \approx 1$ then the ground state involves an approximately equal mixture of $d_{x^2-y^2}$ and d_{z^2} a situation, which is, found to apply with stereochemistries, which are intermediate between square pyramidal and trigonal bipyramidal. Compounds **13** to **16**, **18**, **20** and **22** to **25**, give signals corresponding to axial symmetry. The $g_{\|}$ features are not well defined in these complexes and line broadening is resulted due to small spin lattice relaxation time and large spin –orbit coupling. Still the *g* values for these species are consistent with a copper(II) species with $d_{x^2-y^2}$ ground state. The compounds **17** and **19** gave rhombic spectra. The g_1 and g_2 values are very close to each other in these species, which indicate that the distortion is small. We assumed that such small distortion is due to large spin lattice relaxation time and small spin orbit couplings. The compound **21** show nearly isotropic spectrum and it is inferred that the dipolar interaction is greatest in that species.

The solution spectra of all complexes were recorded in DMF at 298 K. The spectral features of most of the complexes clearly show four well resolved hyperfine lines ($^{63,\ 65}$Cu ,I=3/2) corresponding to -3/2 , -1/2, +1/2, +3/2 transitions ($\Delta m = \pm 1$). The signal corresponding M_I = +3/2 splits clearly in to three peaks with a superhyperfine (shf) or ligand hyperfine coupling constant A ≈ 17.5 G. This is characteristic of compounds bound through azomethine nitrogen and an indication that the bonding in solution state is dominated by the thiosemicarbazones moiety

Table.4.4.

ESR Spectral assignments of Cu(II)complexes with O-N-S donors.(Experimentally determined.). (All A values are reported in units of Gauss)

Compounds*	Solid (300 K)			DMF solution (300 K)			DMF solution (77 K)				
	g_0/ $g_\parallel$ / g_3	$g\perp$ / g_1, g_2	g_{av}	g_0	A_0	A_N	$g_\parallel$	$g\perp$	g_{av}	$A_\parallel$ (Cu)	$A_\perp$ (N)
13	2.1055	2.0328	2.0570	2.0751	74.34	17.1	2.2078	2.0473	2.0979	180.4	17.7
14	2.1069	2.0297	2.0555	2.0634	66.51	15.5	2.186	2.0433	2.0908	164	15.2
15	2.0925	2.0298	2.0507	2.0406	68.12	17.9	2.1679	2.0384	2.0816	164.2	17.1
16	2.1022	2.0419	2.0621	2.0708	83.04	18.96	2.2180	2.0539	2.1086	181.21	18.26
17	g_3 2.0568	g_2 2.0194 g_1 2.0072	2.0278	2.0394	73.16	19.14	2.150	2.042	2.078	180.68	16.51
18	2.099	2.0297	2.0528	2.060	79.86	17.92	2.2018	2.0569	2.1052	179.27	15.52
19	g_3 2.0925	g_2 2.0544 g_1 2.0207	2.0589	2.0827	71.97	18.14	2.15	2.050	2.034	160.6	14.8
20	2.107	2.0293	2.0552	2.085	72.89	16.4	2.197	2.0535	2.1013	173.4	15.3
21	g_0 2.046	---	----	2.032	79.93	17.26	2.2119	2.0537	2.1064	180.7	17.97
22	2.1119	2.0267	2.0551	2.089	79.95	16.91	2.2051	2.0463	2.0992	185	14.69
23	2.089	2.0266	2.0474	2.0793	69.75	15.9	2.2195	2.0472	2.1046	167.86	18.11
24	2.1022	2.0638	2.0766	2.079	63.01	20.87	2.1935	2.0603	2.1047	181.76	16.42
25	g_3 2.115	g_2 2.0544 g_1 2.0267	2.0654	2.0799	72.17	18.8	2.109	2.067	2.095	174.1	15.98

rather than the mono or polyatomic anions [13]. The small variation in the g_{av} value of the complexes in DMF solution from the g_{av} value calculated for polycrystalline spectra can be attributed to the variation in the geometric environment of the compounds upon dissolution [14]. For all complexes, spectra with isotropic features were obtained. .The solution spectra show a little difference among the A_0 and g_0 values of the complexes, suggesting similarity in the bonding of the thiosemicarbazones and interaction with solvent throughout the series of complexes [15].

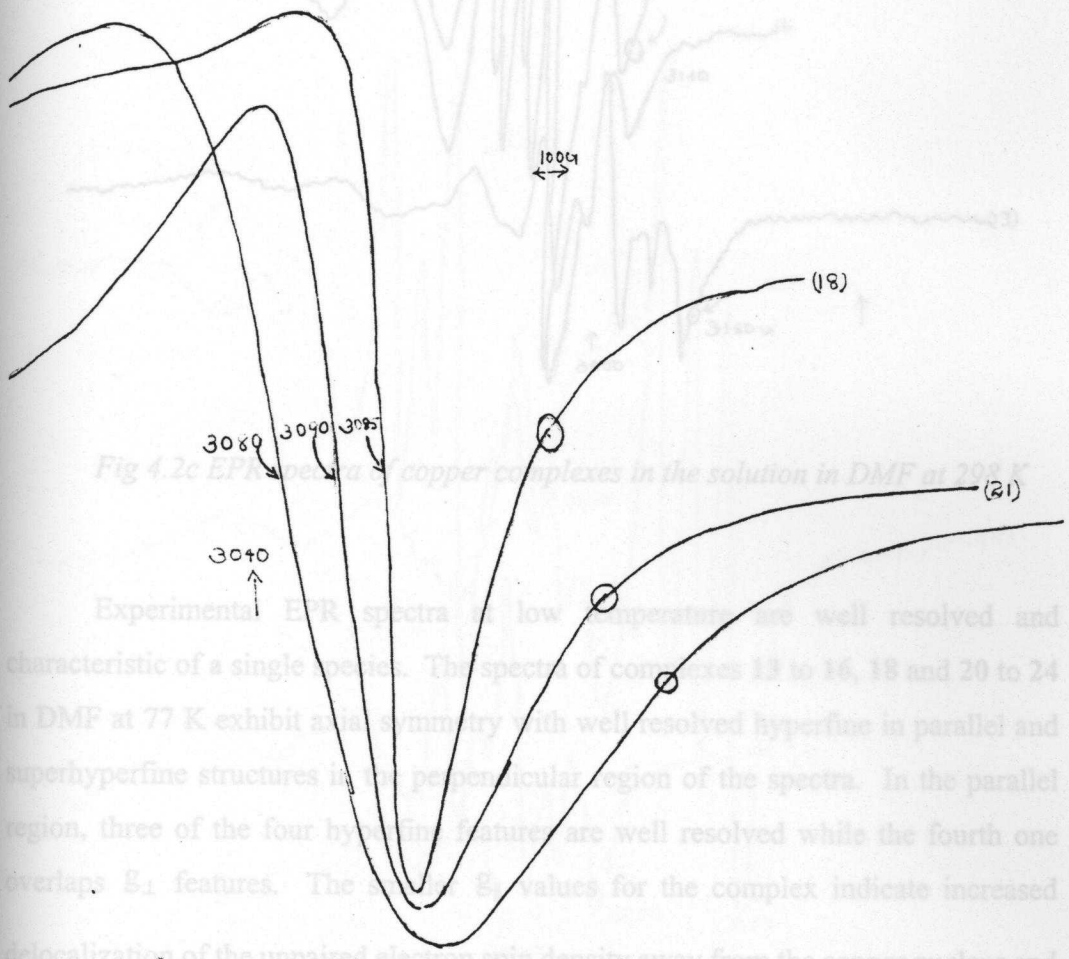

Fig 4.2b EPR spectra of copper complex in the polycrystalline state at 298 K

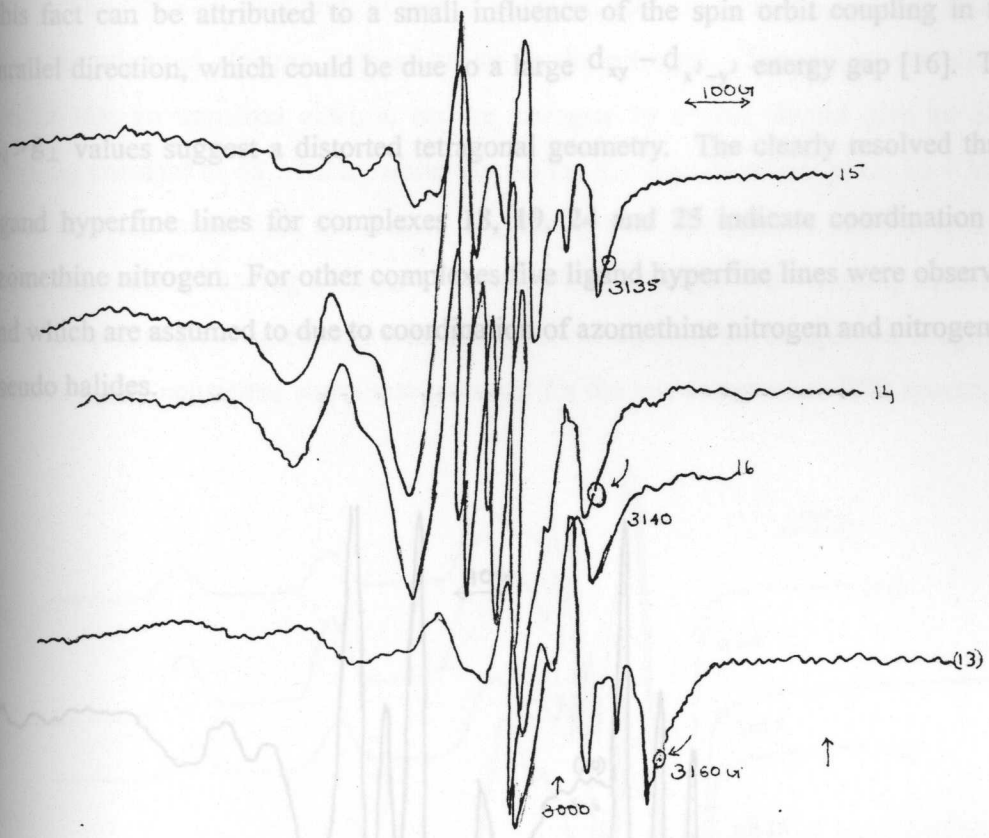

Fig 4.2c EPR spectra of copper complexes in the solution in DMF at 298 K

Experimental EPR spectra at low temperature are well resolved and characteristic of a single species. The spectra of complexes **13** to **16**, **18** and **20** to **24** in DMF at 77 K exhibit axial symmetry with well resolved hyperfine in parallel and superhyperfine structures in the perpendicular region of the spectra. In the parallel region, three of the four hyperfine features are well resolved while the fourth one overlaps $g_{\perp}$ features. The smaller $g_{\parallel}$ values for the complex indicate increased delocalization of the unpaired electron spin density away from the copper nucleus and may be interpreted in terms of increased covalency of the metal – ligand bond. However, the $g_{\parallel}$ or g_{iso} values are relatively small for compounds **14**, **15**, **19** and **25**.

This fact can be attributed to a small influence of the spin orbit coupling in the parallel direction, which could be due to a large $d_{xy} - d_{x^2-y^2}$ energy gap [16]. The $g_{\parallel} > g_{\perp}$ values suggest a distorted tetragonal geometry. The clearly resolved three ligand hyperfine lines for complexes **18**, **19**, **24** and **25** indicate coordination of azomethine nitrogen. For other complexes five ligand hyperfine lines were observed and which are assumed to due to coordination of azomethine nitrogen and nitrogen of pseudo halides.

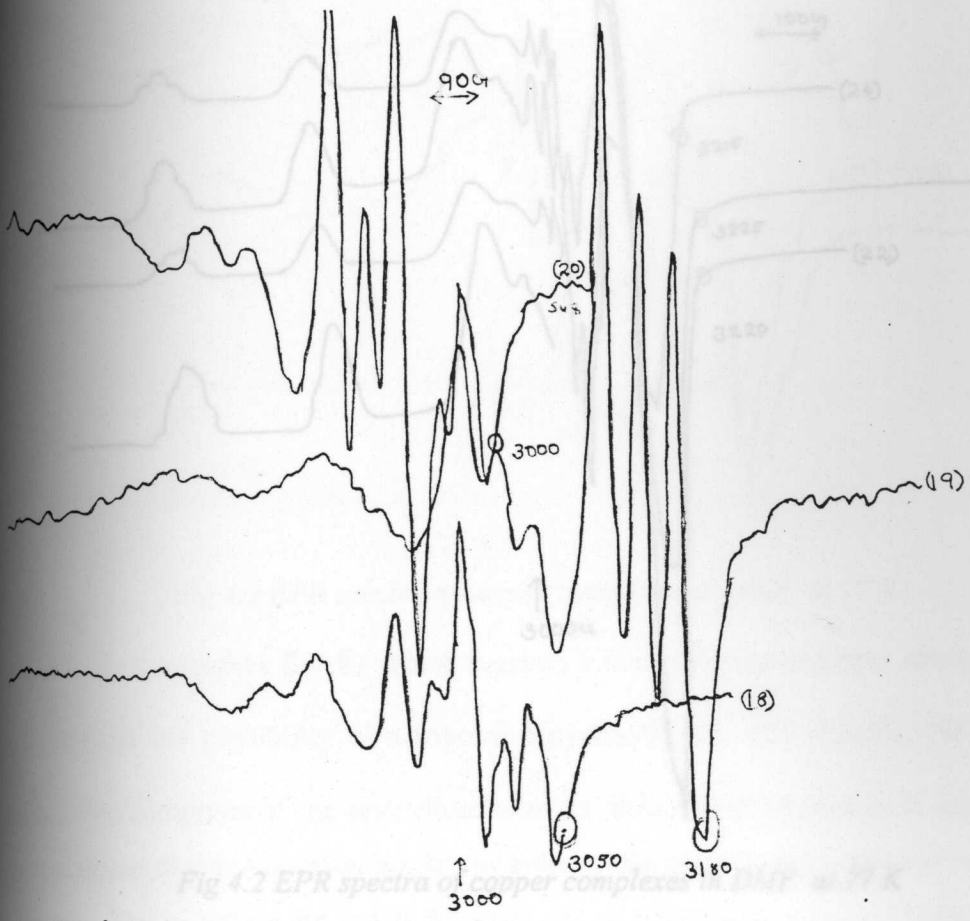

Fig 4.2d EPR spectra of copper complexes in DMF solution at 298 K

The ^{14}N SHF couplings observed in frozen solution EPR spectra arise mainly om the unpaired electron delocalization on the nitrogen. Theoretical calculation redict that an unpaired electron on the nitrogen 2p orbital should give an SHF oupling constant of 48.7 MHz, while that on the nitrogen 2s orbital gives 15.4 MHz hich is much larger than the former, suggesting that the unpaired electron spin on e nitrogen orbital having a higher s / p ratio will give larger SHF coupling constants 7]. This is in good agreement with the observed data for the complexes. Magnetic arameters are consistent with those obtained for the low temperature EPR spectra.

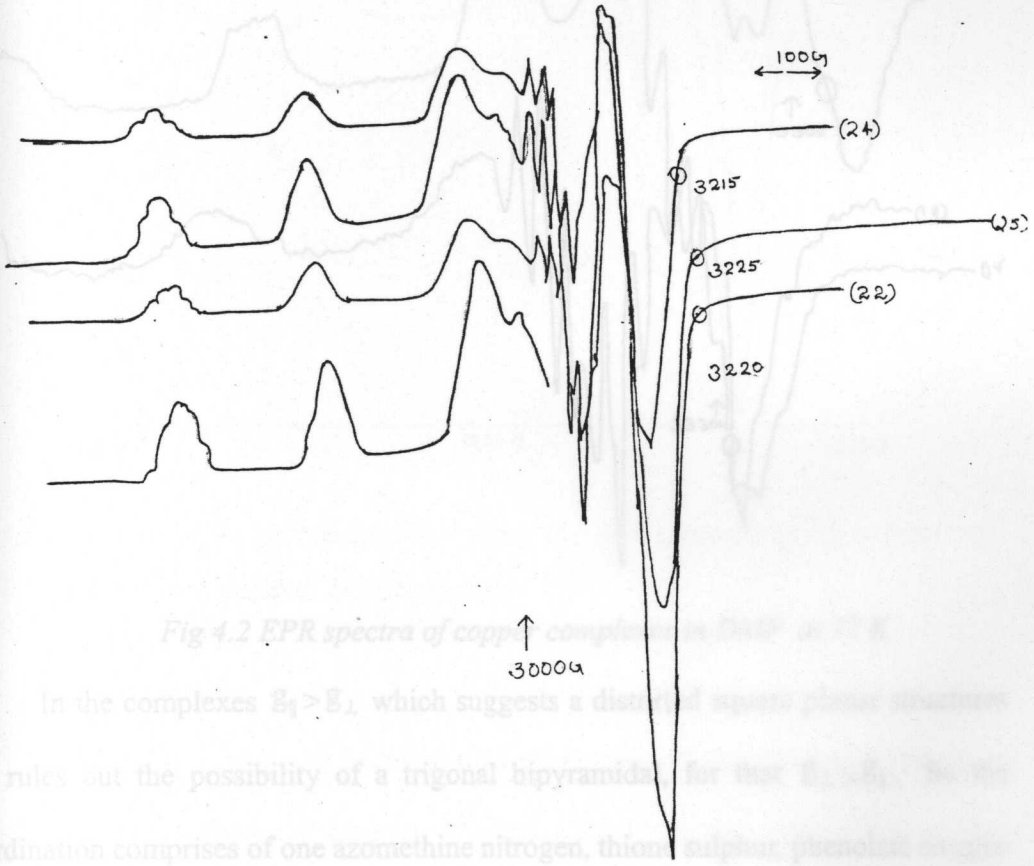

Fig 4.2 EPR spectra of copper complexes in DMF at 77 K

As is evident from analysis of parallel part of the spectra, the line width of I_1= -3/2 component is small compared with the nitrogen coupling constant, leading o the appearance of N superhyperfine pattern. In this case the coordination around

the metal ion can easily be found by analyzing the superhyperfine pattern (SHF) on the $g_{\|}$ region. From this, it is possible to infer metal coordination and precise values for coupling constants of the bound nitrogen. Comparison of the values of the magnetic parameters of these complexes is in agreement with those reported [18] previously for thiosemicarbazones of similar coordination.

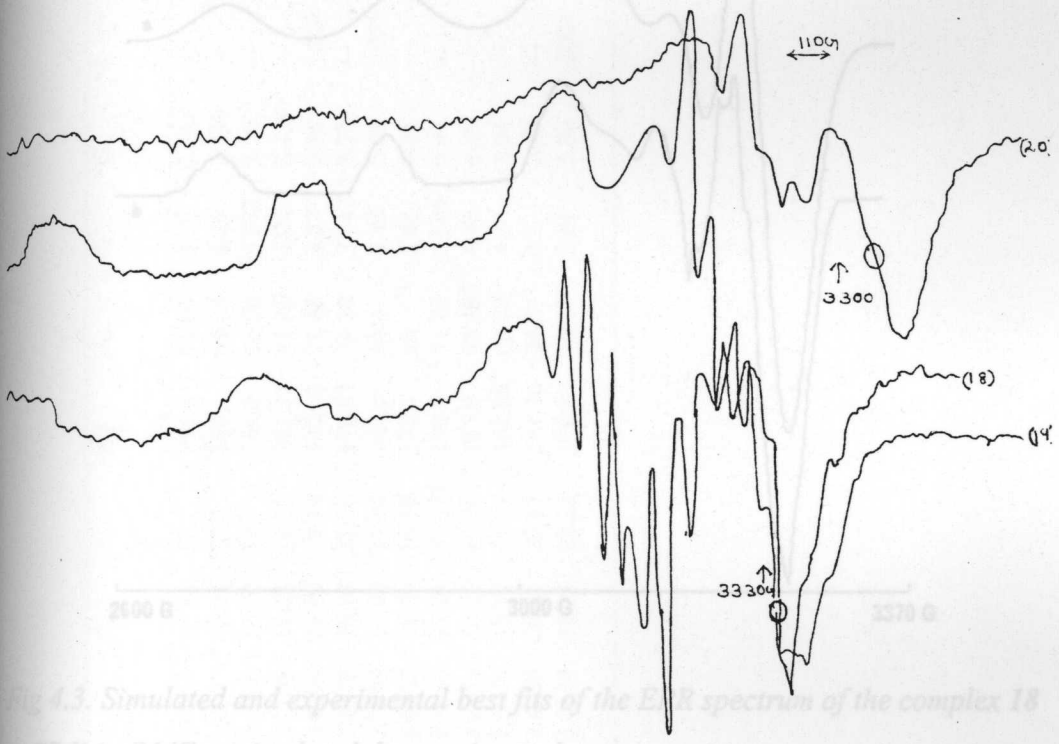

Fig 4.2 EPR spectra of copper complexes in DMF at 77 K

In the complexes $g_{\|} > g_{\perp}$ which suggests a distorted square planar structures and rules out the possibility of a trigonal bipyramidal, for that $g_{\perp} > g_{\|}$. So the coordination comprises of one azomethine nitrogen, thione sulphur, phenolate oxygen and fourth coordination position is taken by either mono or polyatomic anion or water molecule. The g_0 values are nearly the same for all complexes, which indicate that the bonding is dominated by the thiosemicarbazone moiety rather than mono or polyatomic anion. It is also noticed that $g_{\|}$ values are less than 2.3, which indicates

significant covalent bonding in these complexes. In all complexes $g_{\|} > g_{\perp} > g_e$ and $G = (g_{\|} - 2) / (g_{\perp} - 2)$ values are < 4.5 are in consistent with a $d_{x^2-y^2}$ ground state with small exchange coupling.

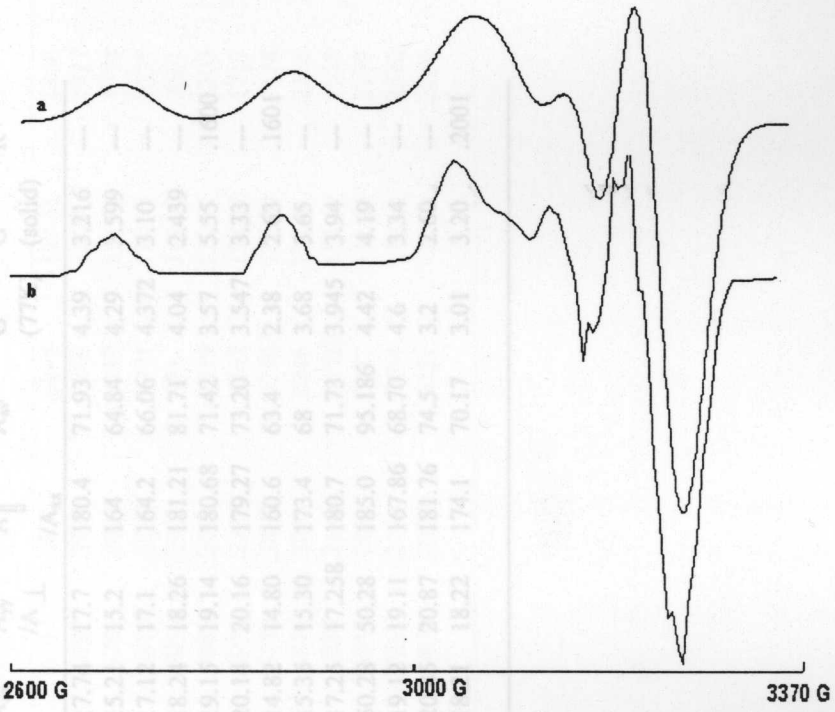

*Fig 4.3. Simulated and experimental best fits of the EPR spectrum of the complex **18** at 77 K in DMF; a-simulated, b-experimental*

The tendency of $A_{\|}$ to decrease with an increase of the tetrahedral distortion in the coordination sphere of copper. The trend for A_{iso} is the same as that of $A_{\|}$. Moving from the planar toward the more distorted complex a decrease of A_{iso} is apparent. The empirical factor $f = g_{\|} / A_{\|}$ (cm^{-1}) is an index of tetrahedral distortion. Its value ranges between 105 and 135 cm^{-1} for square planar complexes, depending on the nature of the coordinated atoms. In the presence of a tetrahedrally distorted,

Table.4.5.a
Spin Hamiltonian parameters of Cu(II) complexes of O-N-S donor ligands.

Compound	g_{xx}	g_{yy} /$g_{\perp}$	$g_{\parallel}$ / gzz	g_{av} (77K)	g_{av} (solid)	g_{av} (dmf)	A_{xx}	A_{yy} /$A_{\perp}$	$A_{\parallel}$ /A_{xx}	A_{av}	G (77K)	G (solid)	R
13	2.0471	2.0473	2.2078	2.0979	2.0570	2.0751	17.74	17.7	180.4	71.93	4.39	3.216	---
14	2.0433	2.186	2.0908	2.0555	2.0634	15.21	15.21	15.2	164	64.84	4.29	3.599	---
15	2.0385	2.0384	2.1679	2.0816	2.0507	2.0406	17.12	17.1	164.2	66.06	4.372	3.10	---
16	2.054	2.0539	2.2180	2.1086	2.0621	2.0708	18.24	18.26	181.21	81.71	4.04	2.439	---
17	2.034	2.050	2.150	2.096	2.0278	2.0394	19.15	19.14	180.68	71.42	3.57	5.55	.1600
18	2.2016	2.0569	2.2018	2.1052	2.060	2.0528	20.14	20.16	179.27	73.20	3.547	3.33	---
19	2.050	2.042	2.15	2.078	2.0818	2.0559	14.82	14.80	160.6	63.4	2.38	2.63	.1601
20	2.0535	2.0537	2.197	2.1013	2.085	2.0552	15.35	15.30	173.4	68	3.68	3.65	---
21	2.0531	2.0535	2.2119	2.1064	2.046	2.1064	17.25	17.258	180.7	71.73	3.945	3.94	---
22	2.0463	2.0463	2.2051	2.0992	2.089	2.0551	50.28	50.28	185.0	95.186	4.42	4.19	---
23	2.0470	2.0472	2.2195	2.1046	2.0793	2.0474	19.12	19.11	167.86	68.70	4.6	3.34	---
24	2.060	2.0603	2.1935	2.1047	2.079	2.0766	20.85	20.87	181.76	74.5	3.2	2.60	---
25	2.0565	2.0565	2.172	2.095	2.0799	2.0654	18.21	18.22	174.1	70.17	3.01	3.20	.2001

A = Gauss

Bonding parameters of Cu(II) complexes of O-N-S donor ligands.

compound	α^2	β^2	γ^2	$K_{\parallel}$	$K_{\perp}$	K_0	P	f	K
13	.7659	.8864	.8296	.6789	.6354	.2928	.0248	122.38	.2286
14	.6986	.9254	.8743	.6448	.6092	.2479	.0259	133.3	.1727
15	.6766	.9150	.8545	.6191	.5781	.2627	.0289	132.18	.1778
16	.7812	.8997	.8802	.7029	.6876	.3297	.0274	122.39	.2575
17	.7058	.8291	.8597	.5852	.7058	.2921	.022	119.00	.2061
18	.7608	.8905	.9317	.6775	.7088	.3027	.0219	122.82	.2303
19	.6508	.8826	.9152	.5744	.5956	.2512	.0202	133.87	.1717
20	.7768	.8903	.9130	.6573	.6740	.2878	.02327	126.00	.2124
21	.7383	.8904	.8772	.6916	.6814	.3033	.0246	122.4	.2356
22	.8020	.8350	.7779	.6696	.6239	.3189	.02015	119.19	.2558
23	.7609	.9406	.8555	.6987	.6353	.2931	.0227	132.22	.2177
24	.7427	.8630	.9506	.6567	.7233	.2774	.0234	120.68	.2110
25	.7165	.8488	.9594	.6082	.6874	.2876	.0221	124.75	.2060

structure the values can be much larger. Values lower than 135 cm^{-1} have been observed for square planar structures and those higher than 150 cm^{-1} for tetrahedrally distorted complex. It is apparent from Table 4.5 that there is a clear tendency for the majority of copper(II) complexes of mono thiosemicarbazones to exhibit a medium distortion from planarity.

The EPR spectra of compounds **16**, **19** and **25**, in frozen state show rhombic symmetry. The lowest g value (2.04).is smaller that usually observed in compounds with square planar geometry. This fact can be attributed to the deviation from planar geometry.

All the spectra were simulated to get values for various magnetic parameters. The bonding parameters α^2, β^2, γ^2 were calculated. Details of calculations are appended in Chapter 3. The α^2, β^2 and, γ^2 have values less than 1.0 which indicates considerable covalent character to the in-plane σ and π bonds in addition to out of plane π bonding. The P values in the range 0.23 cm^{-1} also favour bonding of copper to nitrogen. Reduction in P values from the free ion value might be attributed to the strong covalent bonding. The Fermi contact interaction term K for the complexes is in the range 0.25 to 0.30 and the results are in good agreement with those reported [19]. The observed orbital reduction factors values of $K_{\|} = 0.61$ to 0.70 and $K_{\perp}$ = 0.57 to 0.70 are indicative of the existence of high covalence in the complexes.

The experimental EPR spectra are shown in Fig 4.2 and in Fig 4.3, the experimental frozen solution EPR spectrum of representative complexes paired with simulation that eventually gave the best fit is reported. Based on our spectral studies we proposed square planar structures for the new complexes, Fig 4.4.

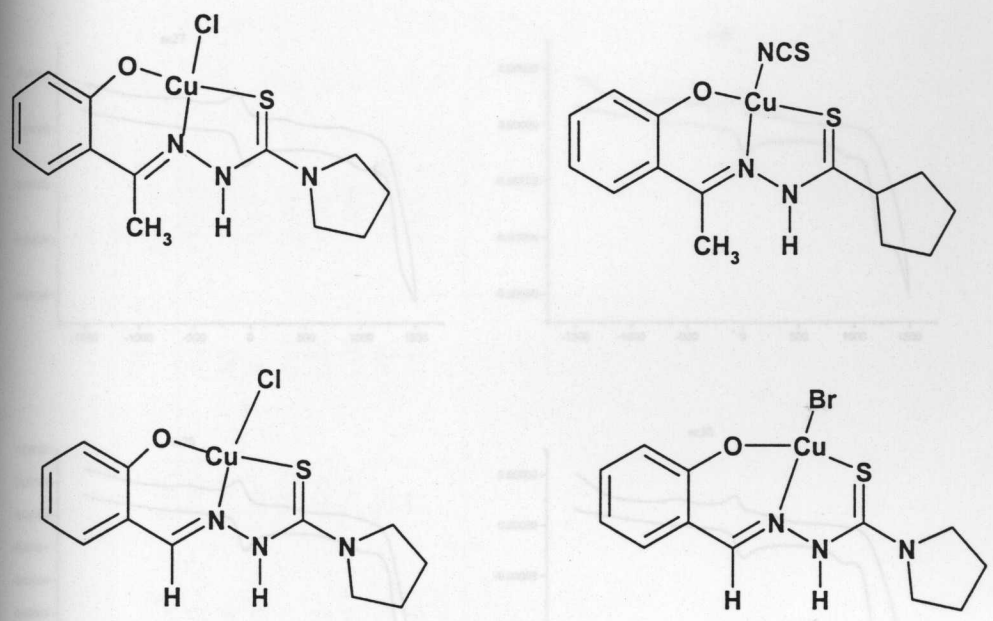

Fig.*4.4 Structures proposed for Cu complexes with O-N-S donor ligands*

4.5 Cyclic voltammetric studies

The results of our cyclic voltammetric studies of Cu(II) complexes **13**, **14**, **15**, **16**, **21**, **22**, **23**, and **24** are reported in Table 4.6. The profiles of representative complexes are given in Fig. 4.5. Details of cyclic voltammetric experiments were reported in Chapter 3.

All complexes gave almost similar cyclic voltammograms. Repeated scans at various rates (100, 200, and 300 mVs^{-1}) showed that the complexes do not dissociate. The anodic peak and cathodic peak current values were found to be independent of scan rates. The entire complexes exhibit quasi-reversible one electron transfer behaviour as indicated by the non equivalent current intensity at the cathodic and anodic peaks at 200 mVs^{-1} as shown in the Table 4.6. The compounds **16** and **24** show almost reversible one electron transfer.

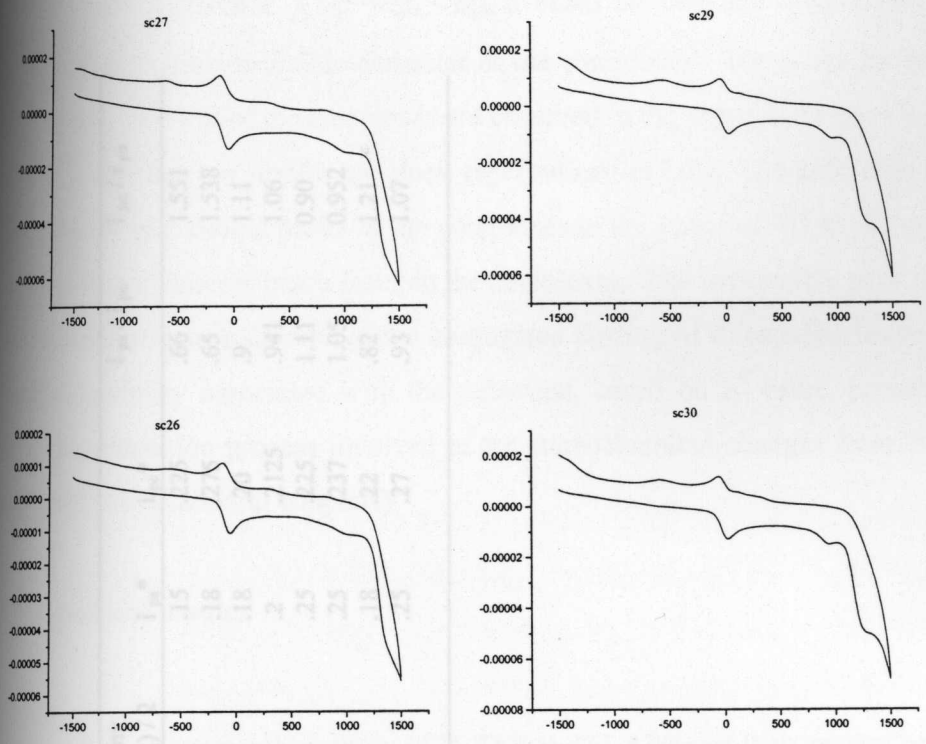

Fig. 4.5 Cyclic voltammograms of Cu(II)complexes with O-N-S donor ligands (x-axis- mill volt, y axis-ampere)

The voltammograms between 0 and - 1.5 V, show peaks in the range -0.33 V, 0.9 mV correspond to successive copper(II) reduction process. The peak at - 0.33 mV corresponds to Cu $^{11/1}$ redox couple and that at -0.9 mV to Cu $^{1/0}$ redox couple. In the positive scan, ranging from +1.5 to 0.0V, the oxidation process Cu(III) / Cu(II) and scanning in the negative range between 0.0 V and -1.5 V, copper reduction centered process Cu(II) /Cu(I) and ligand reduction are observed. The voltammograms of the complexes exhibited an anodic peak in the range - 314 to - 339 mV corresponding to one electron redox couple at platinum electrode. The counter peak is also observed in the range - 231 to - 265 mV. The peak-to-peak separation is found in the range-63 to -89 mV and Ipa/Ipc is the range 0.66 to 1.11, implying quasireversible electrochemical behaviour or heterogeneous electron

Table.4.6
Cyclic voltammetric data of Cu(II) complexes withO-N-S donor ligands

Compound	E_{pa} mV	E_{pc} mV	E_p . mV (E_{pa} -E_{pc})	E^0. mv (E_{pa}+E_{pc}) / 2	i_{pa}*	i_{pc}*	i_{pa} / i_{pc}	i_{pc} / i_{pa}
13	-339	-250	-89	-294	.15	.225	.66	1.551
14	-318	-231	-87	-274	.18	.275	.65	1.538
15	-314	-236	-78	-275	.18	.20	.9	1.11
16	-328	-265	-63	-296	.2	.2125	.941	1.06
21	-312	-247	-65	-279	.25	.225	1.11	0.90
22	-310	-238	-72	-274	.25	.237	1.05	0.952
23	-321	-258	-63	-289	.18	.22	.82	1.21
24	-331	-247	-84	-289	.25	.27	.93	1.07

The reported data corresponds to a scan rate of 200 mV/ s

transfer. The difference $\Delta Ep = Ep_a - Ep_c$ exceeds the Nerstian requirement of 59/n which support quasireversible character of the complexes. The peaks for the Cu^{III} / Cu^{II} couple for most of the complexes are observed in the potential range + 0.410 to + 0. 460 mV, which are similar to values, reported earlier [20]. The difference between the cathodic and anodic peaks of the complexes in the range as -63 to -89 mV infers that electron transfer is much faster in the complexes. The irreversible peak at + 1150 mV corresponds to reduction of the conjugated portion of thiosemicarbazones. The quasireversibility associated with the reduction, based on E^0 value, probably arise from the relaxation process involved in the stereochemical changes from the planar copper(II) to tetrahedral copper(I).

4.6 Biological studies

The *in vitro* antimicrobial activity of H_2SAP and H_2APP and their copper complexes was evaluated against two-Gram positive and nine Gram negative clinical pathogens. The disc diffusion method (Fig 4.7) was used to screen their anti microbial activity, and their MIC was determined by agar diffusion method. Details of these methods and experimental techniques are discussed in Chapter 3. The results of antimicrobial activity by disc diffusion method are tabulated in Table 4.7 and the minimum inhibitory concentrations (MIC) of compounds by agar diffusion method are tabulated in Table 4.8.

It is established that activity increases with increasing concentration of both free and complexed thiosemicarbazones, but we observed that concentration has only very little significance on the antibacterial activity. In general, when tested against Gram-positive bacteria, complexes were found to possess a higher activity than that of the ligand itself but against Gram negative bacteria, complexes were found to possess a little bit lower activity than ligand itself.

E.Coli *Staphylococcus aureus*

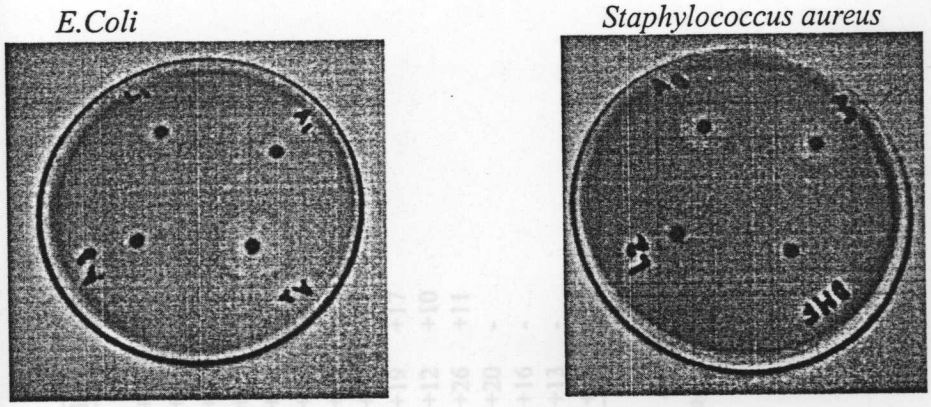

Fig 4.4 Antimicrobial activity (zone of inhibition) of copper complexes

All complexes found to be almost inactive against *E.Coli, Pseudomonas sp, Klebsiella sp, Proteus sp, Salmonella typhi, and Salmonella Para typhi.* A possible mechanism for the poor activity of the compounds studied may be their inability to chelate metals essential for the metabolism of microorganisms and or to form hydrogen bonds with the active centers of cell structures, resulting in an interference with the normal cell cycle. It is reported [21] that the activity of the ligands is affected by the nature of the substituent on the hydrazide group; this is in relation to the lipophilicity of the ligands and their membrane permeability, a key factor in determining the entry inside the cell. Since the present ligands have the similar, substituent at the hydrazide group, no difference in activity is observed. Though copper(II) complexes are better antimicrobial agents the ligands are found to have very high activity against *Vibriocholera O.1* and their activity against this species is almost comparable or even higher to copper(II) complexes and commercially available antimicrobial agents. The compounds **13, 14, 17, 18, 19** to **25** show moderate activity against *Staphylococcus aureus and Bacillus sp* The compounds **21** to **25** show very little activity against *Escherichia coli, Pseudomonas sp, Klebsiella sp, Salmonella typhi, and Salmonella para typhi.* It is also noticed that the ligand H_2SAP has higher antibacterial activity than uncomplexed H_2APP. Chloro complexes of O-N-S donors were found to be more active than corresponding bromo analogues. For bromo analogues, the increase in activity occurs with decreasing '*g*' suggesting

Table4.7
Antimicrobiall studies of O-N-S donors and their Cu(II) complexes with O-N-S donors

Code	Con/Disc.µg	1*	2*	3*	4*	5*	6*	7*	8*	9*	10*	11*
H_2SAP	.5	-	-	-	-	-	-	-	-	-7	+28	-
H_2APP	.5	+8	-	+9	-	-	-	-	-	-7	+27	-6
13	.5	+10	+9	-	-	-	-	-	-	-8	+20	-
14	.5	+9	+9	-	-	-	-	-	-	-8	+18	-
15	.5	-6	-	-	-	-	-	-	-	-7	+16	-
16	.5	-7	+13	-	-	-	-	-	-	+11	+20	-
17	.5	+16	+11	-	-	-	-	-	-	+10	+20	+12
18	.5	+14	+11	-	-	-	-	-	-	-	+16	-
19	.5	+11	+10	-	-	-	-	-	-	-6	+19	+17
20	.5	+10	+13	-	-	-	-	-	-	-8	+12	+10
21	.5	+12	-	-	+9	-	+9	-	-	-7	+26	+11
22	.5	+11	+10	-	-	+10	-	-	-	-8	+20	-
23	.5	+9	+14	-	-	-	-	+7	+9	-	+16	-
24	.5	+10	+11	-	-	+7	+6	-	-	-8	+13	-
25	.5	+9	+11	+8	-	+8	-	-	+10	-6	+13	+10

1* *Staphylococcus aureus*, 2* *Bacillus sp* **(gram positive)**3*. *Escherichia coli*, 4* *Pseudomonas sp*, 5* *Klebsiella sp*. 6* *Proteus sp.*
7* *Salmonella typhi*, 8* *Salmonella Para typhi*,.9* *Shigella sp*, 10* *Vibrio cholerae*.O1.11* *Vibrio parahahaemolyticus*. **(gram negative)**

Table 4.8
MIC Study of O-N-S donors and their Cu(II) complexes.

Code	1*	2*	3*	4*	5*	6*	7*	8*	9*	10*	11*
H_2SAP	-	-	-	-	-	-	-	-	-	5	-
H_2APP	-	-	-	-	-	-	-	4	-	5	-
13	4	4	-	-	-	-	-	-	-	-	-
14	3	4	-	-	-	-	-	-	-	1	-
15	4	4	-	-	-	-	-	-	-	1	-
16	-	1	-	-	-	-	-	-	-	-	-
17	1	1	-	-	-	-	-	-	-	1	1
18	1	1	-	-	-	-	-	-	-	1	-
19	1	1	-	-	-	-	-	-	5	1	1
20	3	3	-	-	-	-	-	-	-	1	3
21	1	1	-	-	-	-	-	-	-	-	-
22	-	4	-	-	-	5	-	-	-	1	-
23	4	4	-	5	-	-	-	-	-	-	-
24	4	5	-	-	-	-	-	-	-	1	3
25	1	1	-	-	-	-	-	-	4	1	1

1* *Staphylococcus aureus*, 2* *Bacillus sp* **(Gram positive)**
3*. *Escherichia coli*, 4* *Pseudomonas sp*, 5* *Klebsiella sp*. 6* *Proteus sp.*
7* *Salmonella typhi*, 8* *Salmonella Para typhi*,.9* *Shigella sp*, 10* *Vibrio cholerae.O1.*
11* *Vibrio parahahaemolyticus*. **(Gram negative)**

that the covalency of the metal ligand bonding is an important factor in biological activity. The extent of inhibitory activities of a given Cu(II) complex against *Vibrio cholera O.1* appears to be related to their '*g*' values. Among the copper(II) complexes, the perchlorate complex of H_2APP is shown greatest activity against *Vibrio cholera O.1* but its activity against *Vibrio parahahaemolyticus* is far less. However, the thiocyanato complex is found to be most active against *Vibrio parahaemolyticus*. For Gram-positive bacteria, the azide and thiocyanate complexes are found to be most efficient.

The MIC of copper(II) complexes is found to be far less than uncomplexed thiosemicarbazones for *Vibrio cholera O.1*, indicating that complexes are very effective in destroying such microorganism even at very low concentration. We also noticed that the MIC of these complexes was less than commercially available antimicrobial agents. The hydrophobic nature of our complexes makes them to stand second to commercially available antimicrobial agents. From the data available, it is found that Cu(II) complexes of the Schiff base containing N-N-S donor ligands are more bacteriostatic than those containing the O-N-S donors.

4.7 Concluding remarks

According to the procedure reported elsewhere, we prepared two O-N-S donor ligands and synthesized thirteen Cu(II) complexes with square planar geometry. They were characterized by usual analytical methods. The ligands were coordinated as monoanionic tridentate manner. Sulphur was coordinated in unusual thione form. The structures of the complexes were determined by various spectroscopic techniques. The spin Hamiltonian and bonding parameters were determined from the simulated EPR spectra of complexes. The electron transfer behaviors of complexes were determined by cyclic voltammetric experiments and observed a quasireversible one electron transfer. Even after repeated scanning at different scan rates gave unassumed results on ligand reduction. The biological

activity of the complexes and ligands were screened against Gram positive and Gram negative bacteria. Thiocyanato, nitrato and perchlorato complexes were found to have considerable antimicrobial activity. The Cu(II) complexes of N-N-S donors exhibited more antimicrobial activity than Cu(II)complexes of O-N-S donors and latter showed activity comparable to former only at very high concentrations.

Reference:

1 E.Ochai, and Bacon, *Bioinorganic Chemistry, An Introduction,* Boston, **1977**, **1**, 456.

2. K. D. Karlin, and J. Zubeta, *Copper Coordination Chemistry:Biological and Inorganic Perspectives* , Adenine Press, NY, 1983, **1**, 231.

3 B. S. Grag, M. R. P. Kurup, S. K.Jain and Y .K. Bhoon, *Transition Met.Chem*, 1988, **13**, 309;

4 M. A. Ali, D. A. Chowdhary and M. Nazimuddin, *Polyhedron*,1984, **3**, 595.

5 D. X. West, D. A. Bin, R. J. Butcher, J. P.Jasinski, R. Y. Pozdiniakiv, R. A Toscano and S. H. Ortega, *Polyhedron*, .1996, **15, 665**.

6 C. B. Castellani, G. Gatti and R. Millini, *Inorg. Chem*, 1983,**23**, 4004.

7 E. W.Ainscough, A. M.Brodie, J. D.Ranford and J. M.Waters, *J.Chem.Soc., Dalton Trans*., 1991,**6**, 1737.

8 B. N. Figgis and R. S. Nyholm, *J. Chem. Soc*., 1958, **4**, 190.

9 P. Bindu and M. R. P. Kurup,*Transition Met.Chem*.,1997, **22,** 578.

10 D. X.West, R. J. Butcher, J. P. Jasinsky and A.E.Liberta, *Polyhedron*,1993, **12,** 2489.

11 E.W.Aincough, A. M. Grodie and N. G.Larsen , *Inorg.Chim.Acta*,1982,**60,** 25.

12 The author acknowledges with thanks Prof. M. V. Rajasekharan, for providing the EPR simulation programme.

13 A. M. Bond and R. L.Martin, *Coord.Chem, Rev*., 1984, 54, 23.

14 D. X. West, A. E. Liberta, S. B. Padhye, R. C. Chikate,, P. B. Sonawane, A. S. Kumbhar and R. S. Yeranda, *Coor, Chem. Rev*, 1993,**123**, 49 and reference therein.

15 B. J Hathaway, G. Wilkinson, R. D. Gillard and J. A. McCleverty (Eds) *Comprehensive Coordination Chemistry*, Pergamon, Oxford, 1987, Vol. 5.

16 H. B. Gray, *Transition Met. Chem.*, 1965, **1**,239.

17 A. H. Maki and B. R. McGarvey, *J.Chem.Phys*, 1958, **29,** 35.

18 U. Sakaguchi and A. W. Addison, *J.Chem.Soc, Dalton Trans.*, 1979, **32**, 600.

19 S. Dutta, P. Basu, A. Chakravorthy, *Inorg. Chem*, 1991, **30**, 4031.

20 J. Ishwara Bhat and P. Bindu, *J. Electrochem. Soc. India* 1993, **42**, 103.

21 C. H. Collins, P. M. Lyne, *Microbial Methods*, University park press, Baltimore, 1970,**1**, 422.

Chapter

5

VANADYL AND VANADATE COMPLEXES WITH TRIDENTATE N_2S DONOR LIGANDS; SYNTHESIS, SPECTRAL, BIOLOGICAL AND ELECTROCHEMICAL PROPERTIES AND CRYSTAL STRUCTURE OF $[VO_2(L4M)]$

5.1 Introduction

5.1.1 History and occurrence of vanadium

In 1802, the mineralogist Andres Manuel del Rio (1764-1849) believed that he discovered a new metal similar to chromium and uranium in a brown lead mineral from Mexico. He first named it *panchromiu*m, because of the varied colours of its salts, but changed the name later on in *erythronium* ('red') as a reference to the red colour of its salts when treated with acids. However, soon he withdrew his discovery, since a French chemist incorrectly declared that this new element was only impure chromium. Vanadium was rediscovered in 1831 by the Swedish chemist Nils Gabriel Sefström (1787-1845) in remnants of iron ore quarried at the Taberg in Småland. He named the element *vanadi*n, after the goddess of beauty, youth and love, Vanadis, referring to the beautiful multi coloured compounds. Vanadis is a common name for Freyja according to the Northern Germanic tribes. After Sefström announced the discovery of vanadium, the brown lead ore from Mexico was reanalyzed and it was shown that it really contained vanadium instead of chromium [1]. Natural vanadium is a mixture of two isotopes, ^{51}V (99.76%) and ^{50}V (0.24%), the latter being slightly radioactive with a half-life of 3.9×10^{17} years [2]. Important sources of the metal are

the minerals *carnotite* [$K_2(UO_2)_2(VO_4)_2$] and *vanadinite* [$Pb(VO_4)_3Cl$]. It is also present in some crude oils in the form of organic complexes. Vanadium occurs with an abundance of 0.014% in the earth's crust and is widespread [3].

The element is the second most abundant transition metal in the oceans (50 nM). Some aquatic organisms are known to accumulate vanadium. For instance, members of an order Oftunicates *(Ascidiacea)* concentrate vanadium to 0.15 M in specialized blood cells [4]. However, the accumulation of vanadium is not restricted to marine organisms, since vanadium, containing haloperoxidases have also been isolated from terrestrial fungi and a vanadium compound of low molecular weight (amavadin) has been isolated from the toadstool *Amanita muscaria*. The actual function of vanadium and the nature of the vanadium compounds present in these organisms remains mystic [5]. In 1983, a naturally occurring vanadium-containing enzyme, vanadium bromoperoxidase (V-BrPO), was discovered in the marine brown alga, *Ascophyllum nodosum*. Since then, several vanadium haloperoxidases have been isolated and studied. Haloperoxidases .are enzymes that catalyse the oxidation of halides to the corresponding hypohalous acids [6]. Vanadium bromoperoxidase isolated from marine algae has been shown to catalyse the oxidation of pseudo halide thiocyanate by hydrogen peroxide [7]. Later vanadium has gained importance as an important element by catalyzing both oxidative (peroxidase) and reductive (nitrogenase) catalytic process of biological importance.

5.1.2 Oxidation states and biochemical importance of vanadium

Vanadium can exist in eight oxidation states ranging from –3 to +5, but with the exception of –2. Only the three highest, *i.e.* +3, +4 and +5, are important in biological systems. Under ordinary conditions, the +4 and +5 oxidation states are the most stable ones. The majority of vanadium(IV) compounds contain the VO^{2+} unit (vanadyl ion). The complexes typically have square planar pyramidal geometries with an axial oxo ligand [8].

The coordination chemistry of vanadium(V) compounds or vanadates is dominated by oxo complexes, containing the VO^{3+} or the VO_2^+ moiety. V^{4+} and V^{5+}

ions are very small with radii of 0.61 Å and 0.59 Å, respectively. These ions are even smaller than lithium (the radius of a Li^+ ion is 0.78 Å) [9].

Vanadium with atomic number 23, atomic weight 50.9415 has a wide variety of biochemical and physiological functions. Among them, an insulin –mimetic antidiabetic effect is the most striking, the effect being provided by the oxidation states of vanadic V(III), vanadyl V(1V) and vanadate V(V). Historically, sodium vanadate was used to treat human diabetes mellitus in 1899, before the discovery of insulin in 1921. A number of vanadium complexes have been shown to alleviate many of the symptoms of diabetes in both *in vitro* and *in vivo* (in rats and mice) studies. These complexes are being studied as potential alternatives to insulin therapy [10]. Recently a compound bis(picolinato) oxovanadium(1V) compound is proved to have insulin mimetic properties and the same is used in rats to cure insulin dependent *diabetes mellitus* [11]. Recently it is reported that vanadium compounds, which are best known as insulin mimetics, have also shown anticancer effects. These compounds are competitive inhibitors of protein tyrosine phosphates [12].

Vanadium has an important role in many biological processes; particularly it has been proposed that salivary of vanadium in higher organism is performed by transferrin. Transferrins are glycoprotein whose primary function is to bind and transport iron. The recognition of vanadium in several biomolecules in azobacter and seaweeds that use haloperoxidases to synthesize organic halides has led a spurt in the investigation of bioinorganic chemistry of vanadium [13]. The identities of vanadium biochromophores in haloperoxisdase enzymes have been under close scrutiny by various spectroscopic investigations. Many phosphorylase enzymes are known to contain histidine residues that coordinate to vanadium center [14]. Over the past few years a few works on the coordination chemistry oxovanadium species, using sulphur containing donors have been reported. The use of tridentate ligands in oxometalate chemistry has an intrinsic advantage because of their ability to form the MOL (metal-oxygen-ligand) primary core, leaving open at least one or more coordination site(s) for the acceptance of ancillary ligands to compete the coordination geometry. These

observations generated sufficient interest in recent years to understand the coordination chemistry of vanadium in biologically relevant ligand environments.

Owing to the d^1 configuration, EPR spectroscopy, easily identifies V(IV) ions. Typical eight-line patterns are observed due to hyperfine interaction of the ^{51}V nucleus (M_I = 7/2). Vanadate(V) is EPR silent due to its d^0 state and therefore diamagnetic, which makes it appropriate for NMR analyses, since the chemical shifts are very sensitive [15] to the nature of the coordination sphere of the ^{51}V metal

In an effort to modal these compounds an attempt was made to synthesize vanadyl(1V) and vanadate(V) complexes with N-N-S donors. In such attempts we used an amphidentate anion, thiocyanate, along with N-N-S donors, as ancillary ligand. The present Chapter describes the syntheses, spectral characterization, cyclic voltammetric, biological and X-ray diffraction studies of vanadyl and vanadate complexes with N-N-S donor ligands.

5.2 Experimental

5.2.1 Materials and method

The synthetic strategy and characterization of ligands HL4M and HL4P are described in Chapter 2. $VO(acac)_2$ (Merck), and potassium thiocyanate (Glaxo) were used as such. The solvents were purified by standard procedures before use.

5.2.2 Measurements

Details of various analytical measurements and characterization techniques such as partial elemental analyses, molar conductivities, magnetic moments, IR, NMR, EPR, cyclic voltammetry and X-ray diffraction studies are described at length in Chapter 2. Various antibacterial studies are elaborated in Chapter 3. The metal content was estimated by 'peaceful pyrolysis' technique by converting a known quantity of the compound in to its stable oxide as V_2O_5.

5.2.3 Syntheses of complexes

The syntheses of all vanadyl(1V) complexes were carried out under inert atmosphere of nitrogen. To a stirred solution of thiosemicarbazone (0.5 mmol) in dichloromethane (15 mL), under nitrogen atmosphere was added an equmolar amount of vanadyl(1V) acetylacetonate (0.5 mmol). When the solution turned in to a homogenous brown solution, was added (0.52 mmol) of potassium thiocyanate. The stirring was continued for 2 h. The vanadate(V) complexes were prepared at reflux conditions (2 h), in the absence of nitrogen atmosphere and potassium thiocyanate, by the same procedure. Finally the solution was cooled in a freezer at 0°C for overnight period. The crystalline compound that deposited at this stage was collected by filtration, washed with dichlomethane, ether and dried *in vacuo*. Crystal suitable for X-ray analysis was obtained by slow evaporation of a CH_3-OH/ CH_3CN solution of the complex [VO2(L4M)], by slow evaporation after keeping its solution for 6 days.

The vanadyl(IV) complexes that we synthesized are [VO(L4M)NCS], **26**; [VO(L4P)NCS], **27**; and vanadate(V) complexes are [VO_2(L4M)], **28**; and [[VO_2(L4P)],**29**.

5.3. Results and discussion

The colours, molar conductivities, magnetic moments, partial elemental analyses, stoichiometry of complexes are presented in Table 5.1. The vanadyl(1V) complexes with N-N-S donors are light green where as the vanadate(V) complexes are yellow in colour.. The N-N-S donors can coordinate metal ions as neutral ligands or as anionic species by the loss of proton at the ^{3}N. The results of partial elemental analysis indicated that the vanadium(IV) and (V) complexes of HL4M and HL4P present one anionic tridentate ligand per metal ion as supported by their behaviour as non electrolytes. The fifth coordination position in vanadyl(1V) complexes is occupied

by thiocyanate anion as confirmed by IR spectra of the complexes and their geometry is probably square pyramidal.

The complexes are soluble in dimethylformamide, in which conductivity measurements were made. The molar conductivity of *ca* 10^{-3} M solution of complexes in DMF ranges between 12-18 Ω^{-1} cm^{-1} $mol,^{-1}$ indicating non-electrolytic nature of them in solution. They are also soluble in dimethyl sulphoxide and acetonitrile.

5.3.1 Magnetic moments

Magnetic susceptibility measurements were carried out at room temperature using Gouy balance and calculations were made using computed values of Pascal constants for diamagnetic corrections. The magnetic moment of the complexes, **26** and **27** are found to be 1.71 and 1.76 BM. The room temperature magnetic moments of the present V(IV) complexes are consistent with the spin only values for mononuclear complexes having d^1 configuration and suggestive of poor orbital contribution [16]. The complexes **28** and **29** are diamagnetic as expected.

5.3.2 Vibrational spectra

The significant IR bands of vanadyl(1V) and vanadate(V) complexes with their tentative assignments in the 4000 to 400 cm^{-1} region are presented in the Tables 5.2.

On coordination of azomethine nitrogen ν(C=N) shifts to lower energy by 25 to 28 cm^{-1}. The band shifting from *ca* 1627 cm^{-1} in the uncomplexed thiosemicarbazones spectra to 1602 cm^{-1} in the spectra of the complexes and ν(N-N) shifts to higher frequency in all complexes, is a clear sign of coordination *via* the azomethine nitrogen atom. This is further supported by the appearance of a new band near 1591 cm^{-1} due to formation of a new ($^2N=^9C$). The spectral band ν(N-H) of the thiosemicarbazones disappears in the complexes indicating the deprotonation of the ^3NH protons and coordination *via* the thiolate sulphur is shown by a decrease in

Table 5.1
Analytical data, colours conductivity, magnetic moments and yield of complexes of vanadyl and vanadate complexes. [a)]

Compound	Emp.formula [b)]	Yield (%)	Colour	μ [c)](BM)	ΛM [d)]	%C	%H	%N	%V
OVL4MNCS,**26**	$C_{13}H_{15}N_5O_2S_2V$	62	Green	1.71	16	40.41 (40.20)	4.01 (3.89)	18.47 (18.03)	13.30 (13.12)
OVL4PNCS, **27**	$C_{13}H_{15}N_5OS_2V$	64	Green	1.76	14	41.74 (41.93)	4.09 (4.06)	18.77 (18.81)	13.57 (13.68)
O_2VL4M, **28**	$C_{12}H_{15}N_4O_3SV$	61	Yellow		11	41.70 (41.62)	4.20 (4.37)	16.24 (16.18)	14.59 (14.71)
O_2VL4P, 29	$C_{12}H_{15}N_4O_2SV$	68	Yellow		11	43.41 (43.64)	4.36 (4.58)	17.02 (16.96)	15.31 (15.42)

[a)] In parentheses calculated values. [b)] Emperical formula. [c)] Magnetic moment [d)] Molar conductivity,10^{-3}M solution(DMF) at 298K

Table 5.2
Selected IR bands (cm^{-1}) with tentative assignments of vanadyl and vanadate complexes with NNS donors

Compound	ν(C=N)	ν(N=C)	ν(N-N)	ν(C=S)	δ(C=S)	δ ip/ op	δ(V=O)	ν(N-N)
HL4M	1627s	-----	1010m	1371m	892m	649m,408m	-----	------
OVL4MNCS	1602s	1591s	1052m	1319m	842m	663m,441m	956s	452m.420s
O2VL4M	1609s	1589s	1049m	1316m	840m	668m,443m	954m	454m
HL4P	1598s	-----	998m	1315m	869m	624m,409m	-----	-----
OVL4PNCS	1548s	1593s	1054m	1261m	836m	653m,439m	959s	452m
O2VL4P	1546s	1602s	1056m	1279m	830m	656m,433m	950s	442m

S=strong; m=medium; w=weak; sh=shoulder

the frequency by 50 to 52 cm^{-1} of the thioamide band which is partially ν(C=S) and found at 1371 and 892 cm^{-1} for HL4M and at 1361 cm^{-1} and 886cm^{-1} for HL4P. A shift to lower wave numbers of these bands occurs on complexation.

Coordination *via* the pyridine nitrogen is indicated by the shifts to lower frequencies of ν(CN) + ν(CC) and shift to higher frequencies of the in plane and out of plane ring deformation bands. Thus the shift in pyridine ring, out of plane and in plane bending vibrations at *ca* 649 cm^{-1} and 408 cm^{-1} by 15 to 22 cm^{-1} to higher frequencies on complexation confirms the coordination of ligand to vanadium *via* pyridine nitrogen.

The strong band at *ca* 866 cm^{-1} is an evidence of for the presence of V=O bond which remained almost undisturbed, and is also characteristic of the coordination of oxygen in the fifth coordination position. The low frequency range observed in the complexes indicates that the V=O bond is weakened by the strong σ and π electron donation by the thiolate and pyridine groups to the antibonding orbital of the V=O group [17]. The ν(C =N), observed in the region of 2080 cm^{-1} for **26** and 2077 cm^{-1} for **27** suggests, bonding through N of the thiocyanate group.

The infrared spectrum of **28** using a KBr disk, reveals two V=O absorptions. The bands are found at 926 and 949 cm^{-1} and are assigned to symmetrical (O=V=O) and asymmetrical (O=V=O) stretching absorptions respectively. These observations correspond to the data known from the literature for stretching frequencies of V=O in similar compounds. IR spectrum of (**29**) shows only one signal, in addition to the N-N-S mode of coordination, at *ca* 929 cm^{-1} for the ν(V=O) stretching mode, which indicates that the two V=O groups are indistinguishable [18].

5.3.3 Electronic spectra

The significant electronic absorption bands in the spectra of the complexes recorded in polycrystalline state (Fig 5.1) and in dimethylformamide are presented in Table 5.3. The VO^{2+} complexes **26** and **27** show the characteristic series of absorption bands common to vanadyl systems. The five coordinate complexes expected to exhibit

three absorption bands but two of them are observed. According to Ballhausen and Gray modal [19] the weak absorption band occurring in the region 720-675 nm can be assigned to the electronic transition $^2B_2 \rightarrow {}^2E$ ($d_{xy} \rightarrow d_{xz}, d_{yz}$) where as those broad band found in the region 550 - 410 nm, can be due to closely lying bands and that correspond to two electronic transitions , $^2B_2 \rightarrow {}^2A_1$ ($d_{xy} \rightarrow d_{x^2}$) and $^2B_2 \rightarrow {}^2B_1$ ($d_{xy} \rightarrow d_{x^2-y^2}$)

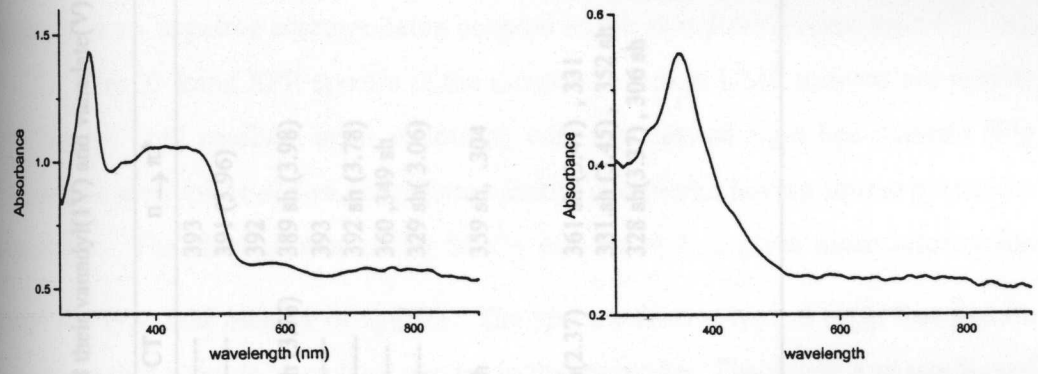

Fig 5.1 UV-Vis DRS of the representative compounds

These closely lying states are indicative of small tetragonal distortion to the vanadyl environment having C_{4v} symmetry. Intraligand and CT are also observed without considerable change in energy as in uncomplexed thiosemicarbazones.

Vanadium(V) is a d^0 species and therefore no d-d transitions are observed. LMCT bands may be expected due to the high oxidation state of the metal centre, but this is not the case for VO_2^+ species since the d orbital energy is raised due to a decrease in net positive charge at the vanadium. In fact, all complexes reported until now containing the VO_2^+ moiety are yellow. The results obtained by us are found to be in good agreement with the above reported observations. The VO_2^+ compounds **28** and **29** do not display intense LMCT bands and even visible CT bands. The

Table .5.3
Electronic spectral assignments (nm), log ε^a for the N-N-S donors and their vanadyl(1V) and vanadate(V) complexes

Compound	Mode	d-d	CT	$n \rightarrow \pi^*$	$\pi \rightarrow \pi^*$
HL4M	Solid	------	-----	393	255
	DMF	------	-----	391 (3.96)	255 (4.02)
OVL4MNCS	Solid	821. , 557	443.	392	255
	DMF	558 (2.49)	440 sh (3.76)	389 sh (3.98)	260 sh (4.57)
O2VL4M	Solid	------	-----	393	255
	DMF	------	------	392 sh (3.78)	256. sh (4.13)
HL4P	Solid		-----	360 ,349 sh	
	DMF	-----	-----	329 sh(3.06)	255
					259
OVL4PNCS	Solid	-------	440 sh	359 sh, .304	
					255
	DMF	823., 547			
			439sh(2.37)	361 sh (3.41) , 331	257 (4.23), 242 sh (4.52)
O2VL4P	Solid	726 (1.98), 550 (2.77)	-----	331.sh (3,45) , 352 sh	254, .245
	DMF		------	328 sh(3.37) , 306 sh	257 (4,34) , 254 sh (4,46)
		-----			

[a] = ε is expressed in (l mol-1 cm-1)

spectra recorded in dimethylformamide exhibit only one broad band at 296 nm and a small shoulder at 340 nm, which closely resembles the spectra of free ligands.

5.3.4 EPR spectra

The EPR parameters of vanadyl complexes obtained from the polycrystalline state at 298 K and in dimethylformamide at 298 K and 77 K are presented in Tables 5.4.

The EPR spectra of the complexes **26** and **27** in the solid state at 298 K (Fig 5.2) give rather broad isotropic signals (495 G) due to enhanced spin lattice relaxation [20]. The solution spectra in dimethylformamide at room temperature (Fig.5.3) showed typical eight line spectra characteristic of mononuclear oxovanadium(1V) containing an unpaired electron being coupled to the vanadium nuclear spin (^{51}V, M_I = 7/2). The X- band EPR spectra of the samples in frozen DMF solution are similar and display well resolved axial anisotropy with two sets of eight line patterns (Fig 5.4) which are typical of five coordinate vanadyl complexes having square pyramidal symmetry. The field corresponding to $A_{\|}$ and M_I = 7 /2 gives more information about the type and number of species. The spectra show a typical eight line pattern indicating that a single Vanadium species in the molecule. The absence of any ligand hyperfine lines in the $g_{\|}$ features due to nitrogen, indicates that the unpaired electron, for the most of the times staying with the d_{xy} ($^2B_2$) ground state. In the frozen solid state, the axial spectrum shows two types of resonance components. One set due to parallel feature and other set, due to the perpendicular feature which indicates axially symmetric anisotropy with well resolved sixteen hyperfine splitting characteristic of interaction between the electron spin and the vanadium nuclear spin. The X- band EPR together with the simulated spectrum is shown in the Fig 5.3.

The Spin Hamiltonian parameters obtained from the spectrum of **27** demonstrates a low symmetry geometric structure of the molecule. The pseudo axial (because the parameters g_x and g_y are very similar) distortion is in agreement with the electronic absorption spectrum. However, this little in-plane observable anisotropy,

$(g_{xx} - g_{yy})$ =0.001, and $(A_{xx} - A_{yy}) = 0.5\times10^{-4}$ cm,$^{-1}$ demonstrates that distortions in **27** is more than those observed in **26**.

It is reported [21] that the *g* and A values are sensitive to the vanadium coordination environment and may be used to distinguish between species with different coordination environment. In the present case, we observed no appreciable change in coordination environment because the *g* and A values of the two species are almost similar. The observed $A_{\|}$ $g_{\|}$ and $g_{\perp}$ values are well in accordance with that of molecules exist in square pyramidal geometry. The molecular orbital coefficients α^2 and β^2 were also calculated for the complexes by using the following equations [22].

$\alpha^2 = (2.0023 - g_{\|})\, E / 8\lambda\, \beta^2$

$\beta^2 = [\,7/6(-A_{\|}/P + A_{\perp}/P + g_{\|} - .5\ g_{\perp} / 12 - 9g_e/14],$

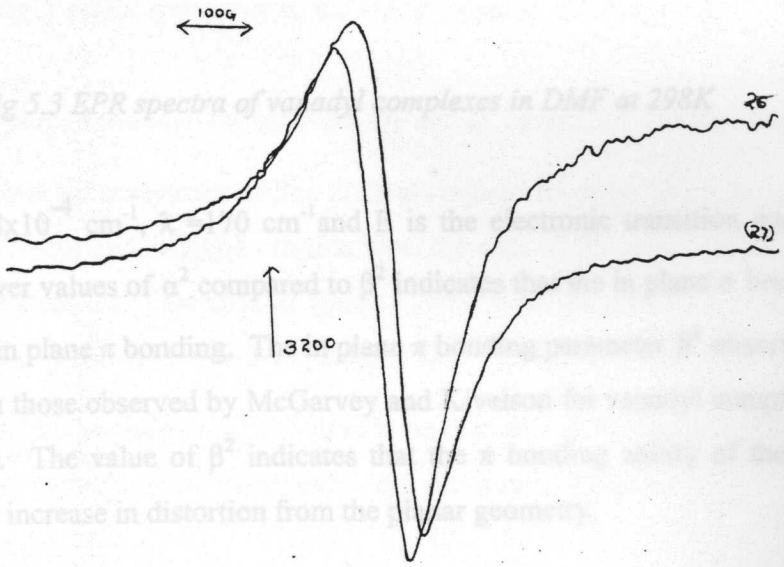

Fig 5.2 EPR spectra of vanadyl complexes in the polycrystalline state at 298K

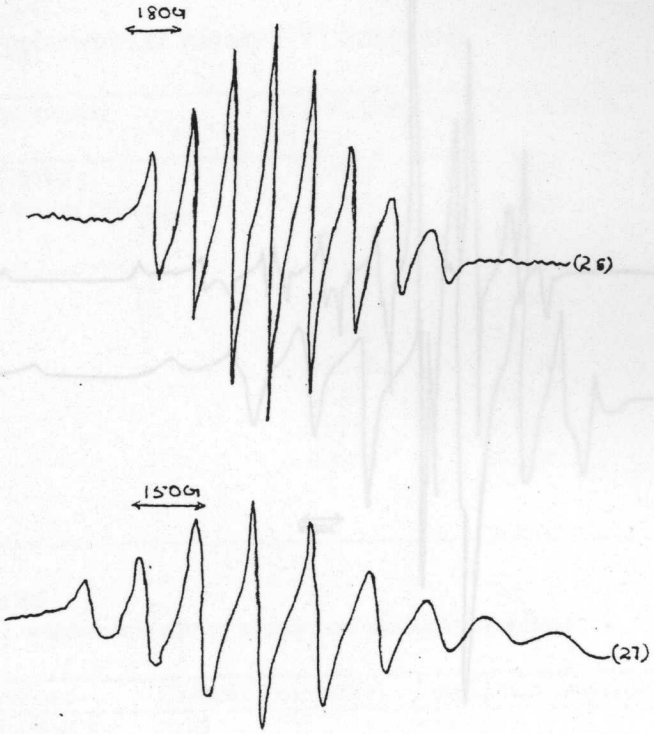

Fig 5.3 EPR spectra of vanadyl complexes in DMF at 298K

Where P =128x10^{-4} cm^{-1}, λ =170 cm^{-1}and E is the electronic transition energy of $^2B_2 \rightarrow {}^2E_2$ Lower values of α^2 compared to β^2 indicates that the in plane σ bonding is more than the in plane π bonding. The in plane π bonding parameter β^2 observed, are consistent with those observed by McGarvey and Kivelson for vanadyl complexes of acetyl acetone. The value of β^2 indicates that the π bonding ability of the ligand decreases with increase in distortion from the planar geometry.

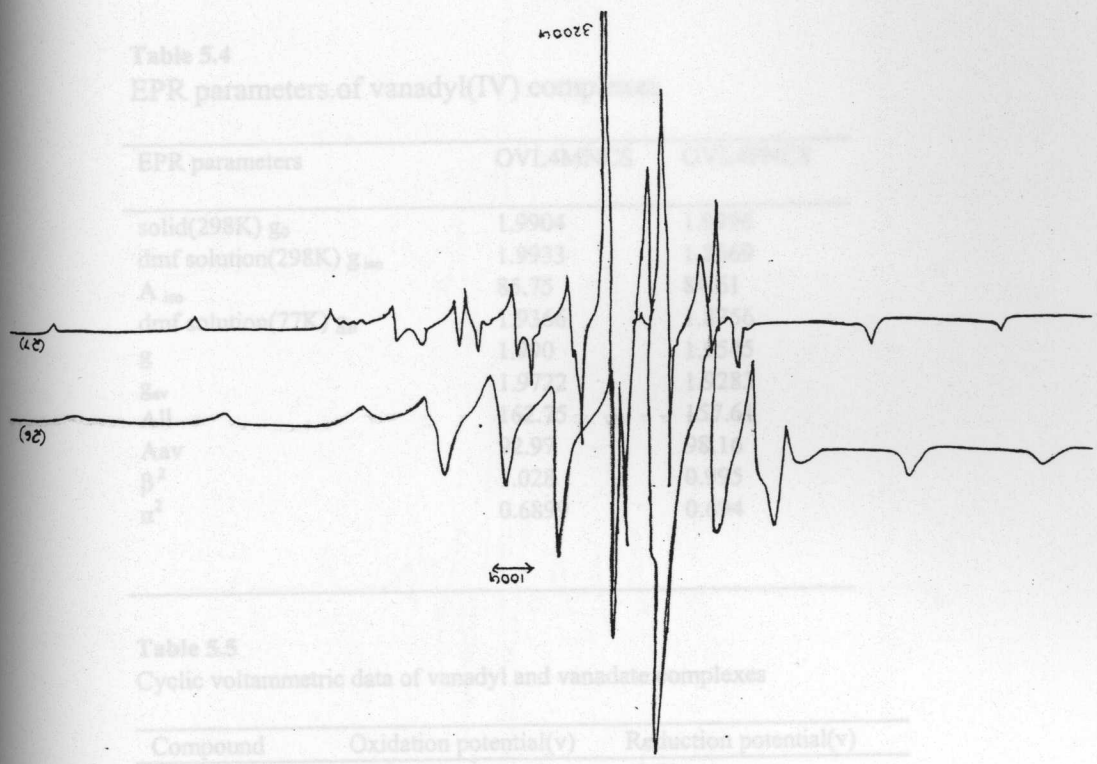

Fig 5.4 EPR spectra of vanadyl complexes in DMF at 77 K

Holyk plotted the relation between $A_{\parallel}$ and $g_{\parallel}$ values for vanadyl complexes and defined zones for complexes having different equatorial donor atom sites, such as VO (N_4), $VO(N_2O_2)$ and $VO(O_4)$. In this plot, the data of the new complexes shift from the main domains. This kind of shifting relative to the reference data implies that the physical mechanism which determines the $A_{\parallel}$ values in the new complexes is not the same as in references.[23] Based on our studies we proposed distorted square pyramidal structures for the vanadyl and vanadate complexes.

Table 5.4
EPR parameters.of vanadyl(IV) complexes

EPR parameters	OVL4MNCS	OVL4PNCS
solid(298K) g_0	1.9904	1.9996
dmf solution(298K) g_{iso}	1.9933	1.8669
A_{iso}	85.75	84.61
dmf solution(77K) g_{II}	1.9366	1.8756
g	1.990	1.9545
g_{av}	1.9722	1.9283
All	162.75	157.61
Aav	92.97	98.16
β^2	1.028	0.995
α^2	0.6899	0.694

Table 5.5
Cyclic voltammetric data of vanadyl and vanadate complexes

Compound	Oxidation potential(v)	Reduction potential(v)
OVL4MNCS	-0.43	-0.72
OVL4PNCS	-0.44	-0.72
O_2VL4M	-1.45	
O_2VL4P	-1.45	

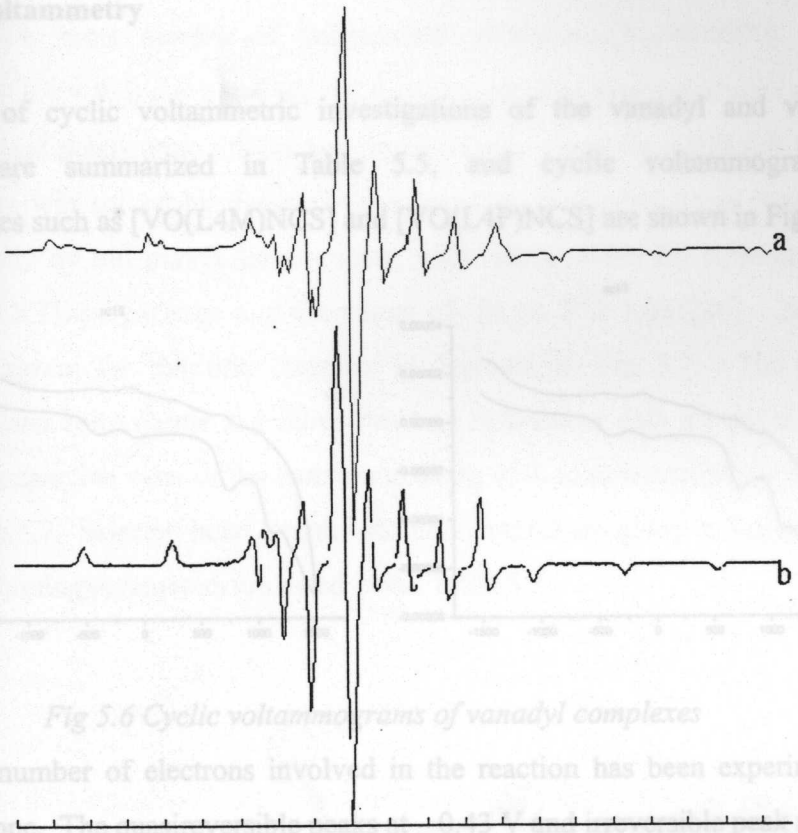

Fig 5.5 Experimental(a) and Simulated(b) EPR spectrum of the compound 26

5.4 Biological activity

All vanadyl(IV) and vanadate(V) complexes were screened against both Gram positive and Gram negative bacteria by disc diffusion method. Repeated the scanning for five times and found all of them were equally ineffective against all microorganisms.

5.5 Cyclic voltammetry

The results of cyclic voltammetric investigations of the vanadyl and vanadate complexes are summarized in Table 5.5, and cyclic voltammograms of representatives such as [VO(L4M)NCS] and [VO(L4P)NCS] are shown in Fig 5.6

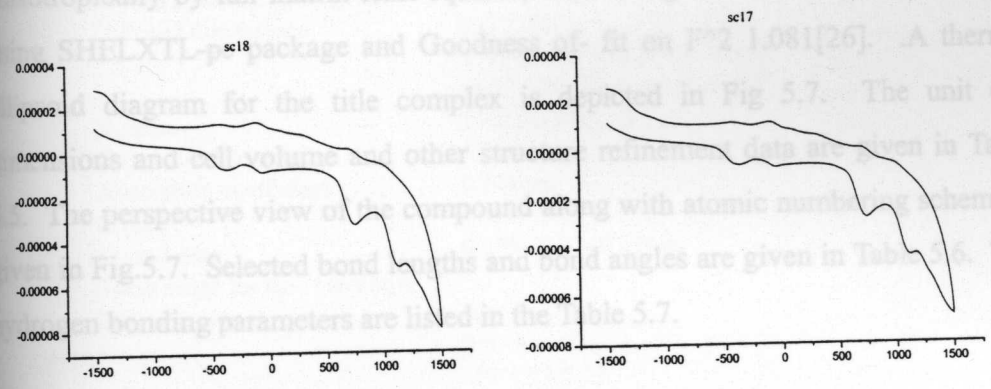

Fig 5.6 Cyclic voltammograms of vanadyl complexes

The number of electrons involved in the reaction has been experimentally found to be one. The quasireversible peaks at – 0.43 V and irreversible peak at – 0.72 mV are due to the successive $V^{(IV\ /\ III)}$ and $V^{(III\ /\ II)}$ redox couples [24]. The quasireversible peaks at + 0.75 mV and 1.02 V correspond to reduction of conjugated portion of coordinated thiosemicarbazones. The irreversible peak at + 0.98 mV in the reverse scan is assigned to $V^{(IV/\ V)}$ oxidation. The small variation in the peak potentials is due to the different substituent in the thiosemicarbazone moiety. The cyclic voltammograms of the vanadate complexes display irreversible peaks at – 1.45mV, indicating the degradation of the formal vanadium species [25].

5.6 X-ray diffraction studies of [VO_2L4M]

An yellow prismatic crystal of 0.275×0.225×0.25mm was chosen for diffraction study. Intensity data were collected on a diffractometer using Graphite monochromatic Mo-K_α radiation (λ=0.7093A°). A total of 2215 reflections were

collected with same number of independent reflections.(R_{int}=0.0000) covering indices 0 < = h < = 9; 0 < = k < = 16; -14 < = 1< = 14. The intensities were corrected for Lorentz and polarization effects and for absorption using the ABSCOR program. The structure was solved by direct method. All non- hydrogen atoms were refined anisotropically by full matrix least squares, with riding model for hydrogen atoms, using SHELXTL-pc package and Goodness of- fit on F^2 1.081[26]. .A thermal ellipsoid diagram for the title complex is depicted in Fig 5.7. The unit cell dimensions and cell volume and other structure refinement data are given in Table 5.5. The perspective view of the compound along with atomic numbering scheme is given in Fig.5.7. Selected bond lengths and bond angles are given in Table 5.6. The hydrogen bonding parameters are listed in the Table 5.7.

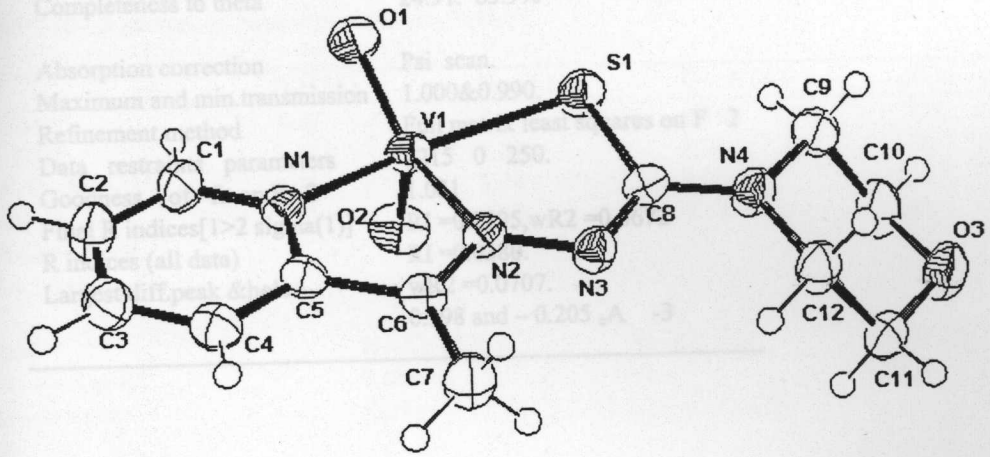

Fig 5.7 ORTEP diagram for compound VO_2L4M Displacement ellipsoids are drawn at the 55% probability level and hydrogen atoms are shown as small spheres of arbitrary radii.

Table 5.6.

Data collection and processing parameters.

Empirical formula	$C_{12}H_{15}N_4O_3SV$
Formula weight	346.28
Temperature	293(2) K
Wave length	$0.7093A^0$
Crystal systems, space group	P 21 n, Monoclinic.
Unit cell dimensions	a=8.3780(6) A; α=90.00(4) ^{0}
	b=13.9600(7) A; β=92.062(5)^0
	c= 12.3280(6) A; γ =90.00(5)^0
Volume	1440.91(14)A 3
Z,Clculated density	4.1.596 Mg m 3
Absorption coefficient	0.848mm 1-
F(000)	712
Crystal size	0.275× 0.25×0.25mm
Theta range for data collection	
Index ranges	0 < = h < 9
	0 < =k < 16
	-14 < = l < 14.
Reflection collected / unique	2215 2215 [R(int)=0.0000]
Completeness to theta	24.91. 83.9%
Absorption correction	Psi scan.
Maximum and min.transmission	1.000&0.990.
Refinement method	Full matrix least squares on F 2
Data restraints parameters	2215 0 250.
Goodness – of –fit on F 2	1.081
Final R indices[1>2 sigma(1)]	RI =0.0295,wR2 =0.0672
R indices (all data)	RI =0.0380.
Largest diff.peak &hole	wR2 =0.0707.
	0.198 and – 0.205 $_e$A -3

Table 5.7

Selected bond lengths (A^0) and angles for the compound [VO_2L4M]

V(1)-O(2)	1.6073(18)	N(1)-V(1)-N(2)	74.26(8)
V(1)-O(1)	1.6228(18) 2.091(2)	O(2)-V(1)-S(1)	103.55(8)
V(1)-N(1)	2.145(2) 2.3676(8)	O(1)-V(1)-S(1)	96.54(7)
V(1)-N(2)	1.752(2)	N(1)-V(1)-S(1)	147.59(6)
V(1)-S(1)	1.305(3)	N(2)-V(1)-S(1)	77.28(6)
S(1)-C(8)	1.375(3)	C(8)-S(1)-V(1)	98.98(9)
N(2)-C(6)	1.325(3)	C(6)-N(2)-N(3)	116.17(19)
N(2)-N(3)		C(6)-N(2)-V(1)	118.31(16)
N(3)-C(8)	109.91(10)	N(3)-N(2)-V(1)	124.44(14)
	100.91(9)	N(1)-C(5)-C(4)	120.7(2)
O(2)-V(1)-O(1)	94.76(9)	N(1)-C(5)-C(6)	114.2(2)
O(2)-V(1)-N(1)	111.07(9)	C(4)-C(5)-C(6)	125.0(2)
O(1)-V(1)-N(1)	138.86(9)	N(2)-C(6)-C(5)	113.9(2)
O(2)-V(1)-N(2)		N(3)-C(8)-N(4)	117.7(2)
O(1)-V(1)-N(2)		N(3)-C(8)-S(1)	123.72(19)

H-bonding and C-H---π interaction parameters of $C_{12}H_{15}N_4O_3SV$

D-H---A	D-H (Å)	H---A (Å)	D---A (Å)	∠D-H—A (Å)
C(4)—H(4).. O(2)^{i}	0.88	2.55	3.38	156
C(7)—H(7).. O(2)^{i}	0.95	2.44	3.38	173
Intra C(9)-- H(9).. S(1)	0.94	2.50	3.03	116
Intra C(12)--H(12).. N(3)	1.02	2.32	2.74	103
Equivalent Position Code				
I =1/2+x,1/2-y,1/2+z				

X-H(I)----Cg(J)	H—Cg (Å)	X—Cg (Å)	∠X-H--Cg (°)
C(12)-H(12A)----- Cg(4)^{ii}	3.28	3.84	119.54
Equivalent position code	Cg(4)= N(1), C(1), C(2), C(3), C(4), C(5)		
ii =1-x,-y,1-z			
D= donor, A= acceptor, Cg= Centroid			

5.6.1 Description of the crystal structure

The ligand HL4M is a potentially interesting oxidation catalyst as it is a bioactive compound and hence it is seemed most suitable for the synthesis of a dioxovanadium(V) complex,

The compound $[VO_2L4M]$ is crystallized in the monoclinic space group $P2_1/n$. The unit cell is comprised of eight molecules. The vanadium atom in each molecule is five coordinate, existing in a distorted square pyramidal (SP) geometry in which the basel plane is defined by N1, N2, S1 atoms, derived from the tridentate ligand and one of the oxygen atoms of the dioxo vanadium moiety.

The compound indeed contains dioxovanadium(V) moiety and the two-oxo groups are *cis* to each other [27]. The bond angle between the oxo groups and the vanadium centre O1-V1-O2 is 109.02^0. The V=O distances are nearly equal, $1.623A^0$ and $1.607A^0$, which is typical of a dioxovanadium complex in which one of the oxygen atoms are involved in hydrogen bonding Fig 5.8.

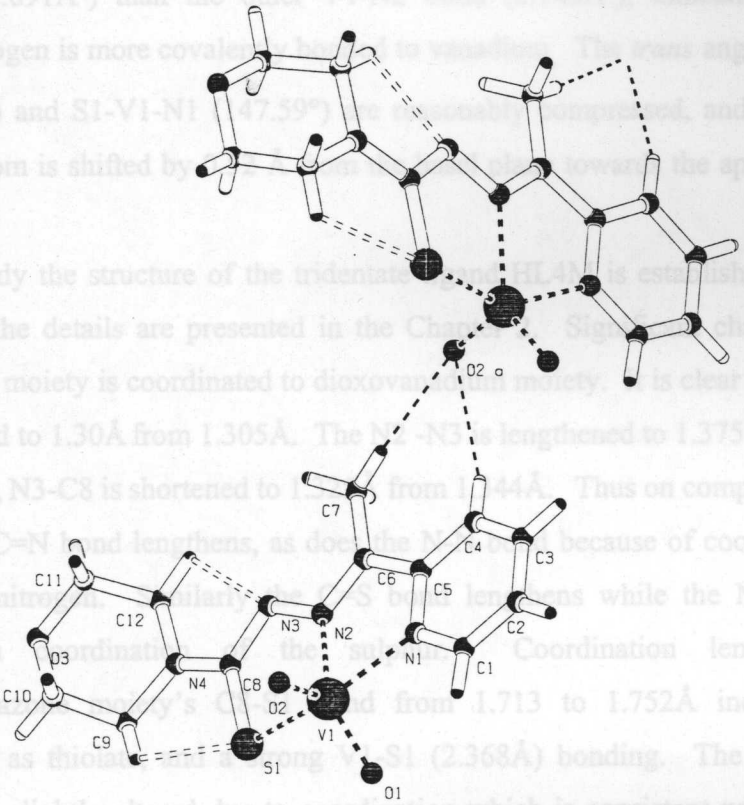

Fig. 5.8. PLATON diagram of compound VO_2L4M showing intermolecular and intra molecular H-bonding interactions.

A trigonal bypyramidal (TBP) structure can also be suggested but the bond angles O1-V1-O2 (109.8°) and O2-V1-N2 (111.07°) suggest considerable distortion from TBP. The vanadium centre is penta coordinated by two nitrogen atoms V1-N1(2.091Å) and V2-N2(2.145Å) with a bond angle of N1- V1- N2 > 74.26° and, one sulphur atom of the deprotonated thiol tautomer with bond angles N1-V1-S1 $=147.59^0$ and N2-V1-S1 =77.29°. Thus the basel positions being occupied by the donors S1, N2, and N1 from the coordinated tri dentate ligand and one of the terminal oxo groups, O2. .The axial site is taken by the remaining oxo atom O1 of the VO_2^+

core. Of the two V1-N bonds generated by the coordinated HL4M, the V1-N1 bond, is shorter ($2.091A^0$) than the other V1-N2 bond ($2.145A^0$), indicating that the pyridine nitrogen is more covalently bonded to vanadium. The *trans* angles, O1-V1-N2 (138.88°) and S1-V1-N1 (147.59°) are reasonably compressed, and the central vanadium atom is shifted by 0.52 Å from the basel plane towards the apical oxygen atom

Already the structure of the tridentate ligand HL4M is established by XRD studies and the details are presented in the Chapter 2. Significant changes occur when HL4M moiety is coordinated to dioxovanadium moiety. It is clear that C6-N2, is compressed to 1.30Å from 1.305Å. The N2 -N3 is lengthened to 1.375 Å from1.30 Å. Similarly, N3-C8 is shortened to 1.325Å from 1.344Å. Thus on complexation the azomethine C=N bond lengthens, as does the N-N bond because of coordination of azomethine nitrogen. Similarly the C=S bond lengthens while the N3-C8 bond shortens on coordination of the sulphur. Coordination lengthens the thiosemicarbazone moiety's C8-S1 bond from 1.713 to 1.752Å indicating the coordination as thiolate, and a strong V1-S1 (2.368Å) bonding. The azomethine bond is only slightly altered due to coordination which is consistent with the bond length C8-N3 and it retained almost a double bond character [27]. It is an indication of weak bonding between V1-N2 as indicated by the bond length.

The bond distance differences in the uncoordinated and coordinated pyridyl ring are within the error limits of the two measurements. On complexation HL4M is altered from a Z isomer to E' isomer because N-C-S bond angle of dioxovanadium complex is smaller than found for HL4M. The packing of the complex (Fig.5.9) is stabilized by the intermolecular H-bonding interactions and C-H----π interactions between the atoms.

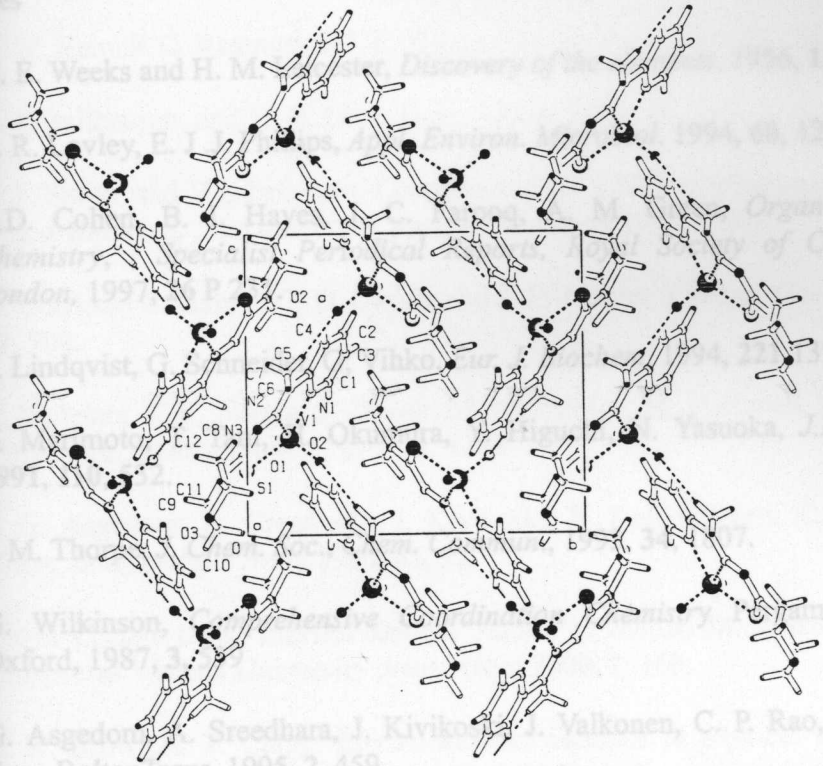

Fig 5.9. Packing diagram compound VO_2L4M view along b axis

5.7 Concluding Remarks.

The work showed that vanadium was prone to give oxovanadium N-N-S complexes under inert atmosphere and dioxovanadium N-N-S complex under normal reflux conditions. Oxo complexes were green, dioxo complexes were yellow, and both classes were nonelectrolytes. Magnetic moments of oxovanadium complexes were very near to spin only values and electronic spectra of dioxovanadium complexes were very similar to ligand spectra. Vanadyl complexes were EPR active due to d^1 configuration and dioxocompounds were NMR active due to d^0 configuration. Both vanadyl and vanadate complexes had no antibacterial activity at the studied concentrations. Electrochemical profiles of complexes showed ligand and metal based redox potentials. The single crystal X-ray diffraction studies of the vanadate(V) complex showed a distorted SP geometry.

References

1 M. E. Weeks and H. M. Leicester, *Discovery of the elements*, 1956, **1**,410.

2 D. R. Lovley, E. J .J. Phillips, *Appl. Environ. Microbiol.* 1994, **60**, 124.

3 K.D. Cohen, B. I. Hayes, J. C. Farooq, A. M. Green, *Organometallic Chemistry*, , *Specialist Periodical Reports, Royal Society of Chemistry, London,* 1997, **26** P 231.

4 Y. Lindqvist, G. Schneider, G; Vihko, *Eur. J. Biochem*, 1994, **221**,139.

5 Y. Marimoto, T. Tani, H. Okumura, Y. Higuchi, N. Yasuoka, *J.Biochem.*, **1991, 110**, 532.

6 J. M. Thorpe, *J. Chem. Soc., Chem. Commun.*, 1993, **34**, 1807.

7 G. Wilkinson, *Comprehensive Coordination Chemistry* Pergamon Press, Oxford, 1987, **3,** 539

8 G. Asgedom, A. Sreedhara, J. Kivikoski, J. Valkonen, C. P. Rao, *J. Chem. Soc., DaltonTrans.* 1995, **2**, 459.

9 M. Balasuramanym and V. Mohan, J, Biol Chem, 1989 **135,** 5106

10 N Raman, and A Kulandaisamy *Proc. Indian Acad. Sci. (Chem. Sci.)*, Indian Academy of Sciences, 2001, Vol. **113**, No. 3, 183

11 R. M. Brand and F. G. Hamel, *Int,J, Pharm* 1999 **183** 117

12 H. S. Anderson, J. F Iversen,.C. B. Jeppesen, and N. P. Moller - *J, Biol Chem*, 2000, **275,** 7101

13 a)P. Schwendt, A. Oravcova, J. Tyrselova, F. Pavelck, *Polyhedron*, 1996, **15,** 4507, b)Zubieta, *J. J. Inorg. Chem.* 1987, **26**, 147.

14 S. Samanta, D. Ghosh, S. Mukhopadhya,*J Inorg. Chem.*2002, **20**, 569.

15 K. V. R. Chary, V. K. Rastogi and G. Govil, *J. Magn. Reson*, 1993, **102**, 81.

16 A. Syamal, K.S. Kale, *J. Inorg. Chem.* 1979, **18,** 992.

17 Z. Xu, Z. .Lin, *Coord.Chem.Rev*, .1996, **156**, 139.

18 C. W. Hahn,P. G. Rasmussen,J. C. Bayon, *Inorg. Chem*, 1992 **3l**, 1963.

19 C. J. Ballhausen, and H. B. Gray, *Inorg. Chem.* 1962, **25**, 234.

20 T. S. Smith and V L Pecoraro, *Corelation of the EPR hyperfine constant with ring orientation*, ,The university press of Michigon 1990,**2**, 567.

21 D. Collison, B. Gahan, C. D. Garner and F. E. Mabbs, *J. Inorg. Chem.* . 1989, **18**, 902.

22 S. Mohanta, K.K. Nanda, S. Ghosh, M. Mukherjee, M. Helliwell, K. Nag, *J. Chem. Soc., DaltonTrans.*, 1996, **23**, 4233.

23 I. G. Asgedom, A. Sreedhara, J. Kivikoski, E. Kolehmainen, C.P. Rao, *J. Chem. Soc., Dalton Trans.*1996, **67,** 93.

24 Eniya Listiani Dewi *Electrochemical Studies of -Dioxo DinuclearVanadium Complexes* Waseda University press Tokyo 2000, **1**, 169.

25 E. R. Brown,R. T. Carge, *Electrochemical methods in physical methods in chemistry* ,; Wiley Interscience, New York,1971, **2**, 6.

26 G. M. Sheldrick, SHELXL-*97. Program for the Re-finementof Crystal Structures.* University of Göttin-gen,Germany **1997.**

27 A. Usman, I. A. Razak, M. K. Fun, S. Sivakumar, A. Sreekanth, M. R. P. Kurup, *Acta,Crystallogr, C. Cryst.Struct. Commun*, 2000, **58**, m46.

Chapter

6

SPECTRAL, ELECTROCHEMICAL AND BIOLOGICAL STUDIES OF IRON(III) COMPLEXES WITH N-N-S DONOR LIGAND

6.1. Introduction

Iron with atomic number 26 and atomic mass 55.8450, is the most wide spread and important transition metal and has an important functional role in living systems. Iron is essential for many life processes such as oxygen transport, nitrogen fixation and DNA synthesis [1]. Physiologically iron is stored in a ubiquitous protein called ferritin. The ferritin can hold up to 4500 iron atoms. Two main functions of iron containing proteins are oxygen transport and electron transfer. There are also molecules whose functions to store and transport iron.

Iron is well known to be an important initiator of free radical oxidation, such as lipid peroxidation. It is established that the exposure of biological membranes to oxidizing species will induce progressive degradation of membrane structure. Lipids containing unsaturated fatty acid moieties are the common targets for oxidative attacks. The degradation process is generally known as lipid peroxidation and it may result in damage to a variety of organic components in living cells and is involved in several diseases states such as postischemic reperfusion injury, xenobiotic toxicity and leucocyte-mediated inflammation [2].

The low solubility of iron (10^{-18} M) at physiological pH is one of the reasons that chelates are present in living systems. Therefore, coordinated iron is the logical form that should be studied physiologically. It is reported that rust red soil in Ochu Island contains over 20% iron but pineapples growing there are iron deficient because

iron is kept in the +3 state by the presence of MnO_2. Under this circumstances farmers resort to the use of iron chelates [3]. The chelate of iron with EDTA are soluble and make iron available to the plants for the manufacture of cytochromes, ferrodoxin etc. In higher animals, iron is transported by the complexing agent transferrin to the site of synthesis, other iron containing compounds such as hemoglobin and cytochromes and its insertion *via* enzymes in to the porphyrin ring. Awareness and understanding of the biological, chemical and physical properties of iron chelates are developing at a rapid rate and it is becoming increasingly easy to identify trends and relationships in structure and reactivity. Therefore, coordination chemistry of iron is intimately connected with its biological activity and hence the papers concerning the classical coordination and inorganic chemistry are very rare.

Iron(III) has five 3d electrons. It is known to exist in three ground states with S=5/2, 3/2 and 1/2 with configurations respectively of $t_{2g}^3 e_g^2$, $t_{2g}^4 e_g^1$ and t_{2g}^5 [4]. Spectral techniques such as vibrational, electronic, EPR, and Mössbauer spectroscopy can be used to give a fair information regarding the electronic and molecular structure of iron(III) complexes. For iron containing complexes ^{57}Fe, Mössbauer spectroscopy and EPR spectroscopy are used as complementary tools for probing molecular magnetism and for elucidating the electronic structure. A good treatment of these techniques is available in Hill and Day's text. Goodman and Raynor had given an excellent combination of experimental and theoretical EPR data. The review "Some Aspects of Coordination Chemistry of Iron(III)" by Cotton gives a good deal of various physical techniques to understand the molecular features of iron(III) complexes.

Inspired by the biological importance of iron complexes, we decided to syntheses and characterize iron(III) complexes of N-N-S donor ligands and the present chapter describes the syntheses, characterization, biological and cyclic voltammetric studies of a series of iron(III) complexes with 2-acetylpyridine -^{4}N-morpholine thiosemicarbazone, (HL4M), a N-N-S donor ligand.

6.2. Experimental

6.2.1 Materials

All reagents were of certified analytical grade and used as received. The solvents were purified by standard procedures before use. Details regarding the preparation and characterization of the ligands are given in Chapter 2.

6.2.2 Syntheses of complexes

Synthesis of [Fe (L4M)$_2$NO$_3$], **30**

Ammonium hydroxide was added in drops to an aqueous solution of $FeCl_3$ (0.325 g, 2 mmol) containing 1 mL of 1N hydrochloric acid, until alkaline. The resulting precipitate of ferric hydroxide was filtered off and washed with distilled water until the filtrate gave no precipitate with dilute silver nitrate solution. The precipitate was dissolved in the minimum quantity of nitric acid and the solution was added to a hot methanolic solution (20 mL) of HL4M (4 mmol, 1.057 g). The resulting solution was boiled under reflux for 4 h and allowed to evaporate to half its volume at room temperature. The resulting crystalline complex was filtered off washed with water, methanol ether and dried over P_4O_{10} *in vacuo*. Yield. 0.91 g (66.5%).

Synthesis of [Fe (L4M)$_2$ClO$_4$]H$_2$O, **31**

Ammonium hydroxide was added in drops to an aqueous solution of $FeCl_3$ (0.325 g, 2 mmol) containing 1 mL of 1N hydrochloric acid, until alkaline. The resulting precipitate of ferric hydroxide was filtered off and washed with distilled water until the filtrate gave no precipitate with dilute silver nitrate solution. The precipitate was dissolved in the minimum quantity of perchloric acid and the solution was added to a hot methanolic solution (20 mL) of HL4M.(4 mmol, 1.057 g). The resulting solution was boiled under reflux for 4 h and allowed to evaporate to half its volume at room temperature. The resulting crystalline complex was filtered off washed with water, methanol ether and dried over P_4O_{10} *in vacuo*. Yield. 0.94 g (68%).

Synthesis of [Fe (L4M)$_2$NCS], **32**

A methanolic solution (25 mL) of HL4M (4 mmol, 0.996 g) was added to a methanolic solution (20 mL) of ferric chloride (0.325 g, 2 mmol). A concentrated

solution of potassium thiocyanate (0.972 g, 10 mmol) was added to the above solution and the resulting solution was concentrated to half its volume at room temperature. The crystalline complex so obtained was washed with water, methanol and ether and dried over P_4O_{10} *in vacuo*. Yield.1.251 g (54.4%).

Synthesis of [Fe (L4M)$_2$] [FeCl$_4$]H$_2$O , **33**

A mixture of 0.325 g (2 mmol) of ferric chloride and 0.598 g (2 mmol) of HL4P in 20 mL of methanol was boiled under reflux for 4 h and cooled to room temperature. The crystalline complex was filtered off, washed successively with water, methanol; and ether and finally dried over P_4O_{10} *in vacuo*. Yield. 0.64 g (69.4%).

6.3 Analytical measurements

The details of analytical measurements such as molar conductivity, magnetic moments, IR, UV-Visible, EPR, Mössbauer spectrometry and, cyclic voltammetry are described in Chapter.2. Procedural details of biological studies are described at length in Chapter.3.

6.4 Results and discussion

All new complexes prepared are either black or olive green. The stoichiometries, partial elemental analyses, molar conductivities, and magnetic moments are shown in Table 6.1.

Analytical data show the presence of 1:2:1 stoichiometry for iron, thiosemicarbazone and gegenions. All new compounds have molar conductivity values in dimethylformamide (10^{-3} M solution), slightly below the expected range for 1:1 electrolytes. The lower value, which seems to predominate for the $[FeCl_4]^-$salt is probably caused by ion association in dimethyl formamide. The complexes are expected to have either a distorted octahedral, a capped octahedral or pentagonal bipyramidal structure (septa coordinated) with two deprotonated ligands and an anion coordinated or non-coordinated to iron(III) centre [5]

6.4.1 Magnetic moments

Magnetic moments have been determined for all complexes at room temperature in the polycrystalline state. Iron(III) is known to exist in three states with S=5/2 (ground term $^6A_1$, μ =5.92 B.M.) , 3/2 (ground term $^4A_2$, μ = 4.00 B.M) and 1/2 (ground term $^2T_2$, μ = 2 to 2.6 B.M) states.

The magnetic moment of nitrate complex **30** at room temperature is 3.816 BM and the value is slightly lower than the spin only value for iron(III) with $^4A_2$ ground state. The slightly low value is suggestive of a spin equilibrium $^6A_1 \leftrightarrow {}^2T_2$. This type of spin equilibrium is reported for iron(III) complexes of o-hydroxy benzaldehyde thiosemicarbazones [6]. The magnetic moments of $[Fe(L4M)_2]ClO_4$ H_2O, **31** and $[Fe(L4M)_2]NCS$, **32** have values respectively of 1.59 B.M and 2.33, which are in the range of low spin iron(III). The slightly low value for iron(III) perchlorate complex (**31**) in polycrystalline state at room temperature may be due to the effective quenching of orbital angular momentum

The compound $[Fe\ (L4M)_2][FeCl_4].H_2O$,**33** has a magnetic moment of 4.4 B.M. The molar susceptibility of the compound is found to be 16020. The susceptibility of the cation $[Fe(L4M)_2]^+$, as determined for $[Fe(L4M)_2]ClO_4H_2O$ is 1032, thus making the susceptibility of the anion to be 14988, this gives a moment 5.9624 for the anion. Previous measurements of the susceptibility of the anion $[FeCl_4]^-$ have given values within the range 5.9-6.0 B.M [7,8]. Thus the majority of the new complexes have the ground state term $^2T_2$.

6.4.2 Vibrational spectra.

The significant IR bands of Fe(III) complexes with their tentative assignments in the 4000 to 300 cm^{-1} region are presented in the Table 6.2.

On coordination of azomethine nitrogen ν(C=N) shifts to lower energy by 20 to 30 cm^{-1}. The band shifting from *ca* 1627 cm^{-1} in the uncomplexed thiosemicarbazones spectra to 1601 cm^{-1} in the spectra of the complexes and ν(N-N) shifts to higher frequency in all, is a clear sign of enolisation of the ligand and coordination *via* the azomethine nitrogen atom. The results are in agreement with

some reported complexes of iron(III) when the ^{4}N has two protons. This is further supported by the appearance of a new band near 1590 cm^{-1} due to formation of a new (N=C) bond.

The second mode of coordination *via* sulphur atom is expected upon deprotonation of the ligand. The spectral band ν(N-H) of the thiosemicarbazones disappears in the complexes indicating the deprotonation of the ^{3}NH and coordination *via* the thiolate sulphur is shown by a decrease in the frequency by 41 to 60 cm^{-1} of the thioamide band which is partially ν(C=S) and found at 1371 and 892 cm^{-1} for HL4M. The shift to lower wavenumbers of these bands occurs on complexation. Another band which is considered to be sensitive to bonding of sulphur to metal ion is the ν(N-N), since there is increased double bond character for N=C-S; ν(N-N) is expected to shift to higher energies. However, we were unable to assign this band with absolute authenticity in various spectra.

Coordination *via* the pyridine nitrogen is indicated by the shifts to lower frequencies of ν(C-N) + ν(C-C) and shift to higher frequencies of the in-plane and out-of plane ring deformation bands. Thus, the shift in pyridine ring, out of plane and in plane bending vibrations 12 to 44 cm^{-1} with N-N-S donors on complexation confirms the coordination of ligand to iron(III) *via* pyridine nitrogen.

The observed low energy bands around 510 cm^{-1}, 440 cm^{-1} and 384 cm^{-1} are assigned to ν(Fe-N) for imine nitrogen , ν(Fe-S) and ν(Fe-N) for pyridine nitrogen.

The nitrate complex **30** has three additional bands at 1410, 1265 and 1020 cm^{1} which are attributed to ν_4, ν_1 and ν_2 modes respectively of the coordinated nitrate ion. The difference (ν_4 - ν_1) $\approx$145 cm^{-1} and hence nitrate ion is coordinated unidentetly [9]. The spectrum of the complex shows an additional medium band at 450 cm^{-1} which is not present in the spectrum of the ligand. This band is attributed to the stretching vibration of Fe-O. Very strong band at *ca* 2056 cm^{-1}, strong band at *ca* 834 cm^{1} (however this band is often obscured by the presence of other bands in the same

Table 6.1

Analytical data, conductivity, magnetic moments, colours and yield of complexes of Fe(III) with HL4M [a)]

Compound	Emp.formula [b]	Yield (%)	Colour	μ[c)](BM)	ΛM [d)]	Analytical data Found / calculated) %			
						C	H	N	Fe
$Fe(L4M)_2NO_3$,**30**	$C_{24}H_{30}FeN_9O_5S_2$	63.8	Black	3.816	95.3	44.57 (44.72)	4.81 (4.69)	19.86 (19.56)	8.86 (8.66)
$Fe(L4M)_2ClO_4.H_2O$,**31**	$C_{24}H_{32}ClFeN_8O_7S_2$	66.5	Brown	1.590	92.8	41.37 (41.18)	4.76 (4.61)	16.37 (16.01)	8.12 (7.98)
$Fe(L4M)_2NCS$,**32**	$C_{25}H_{30}FeN_9O_2S_3$	62.2	Black	2.33	85.7	47.01 (46.87)	4.90 (4.72)	19.90 (19.68)	8.87 (8.72)
$[Fe(L4M)_2[FeCl_4]H_2O$,**33**	$C_{24}H_{32}C_{l4}Fe_2N_8O_3S_2$	61.5	Black	4.44	86.5	36.12 (36.11)	4.12 (4.04	13.86 (14.04)	14.12 (13.99)

[a)] In parentheses calculated values. [b)] Empirical formula. [c)] Magnetic moment [d)] Molar conductivity, 10^{-3}M solution (DMF) at 298 K

Table 6. 2

IR spectral assignments for thiosemicarbazones and their Fe(III) complexes(all absorption are given in cm^{-1})

Compound	ν(C=N)	ν(N-N)	ν(C-S)	δ(C-S)	δop	δip	ν(Fe-N)	$\nu(Fe-N)_p$	ν(Fe-S)
HL4M	1627 s	1371 m	1010 m	892 m	649 m	408 m	--	--	--
$[Fe(L4M)_2[FeCl_4]H_2O$	1600 s	1263 s	1040 m	851 m	661 m	440 w	526 m	364 m	447sh
$[Fe(L4M)_2ClO_4]H_20$	1607 s	1263 s	1001 m	849 m	668 m	444 w	523 m	376 m	448sh
$[Fe(L4M)_2NO_3]$	1601 s	1276 s	1037 m	848 m	667 w	438 m	524 m	389 s	446w
$[Fe(L4M)_2NCS]$	1607 s	1270 s	1034 m	858 m	669 w	441 m	528 m	378 m	445m

s =strong; m=medium; w=weak; sh=shoulder

Table 6.5

Antimicrobial studies of Fe(III) complexes with N-N-S donor

Compounds	1*	2*	3*	4*
$[Fe(L4M)_2[FeCl_4]H_2O$,	+14	+10	+15	+12
$[Fe(L4M)_2ClO_4]H_20$,	+10	+10	+10	+14
$[Fe(L4M)_2NO_3]$,	+18	+12	+17	+11
$[Fe(L4M)_2NCS$,	+12	+13	+14	+15

1* *Staphylococcus aureus*, 2*,*Bacillus sp*, 3**Shigella*, 4**Proteus sp*

region) and a medium band at 483 cm^{-1} in the spectrum of **32** are assigned to ν(CN), ν(CS), δ(NCS) respectively for N coordinated thiocyanate group [10]. We have identified ν(Fe–N) due to thiocyanate group at 283 cm^{-1}.

The spectrum of perchlorate complex **31** exhibits a doubly split strong band with band maxima at 1060 and 1100 cm^{-1}, a weak band at 935 cm^{-1} and a strong doubly split band with band maxima at 615 and 625 $cm.^{-1}$. These bands are not observed in the spectrum of the ligands and are attributed to ν_1, ν_4, ν_2, ν_3 and ν5 modes [11] respectively of the unidentate coordinated perchlorate. The band at *ca* 450 cm^{-1} is attributed to the stretching vibration of ν(Fe-O). The appearance of ν_1(935 cm^{-1}) along with the splitting of $\nu_3(ClO_4)$ in the spectra of the compound is due to interaction *via* hydrogen bonding to water molecule present.

For $[Fe(L4M)_2][FeCl_4].H_2O$, a medium intensity split, band which being observed at 390 cm^{-1} is assignable to $[FeCl_4]^-$. The splitting is likely due to steric factors reducing the symmetry from (T_d) and the same may be due to lattice requirements of the large cation [12].

6.4.3 Electronic spectra

The significant electronic absorption bands (Fig.6.1) in the spectra of the complexes recorded in polycrystalline state and in dimethylformamide are presented in Table 6.3

The U.V. region is dominated by two intense intraligand bands at 335 nm and 395 nm which were assigned to $\pi \rightarrow \pi^*$ and $n \rightarrow \pi^*$ transitions in a similar type of ligands. Usually $n \rightarrow \pi^*$transitions involving N and S occur at a lower energy than $\pi \rightarrow \pi.^*$ Bands which are found between 475 nm and 385 nm in the solid state spectrum of the complexes having pyridyl ligands have assigned to $d \rightarrow \pi^*$ transition and bands between 665 and 475 nm in the spectra of all the solids are also likely due to $d \rightarrow \pi^*$ metal to ligand bands as well as sulphur to iron(III) transitions. The bands below 665 nm can be assigned to d-d transitions of the spin paired d^5 iron(III) complexes.

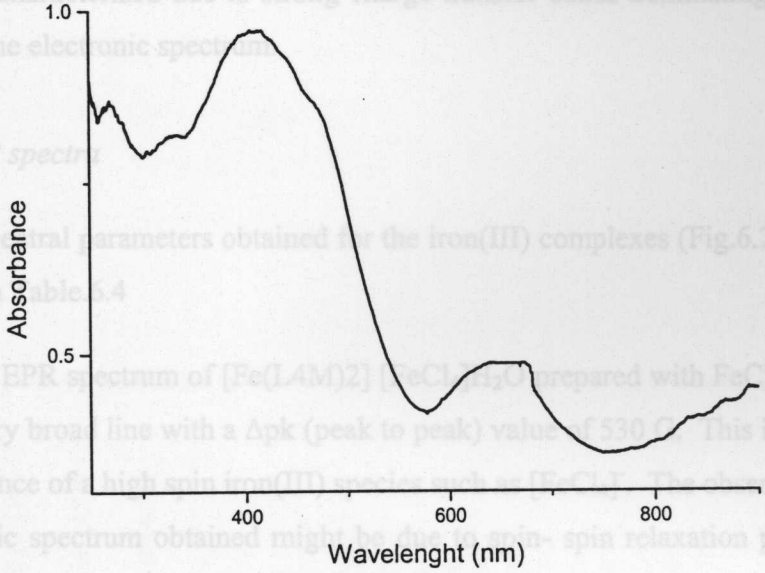

Fig 6.1 UV-Vis-DRS of the compound 33

A comparison of the electronic spectra of $[Fe\ (L4M)_2][FeCl_4].H_2O$ with that of $[Fe(L4M)_2]ClO_4$ shows that no significant difference which indicates that the electronic spectra of cations dominate the spectra of the complexes. Further the spin forbidden transitions between 725-605 nm of $[FeCl_4]^-$ are too weak to be observed. Usually iron(III) has shown a common $(d_{xy})^2\ (d_{xz}\ d_{yz})^3$ configuration. The iron(III) of in these complexes have exhibited the presence of a less common $(d_{xz}\ d_{yz})^4(d_{xy})^1$ configuration. Occurrence of the less common configuration has been ascribed to the electronic interaction between d orbital of iron and π^* orbital of ligand. The interaction stabilizes the d orbital and induces $(d_{xz}\ d_{yz})^4(d_{xy})^1$ configuration [13].

There is no significant difference between the band energies for tetrachloferrate(III) and perchlorate solids with same ligands indicating that the electronic transitions of the cation dominates the spectra. Therefore, the spin forbidden transitions between 730 – 602 nm of the $[FeCl_4]^-$ are too weak to be observed. The electronic spectra of low spin iron(III) complexes have not been

adequately characterized due to strong charge transfer bands dominating the visible portion of the electronic spectrum.

6. 4. 4. EPR spectra

The EPR spectral parameters obtained for the iron(III) complexes (Fig.6.2 & 6.3) are presented in Table.6.4

The EPR spectrum of [Fe(L4M)2] $[FeCl_4]H_2O$ prepared with $FeCl_3$ consist of a single, very broad line with a Δpk (peak to peak) value of 530 G. This is indicative of the presence of a high spin iron(III) species such as $[FeCl_4]^-$. The observed g value and isotropic spectrum obtained might be due to spin- spin relaxation possibly *via* dipole- dipole interactions. However, the isotropic spectrum changes to a rhombic one in frozen solution, since the value of g_{av} of the frozen solution is essentially the same as the g_{iso} value in the polycrystalline state, it is likely that lattice effects in the solid may account for this change from isotropic to rhombic and it is common for spin paired iron(III) complexes. The observed anisotropic character with three *g* values due to rhombic distortion is common for spin – paired iron(III) complexes. The small deviation of the anisotropic *g* value from 2 suggests that the unpaired electron is in the d_{xy} orbital with ground state configuration $d^2_{xz}d^2_{yz}d^1_{xy}$. The presence of signal at 4.3 indicates the presence of high spin iron(III). The observed EPR spectra are in general agreement with earlier results for complexes of similar type [14]. No change in iron(III) centre is observed when the solvent is changed. There is gradual / little difference in the spectrum obtained in frozen chloroform / ethanol and spectrum obtained in frozen DMF and those of the solid state spectra, indicating that the iron(III) centre does not undergo alteration in solution.

The room temperature EPR spectrum of the-nitrate complex exhibits a broad absorption at $g \approx 4$ (typical for high spin iron(III) complexes), and a strong axial signal ($g_\perp$ = 2.1573, $g_\parallel$ = 2.0282), typical for low – spin ferric complexes,

Table.6.3

Electronic spectral assignments (nm),(log ε^a)of Fe(III) complexes with N-N-S donor.

Compound	Mode	d-d	CT(d-π^*)	Intraligand.
$[Fe(L4M)_2[FeCl_4]H_2O$	DMF	843 sh (2.19)	645 (2.74) ; 374 (4.02)	328 (4.02), 294 sh (4.12)
	Solid	844 sh	644 sh	326, 292.sh
$[Fe(L4M)_2ClO_4]H_20$	DMF	881(2.16)	607 (2.71);375 (3.98)	329, (3.98), 297 (4.11)
	Solid	883	613 ;385	330 ;299 sh
$[Fe(L4M)_2NO_3]$	DMF	838 (2.22)	601.(2.69) ; 376 (4.03)	326 (4.03);296 sh (4.14)
	Solid	846 sh	617 ; 379 sh	330 sh; 298
$[Fe(L4M)_2NCS$	DMF	846 (2.33)	624 (3.01) ; 380 (4.23)	329 (4.01) 296 sh (4.34)
	Solid	847	625 sh ; 380	330, 298 sh

[a] = ε is expressed in (l mol^{-1} cm^{-1})

Table 6.4

EPR spectral parameters of Fe(III) complexes with N-N-S donor ligands. (RT = 298 K, LNT = 77 K)

Compound	Mode	Feature		
$[Fe(L4M)_2[FeCl_4]H_2O$	Solid(RT)	----	-----	Δpk=530 G
	DMF(LNT)	$g_2 = 2.1337$	$g_3 = 2.1910$	g_{av} =2.1037
	$CHCl_3$ + C_2H_5OH (LNT)	$g_2 = 2.1442$	$g_3 = 2.1989$	g_{av}=2.1107
$[Fe(L4M)_2ClO_4]H_20$	Solid(RT)	----	---	Δpk=518 G
	DMF (LNT)	$g_2 = 2.1418$	$g_3 = 2.1888$	g_{av} =2.1080
	$CHCl_3$ + C_2H_5OH (LNT)	$g_2 = 2.1424$	$g_3 = 2.1860$	g_{av}= 2.1314.
$[Fe(L4M)_2NO_3]$	Solid(RT)	$g\perp$ =2.157,$g\perp$ =4	----	g_{av}= 2.1142
	DMF (LNT)	$g_2 = 2.112$	$g_3 = 2.164$	g_{av}= 2.091
	$CHCl_3$ + C_2H_5OH (LNT)	$g_2 = 2.107$	$g_3 = 2.161$	g_{av}= 2.0876
$Fe(L4M)_2NCS$	Solid(RT)	$g_2 = 2.1471$	$g_3 = 2.2084$	g_{av}= 2.2241
	DMF (LNT)	$g_2 = 2.1384$	$g_3 = 2.1854$	g_{av}= 2.1061
	$CHCl_3$ + C_2H_5OH (LNT)	$g_2 = 2.1420$	$g_3 = 2.1928$	g_{av}= 2.1104

indicating the existence of two types of iron species. Spectroscopic characteristic of the complexes in which ferric ion take the $(d_{xz}\ d_{yz})^4(d_{xy})^1$ configuration is an axial type spectra. Occurrence of the less common configuration has been ascribed to the electronic interaction between d orbital of iron and π^* orbital of ligand [15]. The interaction stabilizes the d orbital and induces $(d_{xz}d_{yz})^4(d_{xy})^1$ configuration. However, at 77K a rhombic spectrum with three g values typical of a low spin complex is obtained. This explains the anomalous magnetic moment of 3.816 B.M at room temperature and confirms the existence of spin equilibrium $^6A_1 \leftrightarrow ^2T_2$. The observed anisotropic character with three *g* values due to rhombic distortion is common for spin – paired iron(III) complexes. The *g* values confirm the low spin character of iron(III). The small deviation of the anisotropic g values from 2 suggests that the unpaired electron be in the d_{xy} orbital.

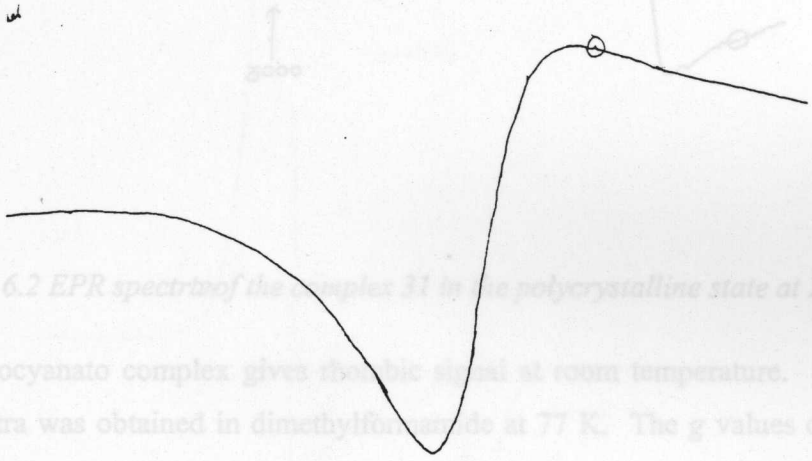

*Fig 6.2 EPR spectra of the complex **33** in the polycrystalline state at 298 K*

The perchlorate solid gives isotropic signal at room temperature. The isotropic spectra observed may be due to spin- spin relaxation possibly *via* dipole interaction. At liquid nitrogen temperature the complex give anisotropic spectra. The anisotropic spectra with three *g* values due to rhombic distortion is not uncommon for spin paired iron(III) ,since this behavior has been reported for Iron(III) complexes

with other Schiff bases. The small deviation of the anisotropic *g* values from 2 .0 suggests that the electronic structure of the ground state is $(d_{xz}\ d_{yz})^4(d_{xy})^1$ configuration. There is gradually little difference in the spectrum obtained in frozen chloroform / ethanol and those of the solid state spectra indicating that the iron(III) centre does not undergo alteration in solution.

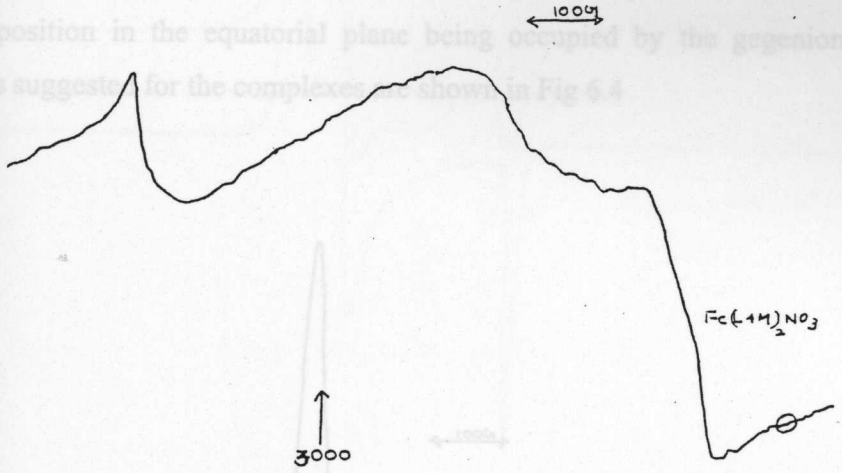

Fig 6.2 EPR spectrum of the complex 31 in the polycrystalline state at 298 K

N-thiocyanato complex gives rhombic signal at room temperature. Similar type of spectra was obtained in dimethylformamide at 77 K. The *g* values confirm the low spin character of iron(III). The small deviation of the anisotropic *g* values from 2 suggests that the unpaired electron is in the d_{xy} orbital. There is gradually little difference in the spectrum obtained in frozen chloroform / ethanol and those of the solid-state spectra indicating that the iron(III) centre does not undergo alteration in solution.

From the spectral studies we assumed that the cation of $[Fe(L4M)_2]$ $[FeCl_4].H_2O$ has an octahedral geometry and coordination around tetrachlo ferrate is

tetrahedral. Complexes with nitrate, perchlorate and thiocyanate as anions are assigned either a capped octahedral or pentagonal bipyramidal geometry. In the capped octahedral structure, two L4M ligands occupy six corners of an octahedron and an additional position is occupied by an anion at one triangular faces of this octahedron. In alternate pentagonal pyramid structure, two L4M moieties can occupy two axial positions and four positions in the equatorial plane with an additional seventh position in the equatorial plane being occupied by the gegenions. The structures suggested for the complexes are shown in Fig 6.4

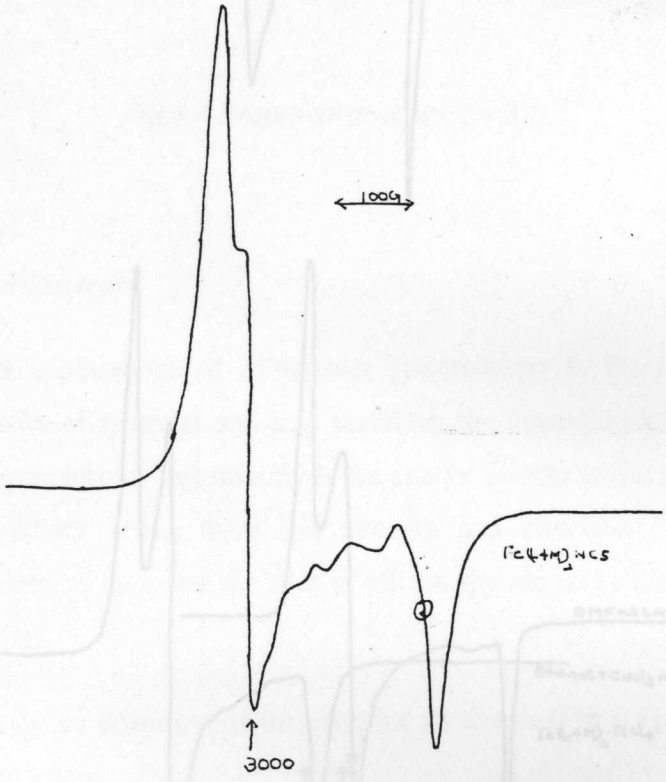

Fig 6.2 EPR spectra of the complexes in the polycrystalline state at 298 K

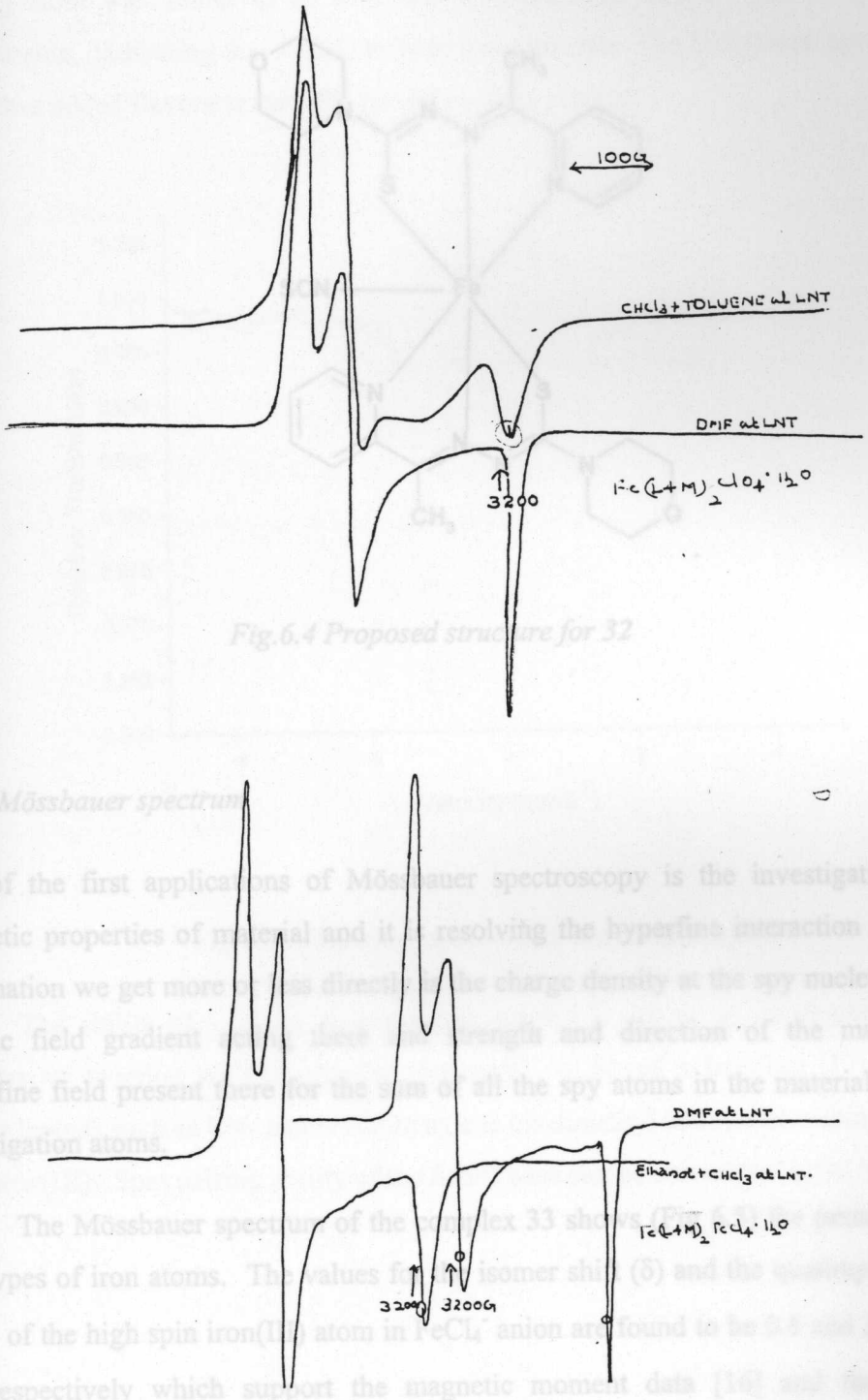

Fig 6.3 EPR spectra of the complexes in solution at 77K

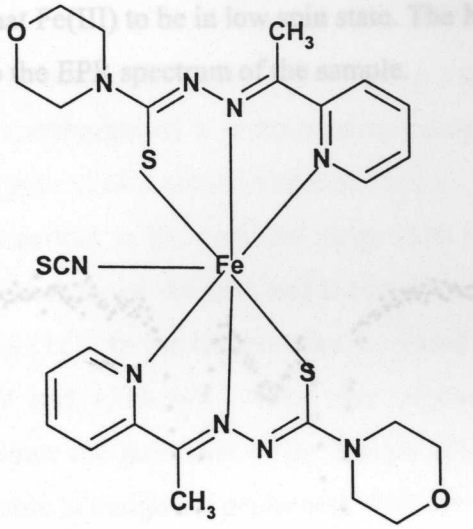

Fig.6.4 Proposed structure for ***32***

6 .4 5 Mössbauer spectrum

One of the first applications of Mössbauer spectroscopy is the investigation of magnetic properties of material and it is resolving the hyperfine interaction so the information we get more or less directly is the charge density at the spy nucleus, the electric field gradient acting there and strength and direction of the magnetic hyperfine field present there for the sum of all the spy atoms in the material under investigation atoms.

The Mössbauer spectrum of the complex **33** shows (Fig 6.5) the presence of two types of iron atoms. The values for the isomer shift (δ) and the quadruple split (ΔE_q) of the high spin iron(III) atom in $FeCl_4^-$ anion are found to be 0.8 and 3.2 mm s^{-1} respectively which support the magnetic moment data [16] and the large quadruple splitting indicates only slight distortion from Td symmetry which supports the EPR parameters. The isomer shift and the quadruple split (ΔE_q) for the low spin

iron(III) atom was found to be 0.49 mm s^{-1} and 0.22 mm s^{-1} with respect to nitroprusside, indicating that Fe(III) to be in low spin state. The Mössbauer spectrum of **33**, thus added flavors to the EPR spectrum of the sample.

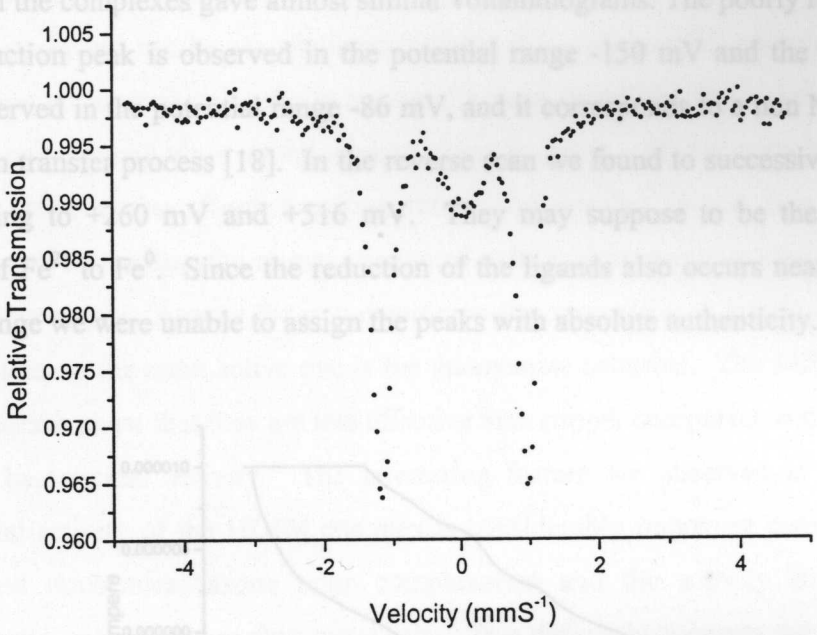

Fig 6.5 Mössbauer spectrum of the compound 33

The ability of a ligand to cause spin pairing is related to its degree of << softness >> together with its capacity for metal → ligand π bonding [17]. Only softest ligands such as CN- and orthophenylene bis dimethyl arsine cause spin pairing with iron(III). Spin pairing ability of the Schiff base can be considered quite high [5].

6.5 Cyclic voltammetry

Details of cyclic voltammetric experiments are presented at length in Chapter.2. The cyclic voltammogram of a representative complex is presented in Fig.6.6. All the complexes gave almost similar voltammograms. The poorly resolved $Fe^{III/II}$ reduction peak is observed in the potential range -150 mV and the counter peak is observed in the potential range -86 mV, and it corresponds to a non Nerstian one electron transfer process [18]. In the reverse scan we found to successive peaks corresponding to +260 mV and +516 mV. They may suppose to be the due to reduction of Fe^{2+} to Fe^{0}. Since the reduction of the ligands also occurs near to this potential range we were unable to assign the peaks with absolute authenticity.

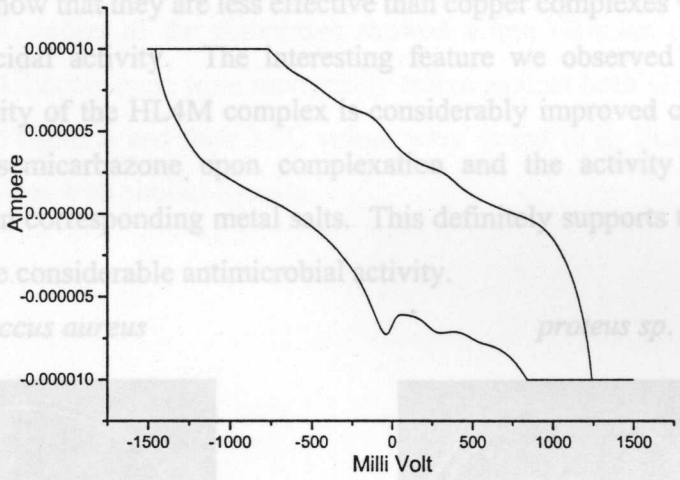

Fig 6.6 Cyclic voltammogram of **33**

6.6 Biological studies

Details of antimicrobial screening of complexes are described at lengths in Chapter.2

All Fe(III) complexes are screened against both Gram positive and Gram negative bacteria and results are tabulated in Table 6.5. All iron(III) complexes are found to have no bactericidal activity against the most dreadful Vibrio cholerae O1 and Vibrio parahaemolyticus, at the studied concentrations. All the complexes are moderately active against *Staphylococcus aureus* and *Bacillus sp* and *Shigella* and *proteus sp*. All above this, the nitrato compound exhibited moderate activity against *Salmonella paratyphi*. Among the iron complexes the most active is nitrato complex but for *Proteus sp* the most active one is the thiocyanate complex. The MIC values of the complexes show that they are less effective than copper complexes with similar ligands in bactericidal activity. The interesting feature we observed is that the antimicrobial activity of the HL4M complex is considerably improved compared to uncomplexed thiosemicarbazone upon complexation and the activity is seen to slightly greater than corresponding metal salts. This definitely supports the fact that the complexes have considerable antimicrobial activity.

Staphylococcus aureus *proteus sp.*

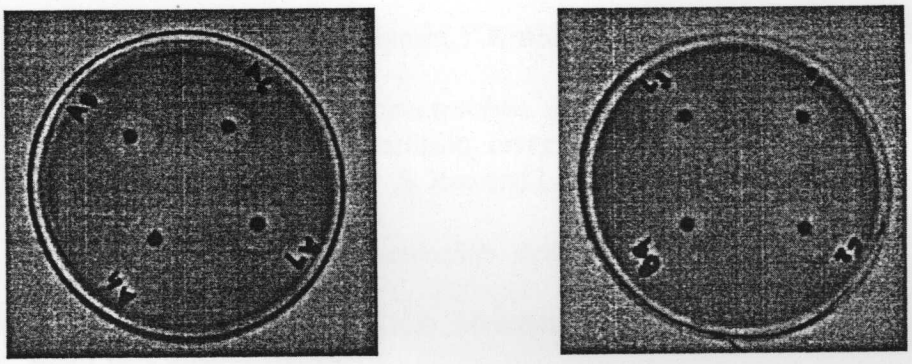

Fig 6.7 Antimicrobial activity (inhibition zone) of the compounds.

6.7 Concluding remarks

The N-N-S donor ligand, HL4M gave low spin iron(III) complexes at reflux temperature. The complexes were either shiny black or deep green colour. The molar conductivity was found to be slightly below the expected range for 1:1 electrolyte which might be attributed to the ion pairing in solution. Higher magnetic moments for the two complexes were found to be due to either the presence of a high spin anion containing iron(III) or spin equilibrium. Iron in theses complexes exhibited less common electronic configuration. The IR spectral assignments were in agreement with N_2, N_2 and S_2 coordination. The EPR spectral features are almost similar and gave three g value spectra in solution at liquid nitrogen temperature. The EPR spectra support the less common configuration of iron(III) in complexes. The Mössbauer spectrum of the complex showed the presence of two types of iron in the complex. The CV studies of the complexes showed a non Nerstian one electron transfer process. All complexes were moderately active against both Gram positive and Gram negative bacteria and their MIC values were found to be little bit higher than copper complexes with similar ligands.

References

1 a) J. H. Dawson, *Science*, 1988, **240**, 433, b) J. Reisach, K. Gersonde, Biochemistry, 1977, **16**, 2539.

2 P. R. Ortiz de Montello, *Cytochrome, Structure,Mechanism,andBiochemistry*; Plenum Press: NewYork, 1986, **1**, 480.

3 J. F. Deatherage, R. S. Loe, K. J. Moffat, *J. Mol. Biol*, 1976, **104**, 723.

4 (a) R. L. Martin, A. H. White, *Transition. Metal Chem*, 1968, **4**, 113. (b) E. Konig, *Coord.Chem. Rev.* 1968, **3**, 471.

5 P. S. Rao, P. Ganguli and B. R. McGarvey, *Inorg. Chem.*, 1981, **20**, 3682.

6 P. S. Rao, A. Reuveni, B. R. McGarvey, P. Ganguli and P. Gütlich, *Inorg. Chem.*, 1981, **20**, 204.

7 S. Vasudevan, H. N. Vasan and C. N. R. Rao, *Chem. Phys. Lett*, 1979, **65**, 444.

8 G. Sankar, J. M. Thomas, V. Varma, G. U. Kulkarni and C. N. R. Rao, *Chem. Phys. Lett.*, 1996, **251**, 79.

9 M. G. Finn, and K. B. Sharpless, *J. Am. Chem. Soc.* 1991, **113**, 113.

10 M. E. De Vries, ,R. M. La Crois, G. Roelfes, H. Kooijman, A. L. Spek, R Hage,*J. Chem. Soc., Chem. Commun.* 1997, **45**, 1549.

11 N.Mikio,I.Takahisa,I.Akira,O.Yoshiki,F.Hiroshi,*Inorg.Chem. 1999,* **38**, 3857

12 T.Mizuta,T.Yamamoto,K.Miyoshi,Y.Kushi, *Inorg. Chim. Acta* 1990, **175**, 121

13 a) E. König and K. Madeja, *Spectrochim. Acta*, *Part* A, 1967, **23**, 477.
b) J. H. Takemoto and B. Hutchison, *Inorg. Chem.*, 1973, **12**, 705.

14 B. Maiti, B. R. McGarvey, P. S. Rao and L. C. Stubbs, *J. Magn.Reson.*, 1983, **54**, 99.

15 E. König and K. Madeja, *Spectrochim. Acta*, *Part* A, 1967, **23**, 45.

16 N. N. Greenwood and T. C. Gibb, *Mossbauer Spectroscopy*, (Chapman and Hall Ltd, London) 1971.

17 C. Roux, J. Zarembowitch, J. P. Itie, A. Polian and M. Verdaguer, *Inorg. Chem.*, 1996, **35**, 574.

18 G. R. Hall, D. N. Hendrickson, *Inorg. Chem.* 1976, **15**, 607.

Chapter

7

SPECTRAL, BIOLOGICAL AND ELECTROCHEMICAL STUDIES OF Mn(II) COMPLEXES WITH N_2S AND O-N-S DONOR LIGANDS AND SINGLE CRYSTAL X-RAY DIFFRACTION STUDIES OF $[Mn(C_{14}H_{13}N_4S)_2]$

7.1 Introduction

Manganese with atomic number 25 and atomic weight 54.9380 exhibits a wide variety of oxidation states ranging from -3 to +7 is very common in biochemical systems. The most well known of the manganese enzyme is the tetranuclear system which is active in oxygen evolution step [1]. This tetranuclear manganese(1V) complex has led to a spurt in research in this field and as a consequences different oxygen-evolving model were synthesized and their importance investigated. In such studies, manganese complexes in different oxidation states were obtained and studied their magnetic and spectral properties in depth. Their spectral and magnetic properties were an active domain of research.

It is reported that +2 is most common among different oxidation states. Due to absence of LFST of d^5 configuration the formation constants of manganese complexes are smaller than those of other first transition series metals and hence exist fewer number of manganese enzymes that contain manganese [2]. It is reported that Mn^{2+} can replace Mg^{2+} in a number of biological systems [3]. It is reported [4] that manganism is a disease caused by exposure to excessive levels of manganese, attacks the central nervous system, kidney and liver. Manganese poisoning is characterized by motor skill and psychological disturbances. Manganism is almost identical to

those of Parkinson's disease. Due to these similarities, manganism has been classified as a Parkinson's syndrome.

This Chapter describes the syntheses, characterization and biological and cyclic voltammetric studies of manganese complexes with various N_2S and O-N-S donor ligands.

7.2 Experimental

7.2.1 Materials and method

Manganese(II) acetate tetrahydrate (Reagent Grade, E. Merk) was used with out prior purification. The solvents were purified by standard procedures before use. Details regarding the preparation and characterization of the ligands HL4M, HL4P, H_2SAP and H_2APP are given in Chapter 2.

7.2.2 Measurements

The details of magnetic moments, molar conductivity, partial elemental analyses, atomic absorption, IR, UV-Visible, EPR spectroscopy and X-ray diffraction studies are described in Chapter 2. The details of biological investigation and cyclic voltammetry are presented in Chapters 3 and 2 respectively.

7.2.3 Preparation of complexes

The general method of synthesis of the manganese (II) complexes is as described below.

To a hot methanolic solution (20 mL) of the thiosemicarbazones (2 mmol) was added a hot methanolic solution (15 mL) of manganese(II) acetate tetra hydrate (1 mmol) with stirring. The solution after refluxing for 2 h was allowed to cool, when micro crystals of the manganese(II) complexes crystallized out. The complexes were filtered off, washed with hot water, methanol and ether and finally dried over P_4O_{10} *in vacuo*.

The complexes synthesized with N-N-S donor ligands are $Mn(L4M)_2$, **34** and $Mn(L4P)_2$, **35,** and with O-N-S donor ligands are $Mn(HSAP)_2$, **36**, and $Mn(HAPP)_2$, **37**.

7.3 Results and discussion

The colours, molar conductivity, magnetic moments, partial elemental analyses, stoichiometries of complexes are presented in Table 7.1

The manganese complexes with N_2S donors are pale yellow or orange where as that with O-N-S donors are black. The N_2S donors can coordinate metal ions, either neutral ligands or anionic species by the loss of proton at the ^{3}N. The analytical data for all manganese(II) complexes show the presence of two monoanionic tridentate ligand per metal ion which is supported by their behaviour as non electrolytes and their geometry is probably distorted octahedral.

The complexes are soluble in dimethylformamide, in which conductivity measurements were made, dimethyl sulphoxide and acetonitrile. The molar conductivity of *ca* 10^{-3} M solution of complexes in dimethylformamide, ranges between 8 to 12 Ω^{-1} cm^{-1} $mol,^{-1}$ indicating non-electrolytic nature of complexes in solution [5]. The manganese complexes with O-N-S donors were soluble in dimethyl formamide with decomposition and hence conductivity measurements were made in acetonitrile. Single crystals of manganese(II) complex with N-N-S donor, suitable for X-ray scattering studies were obtained by slow evaporation of solution of complex in dimethylformamide.

7.3.1 Magnetic susceptibility

Because of the additional stability of d^5 configuration, Mn(II) generally forms high spin complexes which has an orbitally degenerate ^{6}S ground state term and the spin only magnetic moment of 5.91 B.M. which will be independent of the temperature and of the .stereochemistry. The room temperature magnetic moments of the complexes in the polycrystalline state fall in the 5.3-6.01 B.M range, which are very close to spin only value of 5.91 B.M. for $d.^5$ There is no magnetic evidence for any manganese –manganese interaction [6].

7.3.2. IR spectra.

The significant IR bands of Mn(II) complexes with their tentative assignments in the 4000 to 300 cm^{-1} region are presented in the Table 7.2.

With N-N-S donors coordination is expected *via* pyridine nitrogen, azomethine nitrogen and thiolate sulphur. On coordination of azomethine nitrogen ν(C=N) shifts to lower energy by 23 to 35 cm^{-1}. The band shifting from *ca* 1630 cm^{-1} in the uncomplexed thiosemicarbazones spectra to 1601 cm^{-1} in the spectra of the complexes and ν(N-N) shifts to higher frequency side in all, is a clear sign of coordination *via* the azomethine nitrogen atom. The results are in agreement with Raina and Srivastava who studied complexes of iron(III) when the ^{4}N has two protons. This is further supported by the appearance of a new band near 1450 cm^{-1} due to formation of a new (N=C).

The mode of coordination *via* sulphur atom is expected upon deprotonation of the ligand. The spectral band ν(N-H) of the thiosemicarbazones disappears in the complexes indicating the deprotonation of the ^{2}NH and co ordination *via* the thiolate sulphur is shown by a decrease in the frequency [7] by 52 to 58 cm^{-1} of the thioamide (IV) band which is partially ν(C=S) and found at 1371 and 892 cm^{-1} for HL4M. A shift to lower wavenumbers of these bands occurs on complexation. Another band which is considered to be sensitive to bonding of sulphur to metal ion is the ν(N-N), since there is increased double bond character for N=C-S; ν(N-N) is expected to shift to higher energies.

Coordination *via* the pyridine nitrogen is indicated by the shifts to lower frequencies of ν(C-N) + ν(C-C) and shift to higher frequencies of the in plane and out of plane ring deformation bands. Thus, the shift in pyridine ring, out of plane and in plane bending vibrations 10 to 12 cm^{-1} with N-N-S donor on complexation confirms the coordination of ligand to manganese(II) *via* pyridine nitrogen [8]. The observed low energy bands around 521, 416 and 318 cm^{-1} are assigned to ν(Mn-N) for imine nitrogen , ν(Mn-S) and ν(Mn-N) for pyridine nitrogen.

With O-N-S donors coordination is expected *via* phenolic O, azomethine nitrogen and thione sulphur. The bands at 1634 and 1602 cm^{-1} are characteristic of the azomethine nitrogen atom present in H_2SAP and H_2APP. On coordination the azomethine nitrogen, $\nu[^7C=^1N]$ shifts to lower wavenumbers by 21-34 cm^{-1}. The lowering in the frequency region 1600 -1580 cm^{-1} is observed in complexes indicating the involvement of the azomethine nitrogen atom in coordination. It is further confirmed by the presence of a new band at 443 cm^{-1} assignable to ν(Mn-N) for these complexes. The increase in $\nu(^1N-^2N)$ in the spectra of complexes is due to the increase in double bond character offsetting the loss of electron density *via* donation of the metal is a another confirmation of the coordination of the donors through the azomethine nitrogen.

The ligand and the complexes show an intense peak at 3150 cm^{-1} that is characteristic of the –N-H stretching, indicating the existence of free –N-H group .The band in the region 2600-3800 cm^{-1} of the IR spectra of O-N-S donors suggests the presence of thioketo form in the solid state. The O-N-S donors show a strong and medium band in the region 1371 and 1362 cm^{-1} due to ν(C=S) stretching but no band due to ν(S-H) near 2570 $cm.^{-1}$ Coordination *via* the sulphur atom is indicated by a decrease in the frequency of the thioamide band by 47 to 49 cm^{-1}. The thioamide (1V) band appears at *ca* 804 cm^{-1} and 839 cm^{-1} is shifted by approximately 37 cm^{-1} in the spectra of complexes, indicating coordination of the thione sulphur atom. Thus a substantial shift to lower energies of the above two bands is an indicative of thione coordination. This fact can be due to both a decrease in the double bond character of C=S bond and the change in the conformation along N-C bond on complexation [9]. The presence of a new band at *ca* 410 cm^{-1}, which is assignable to ν(Mn-S), is another indication of involvement of sulphur coordination. In H_2SAP and H_2APP, the ν(O-H) band appears at 3383 and 3410 cm^{-1} respectively. The phenolic oxygen by loss of proton occupies the third coordination site, causing ν(C-O) to shift to lower wave numbers by 82 cm^{-1}. The presence of a non-ligand band in the region 341-343 cm^{-1} that is assignable to ν(Mn-O) further confirms phenolic oxygen coordination.

7.3.3 Electronic spectra.

Electronic spectra of complexes were recorded in polycrystalline state (Fig. 7.1) and in solution (DMF / dichloromethane) and the details are presented in Table 7.3

The Mn(II) complexes with high spin d^5 state register no characteristic bands in the visible region. However, the two broad bands at 392 and 406 nm are typical charge transfer transitions as expected for octahedral manganese(II) complex [10]. The six coordinate high spin manganese(II) belongs to the d^5 system. The Tanabe-Sugano diagram corresponding to such a system shows that the only high spin state Russell-Saunders term is ^6S which in an octahedral geometry, changes its notation to $^6A_{1g}$. Since there is no excited state with the spin multiplicity 6, all electronic transition in a high spin d^5 complexes are doubly forbidden (Laporte forbidden and spin forbidden) [11]. Consequently all electronic transitions have an extremely low molar extinction coefficient value and hence it is difficult to locate these doubly forbidden transitions. In the visible region, the complexes show weak absorption and it suggests a near octahedral geometry around manganese(II). It is attributed to forbidden nature of spin doublets [12]

.The electronic spectra of manganese(II) complexes with O-N-S donors have high intensity charge transfer. The intense peaks in the visible region ($\log \epsilon \approx 3$), is attributed to the intensity stealing influence of the sulphur containing ligands. The shoulders in the 455, 527 and 624 nm are attributed to the LMCT of phenolate and thiolate to Mn(II).

The shoulders seen at *ca* 552, 446, 406 and 392 nm represent the following transitions which in terms of Racah parameters are

$^6A_{1g} \rightarrow {}^4T_{1g}$ ($E = 18100\ cm^{-1}$), $\epsilon = 0.01332\ L\ mol^{-1}\ cm^{-1}$ [10B+5C]

$^6A_{1g} \rightarrow {}^4T_{2g}$ ($E = 22400\ cm^{-1}$), $\epsilon = .009260\ L\ mol^{-1}\ cm^{-1}$ [10B+5C]

$^6A_{1g} \rightarrow {}^4E_g$ ($E = 24600\ cm^{-1}$), $\epsilon = 0.0323\ L\ mol^{-1}\ cm^{-1}$ [17B+5C]

$^6A_{1g} \rightarrow {}^4A_{1g}$ ($E = 25500\ cm^{-1}$), $\epsilon = 0.01425\ L\ mol^{-1}\ cm^{-1}$ [7B+5C].

Table 7.1
Analytical data,conductivity, magnetic moments, colours and yields of complexes of Mn(II) with N-N-Sand O-N-S ligands [a)]

Compound	Emp.formula [b)]	Yield (%)	Colour	μ[c)](BM)	ΛM [d)]	Analytical data Found / (Calculated) %			
						C	H	N	Mn
$Mn(L4M)_2$,34	$C_{24}H_{31}N_8O_2S_2Mn$	67	Yellow	6.014	5.5	49.33 (49.56)	5.28 (5.20)	19.45 (19.27)	9.52 (9.45)
$Mn(L4P)_2$, 35	$C_{24}H_{31}N_8S_2Mn$	63	Yellow	5.912	6.3	52.22 (52.45)	5.21 (5.50)	20.53 (20.39)	9.88 (9.98)
$Mn(HSAP)_2$, 36	$C_{24}H_{29}N_6O_2S_2Mn$	68	Black	5.990	6.1	52,43 (52.26)	5.08 (5.12)	15.39 (15.24)	10.06 (9.96)
$Mn(HAPP)_2$, 37	$C_{26}H_{33}N_6O_2S_2$	63	Black	6.102	6.5	53.54 (53.87)	5.62 (5.56)	14.33 (14.50)	9.73 (9.48)

[a)] In parentheses calculated values. [b)] Emperical formula. [c)] Magnetic moment [d)] Molar conductivity,10^{-3}M solution(DMF) at 298 K

Table.7.3 Electronic(Diffuse reflectance) spectral data of Mn(II) with N-N-S and O-N-S ligands (nm) and Racah parameters

Compound	$^6A_{1g} \rightarrow {}^4T_{1g}$	$^4T_{2g} \rightarrow {}^6A_{1g}$	$^6A_{1g} \rightarrow {}^4E_g$	$^4A_{1g} \rightarrow {}^6A_{1g}$	$n \rightarrow \pi^*$	$\pi \rightarrow \pi^*$	B(cm^{-1})	B (B/B_0)	Dq (cm^{-1})	C(cm^{-1})
$Mn(L4M)_2$	553	446	406	392	317	277	694	0.81	8584	2232
$Mn(L4P)_2$	551	448	402	395	315	279	688	0.80	8448	2256
$Mn(HLSAP)_2$	552	446	402	392	320	273	690	0.80	8533	2246
$Mn(HLAPP)_2$	554	440	405	393	330	269	694	0.80	8744	2222

Table.7.2
IR spectral assignments (cm^{-1}) of Mn (II) complexes with N-N-S and O-N-S donors

compound	$\nu(^6C=^2N)$	$\nu(^3N-^8C)$	$\nu(^2N-^3N)$	ν(C=S)	δ(C=S)	δo.p	δi.p	ν(Mn-N)	ν(Mn-S)	$\nu(Mn-N)_{py}$
HL4M	1627 s	---	1010 m	1371 s	892 m	649 m	408 m	---	---	---
$Mn(L4M)_2$	1592 s	1450 s	1029 m	1301 s	840 m	66 2 m	418 m	521 w	416 m	318 m
HL4P	1604 sh	---	998 m	1380 s	843 w	63 7 m	406 m	---	---	---
$Mn(L4P)_2$	1581 s	1476 s	1019 m	1310 s	785 m	648 m	418 m	522 m	416 m	314 m

compound	$\nu(^7C=^1N)$	$\nu(^3N-^8C)$	$\nu(^1N-^2N)$	ν(C=S)	δ(C=S)	ν(C-O)	----	ν(Mn-N)	ν(Mn-S)	ν(Mn-O)
H2SAP	1634 s	1495 s	1000 m	1371 m	804 m	1270 s	---	---	---	---
$Mn(HLSAP)_2$	1593 s	1453 s	1055 m	1322 s	778 m	1188 s	---	448 w	410 m	343 m
H2APP	1602 s	1491 s	996 m	1362m	839 m	1253 s	---	---	---	---
$Mn(HLAPP)_2$	1589 s	1457 s	1058 m	1315 s	791 m	1171 s	---	443 sh	412 m	341 m

S=strong; m=medium; w=weak; sh=shoulder

Table.7.4
EPR spectral data, cyclic voltammetric and antimicrobial data of Mn(II) complexes with N-N-S and O-N-S donors

compound	g_o [a]	g_{iso} [b]	A_{iso} [c]	Oxidation(E)V	Reduction(E)V	Con/Disc in.µg	1*	2*	3*	4*	MIC in µl			
											1*	2*	3*	4*
$Mn(L4M)_2$	2.0095	2.0089	90G	0..65, 0.89	0.68, 0.82, 1.3	50	+14	+11	+20	+12	1	2	1	2
$Mn(L4P)_2$	2.001	1.9996	85G	0.47, 0.67 , 0.90	0.62, 0.94	50	+14	+13	+20	+13	1	2	1	1
$Mn(HLSAP)_2$	1.9992	1.9996	95G	0.41, O.69	0.59, 0.93	50	+10	---	+13	---	2	--	1	2
$Mn(HLAPP)_2$	2.0105	2.0089	88G	0.39, 0.65	0.56, 0.90	50	+10	---	+14	---	2	--	1	---

[a] = (polycrystalline) 298 K [b] = (DMF solution) 77 K, [c] = (DMF solution) 77 K

1* =*Staphylococcus aureus*, 2*=*Salmonella paratyphi* , 3*=*Shigella sp*, 4*=*Vibreo parahaemolyticus.*

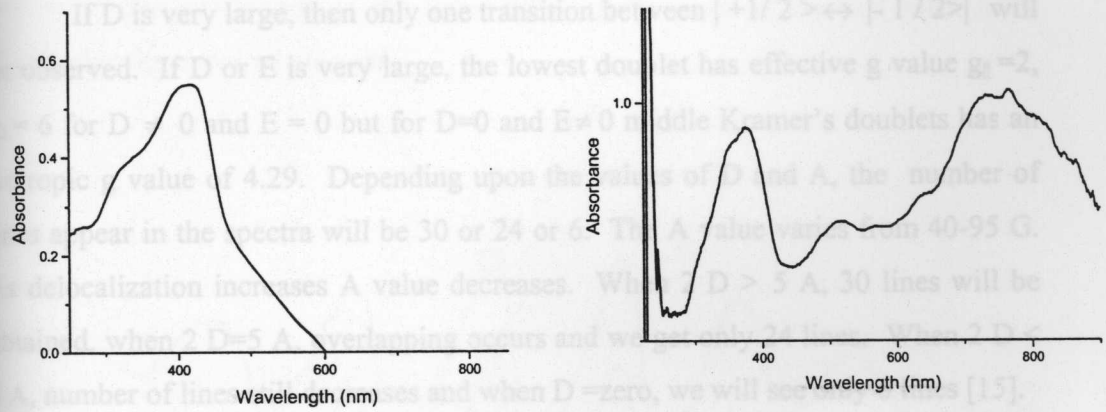

Fig 7.1 UV-Vis DRS of manganese complexes

The energies of last two transitions are independent of Dq, but dependent only on the values of Racah parameters B and C and hence one can obtain the values of B, C and Dq from the Tanabe–Sugano diagram for ^{5}d systems [13]. The results have been calculated and presented in Table 7.3. The B values are lower than free ion value for octahedral environment showing distortion from regular octahedral geometry and C values are almost consistent with reported results for similar kind of complexes. These transitions are characteristics of a tetragonally distorted octahedral environment of d^5 ion. The $n \rightarrow \pi^*$ and $\pi \rightarrow \pi^*$ transitions (intra ligand transitions) remained almost unaltered.

7.3.4 EPR spectra

The spin Hamiltonian, $H = g\beta H_s + D\,[S^2_z - S(S+1)] + E(S^2_x - S^2_y)$ may be used to describe the EPR spectra of Mn(II) complexes. In the expression H is the magnetic field vector, D is the axial zero field splitting term and E is the rhombic zero field splitting parameter.[14]. If D and E are very small compared to $g\beta H_s$, five EPR transitions are expected with g value of 2.0. $|+5/2> \leftrightarrow |+3/2>, |+3/2> \leftrightarrow |+1/2>$ $|+1/2> \leftrightarrow |-1/2>, |-1/2> \leftrightarrow |-1/2>$ and $|-3/2> \leftrightarrow |-5/2>$.

If D is very large, then only one transition between $|+1/2> \leftrightarrow |-1/2>|$ will be observed. If D or E is very large, the lowest doublet has effective g value $g_{\|} = 2$, $g_{\perp} = 6$ for $D \neq 0$ and $E = 0$ but for $D=0$ and $E \neq 0$ middle Kramer's doublets has an isotropic g value of 4.29. Depending upon the values of D and A, the number of lines appear in the spectra will be 30 or 24 or 6. The A value varies from 40-95 G. As delocalization increases A value decreases. When $2D > 5A$, 30 lines will be obtained, when $2D = 5A$, overlapping occurs and we get only 24 lines. When $2D < 5A$, number of lines still decreases and when D =zero, we will see only 6 lines [15].

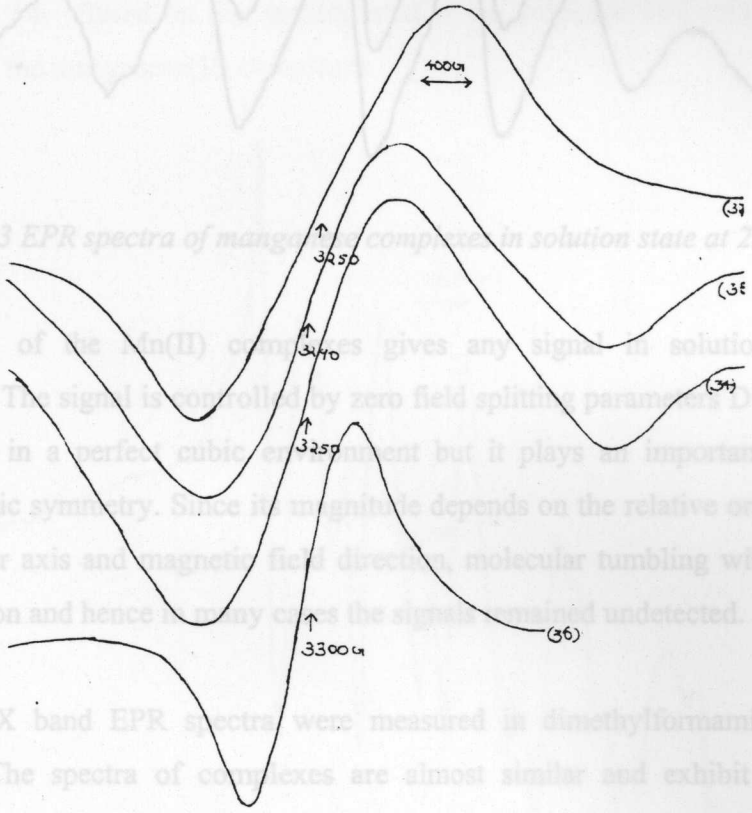

Fig 7.2 EPR spectra of manganese complexes in polycrystalline state at 298 K

In the polycrystalline state at room temperature, Mn(II) complexes give very broad signals (Fig. 7.2) due to dipolar interactions and enhanced spin lattice relaxation. Another reason attributed to broad signals is restriction of rotational motion of Mn(II) [16]. The higher *g* values is suggestive of spin orbit coupling and

the promotion of electron in the inner filled ligand levels to the half filled levels containing the unpaired electron.

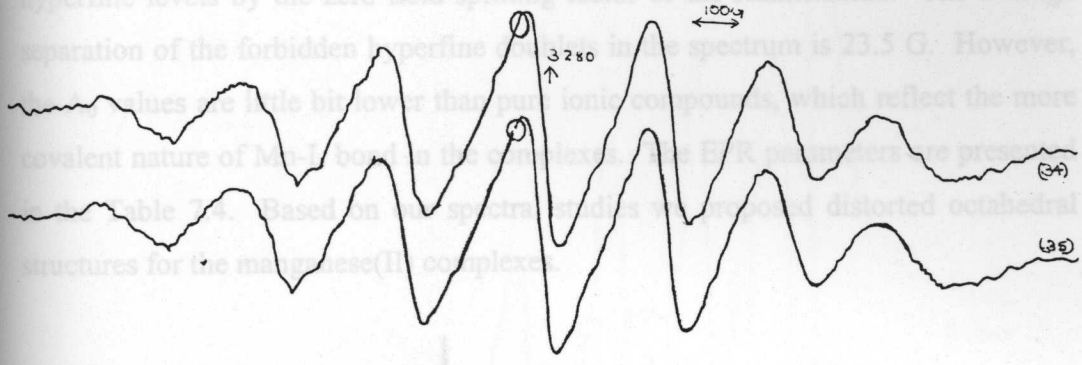

Fig 7.3 EPR spectra of manganese complexes in solution state at 298 K

None of the Mn(II) complexes gives any signal in solution at room temperature. The signal is controlled by zero field splitting parameters D and E. It is insignificant in a perfect cubic environment but it plays an important role in a distorted cubic symmetry. Since its magnitude depends on the relative orientation of the molecular axis and magnetic field direction, molecular tumbling will modulate this interaction and hence in many cases the signals remained undetected.

The X band EPR spectra were measured in dimethylformamide at 77K (Fig.7.4). The spectra of complexes are almost similar and exhibit a six line manganese hyperfine pattern centered at g =2.001 and coupling constant A_0, = 95 G, which is that expected of an odd unpaired electron system (S=± 5/2), m_S = ± 5/2, ± 3/2 ,± 1/2 and I= 5/2,m_I =±5/2, ±3/2 ,±1/2, with g and A tensors isotropic, resulting from allowed transitions (Δm_S= ± 1, Δm_I =0). The observed g values are very close to the free electron spin value of 2.0023 which is consistent with the typical manganese(II) and also suggestive of the absence of spin orbit coupling in the ground

state $^6A_1$with out another sextet term of higher energy [17]. The A_0 values are consistent with octahedral coordination. Besides, between every adjacent pair of the allowed six hyperfine lines of the $g \approx 2$, resonance there is a pair of relatively weak "forbidden "($\Delta m_S = \pm 1$, $\Delta m_I = 0$) transition. This is due to the mixing of nuclear hyperfine levels by the zero field-splitting factor of the Hamiltonian. The average separation of the forbidden hyperfine doublets in the spectrum is 23.5 G. However, the A_0 values are little bit lower than pure ionic compounds, which reflect the more covalent nature of Mn-L bond in the complexes. The EPR parameters are presented in the Table 7.4. Based on our spectral studies we proposed distorted octahedral structures for the manganese(II) complexes.

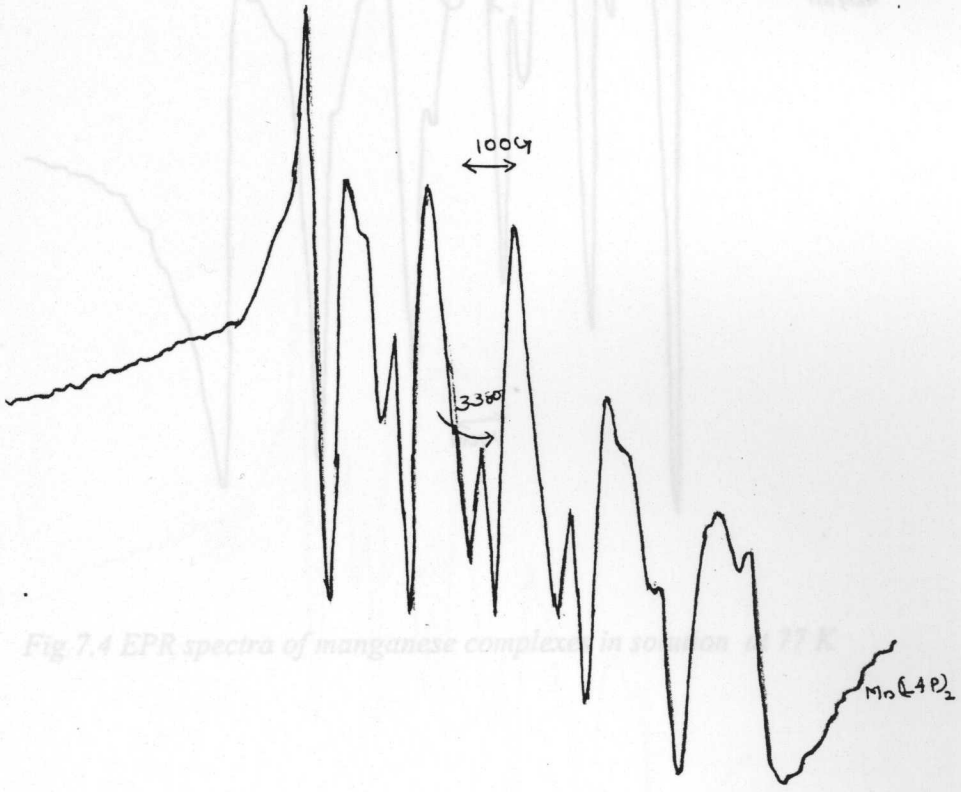

Fig 7.4 EPR spectra of manganese complexes in solution at 77 K

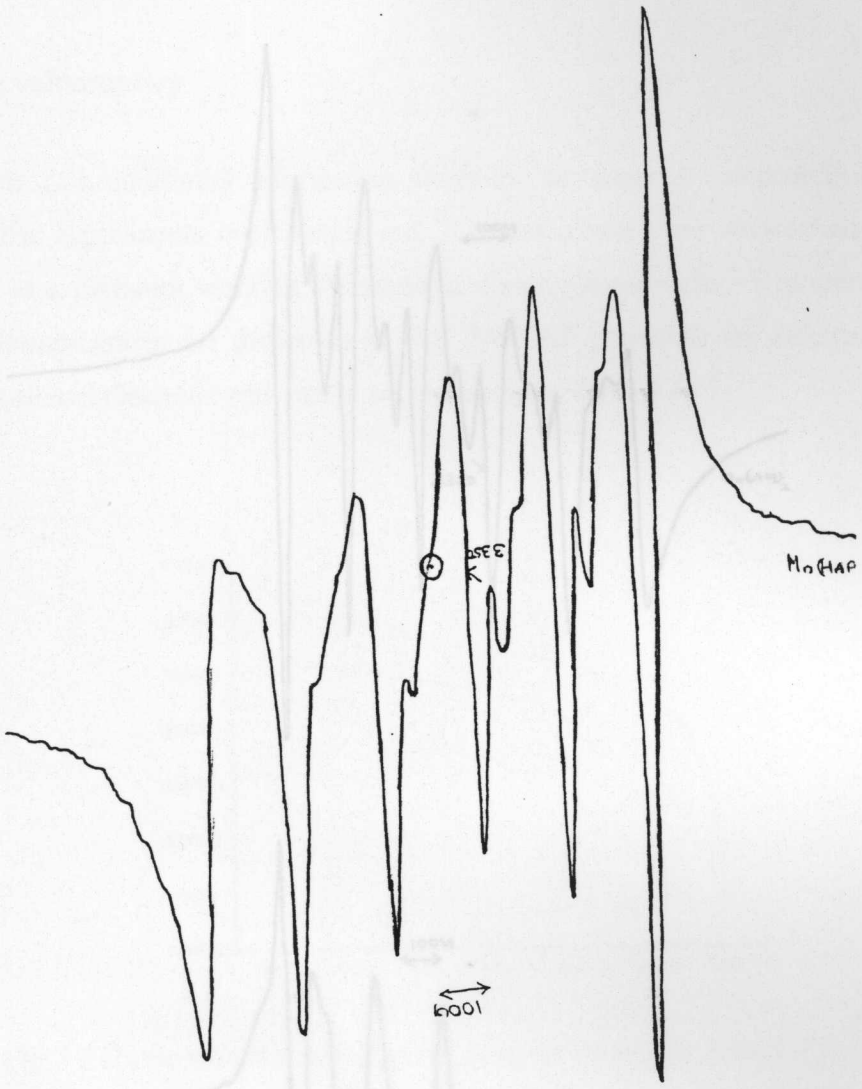

Fig 7.4 EPR spectra of manganese complexes in solution at 77 K

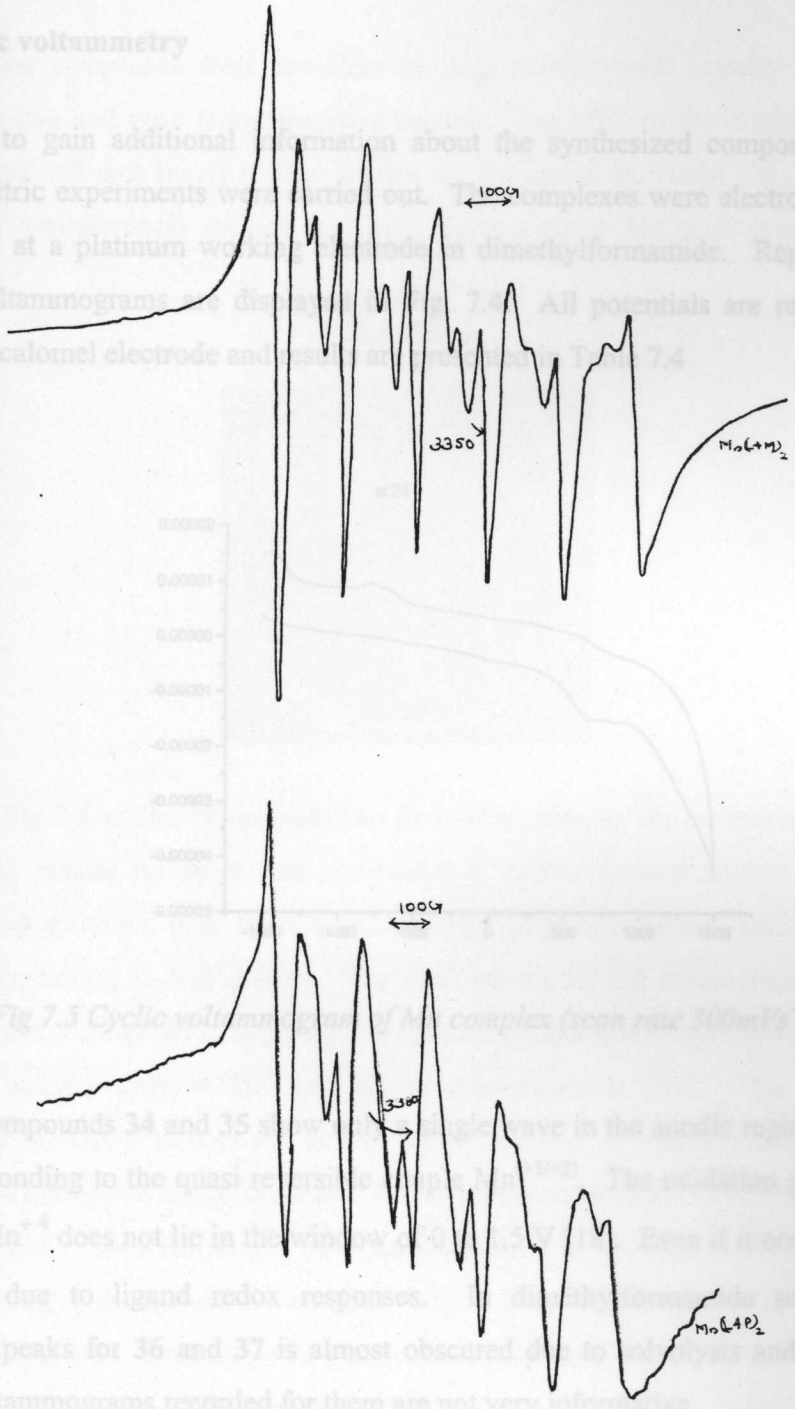

Fig 7.4 EPR spectra of manganese complexes in solution at 77 K

7.4 Cyclic voltammetry

In order to gain additional information about the synthesized compounds cyclic voltammetric experiments were carried out. The complexes were electrochemically examined at a platinum working electrode in dimethylformamide. Representative cyclic voltammograms are displayed in Fig. 7.4. All potentials are referred to a saturated calomel electrode and results are presented in Table 7.4

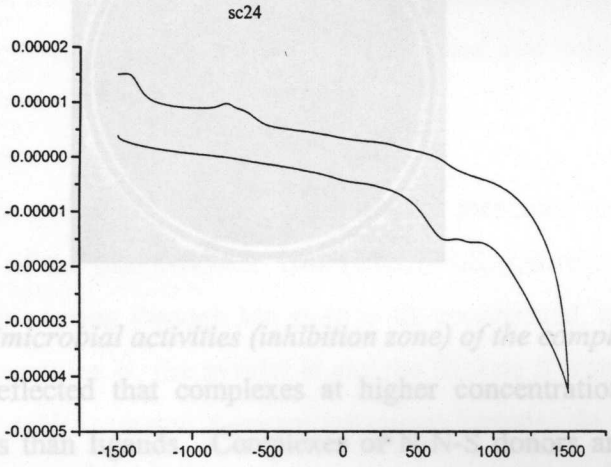

Fig 7.5 Cyclic voltammogram of Mn complex (scan rate 300mVs^{-1})

Compounds **34** and **35** show only a single wave in the anodic region at +0.89 V corresponding to the quasi reversible couple $Mn^{(+3/+2)}$. The oxidation potential of $Mn^{+3} \rightarrow Mn^{+4}$ does not lie in the window of 0 to 1.5 V [18]. Even if it occurred, it is obscured due to ligand redox responses. In dimethylformamide solution the oxidation peaks for **36** and **37** is almost obscured due to solvolysis and hence the cyclic voltammograms recorded for them are not very informative.

7.5 Biological activity

All the four complexes were screened for their antimicrobial activity against two Gram positive and nine Gram negative bacteria .The MIC of the compounds were also determined and result of our studies are presented in Table 7.4. Procedural details of antimicrobial studies and MIC determination are well documented in Chapter 3

Bacillus sp

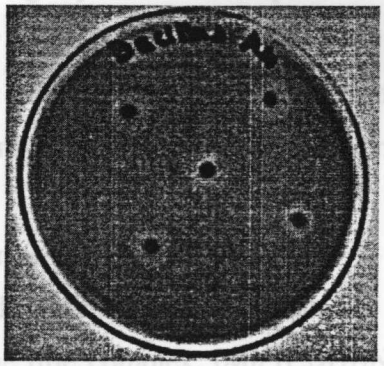

Fig 7.5 antimicrobial activities (inhibition zone) of the complexes

The results reflected that complexes at higher concentrations have more antibacterial activities than ligands. Complexes of N-N-S donors are more active than corresponding O-N-S donors. The MIC values for the compounds supported this argument. Compared to copper(II) complexes manganese complexes show, even, moderate activity only at 10^2 fold higher concentrations [19]. The manganese complexes of N-N-S donors are active against *Bacillus sp,Staphylococcus aureus, Salmonella paratyphi, Shigella sp and, Vibrio parahaemolyticus*. The complex of 2-acetylpyridine ^{4}N-pyrrolidine thiosemicarbazone is more active than the corresponding manganese complex of 2-acetylpyridine ^{4}N-morpholine thiosemicarbazones. Both show very high activity against *Shigella sp* and the activity is comparable to copper(II) complexes of N-N-S donors.. The complexes of O-N-S donors are active only against *Staphylococcus aureus* and *Shigella sp* at higher concentration.

7.6 X-ray diffraction studies of bis(2-acetylpyridine -$_K$N-phenylthiosemicarbazonato K^2N^1,S) manganese(II), [Mn ($C_{14}H_{13}N_4S)_2$],

The title complex was reported elsewhere [20] but to our best of knowledge, no attempt was made on its crystal studies.

7.6.1 Synthesis of complex

An ethanolic solution of $MnCl_2.4H_2O$ and HL (ligand) in 1:2 molar ratios was warmed for 1 h to yield a light yellow colored product. Reddish brown monoclinic single crystals suitable for X-ray diffraction studies were grown by slow evaporation of a dilute solution of the title complex in dimethylformamide. The reddish brown crystals formed after twenty days were isolated and dried and subjected to X-ray diffraction studies.

7.6.2 Description of crystal structure.

Details of crystal data and structure refinement data are presented in Table 7.5.One half of the molecule of the title complex, [Mn ($C_{14}H_{13}N_4S)_2$],is related to the other half by a twofold axis passing through Mn atom is six coordinated, in an octahedral geometry, by the azomethine N, the pyridyl N and the thiolate S atom of two planar 1-pyridin -2-ylethanoneN(4)-phenyl thiosemicarbazones ligands. In the crystal, the molecule are interconnected by N-H---S and C-H---N interactions, forming a three dimensional network.

The six coordinate distorted octahedral high-spin Mn(II) complex containing two-deprotanated ligand has a structure, identical to the closely related Fe(III) and Co(III) species where the two coordinating azomethine nitrogen atoms are trans to each other and the other two sets of identical donor atoms are *cis* to each other. The title compound crystallizes in to a monoclinic C2/c space group symmetry. The perspective view of the complex (Fig.7.4) shows that the thiosemicarbazones is functioning as N-N-S donor ligand and it is coordinated in a meridonal arrangement [21]. The selected bond lengths and bond angles are presented in Table.7.6.

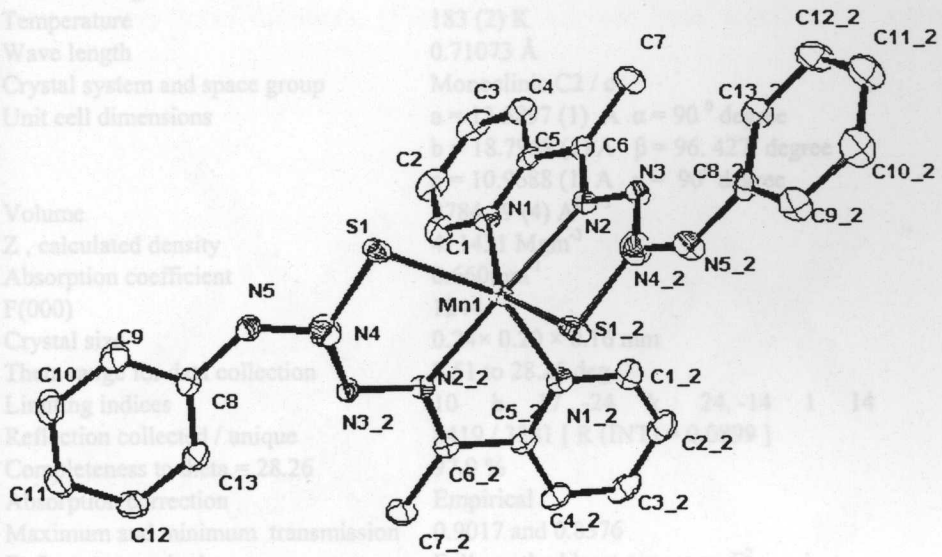

Fig 7.6 ORTEP diagram of the title complex in 50% probability level. Hydrogen atoms are removed for clarity.

As observed, one L, and azomethine nitrogen of the other ligand are approximately in the same plane of the Mn atom exhibiting considerable distortion from octahedral symmetry indicated by the bond angles N2-Mn1-N2-2 (170.41°) and N1-Mn1-S1-2(147.77°). The apical positions of the octahedron are occupied by one of the nitrogen N1 of the pyridine ring and S1 of the same ligand with bond lengths 2.262 Å(Mn1-N1) and 2.513 Å (Mn1-S1). The bond angles N2-Mn1-N2-2 (170.41°) and N1-Mn1-S1-2 (147.77°), N2-Mn1-N1 (71.62°) and S1-Mn1S1-2 (101.08°) are quite far from a perfect octahedron indicating considerable distortion in the geometry. Co ordination lengthens the thiosemicarbazone moiety's C8- S1 bond from 1.699 Å to 1.739 Å and shortens C8-N3, a partial double bond character. Comparatively larger bond lengths Mn1-N2 (2.252 Å), Mn1-S1 (2.5132 Å) and Mn1-N1 (2.262 Å) indicate weak coordination (21) of the ligand with Mn(II). The azomethine (N2) nitrogens of the ligands are *trans* to each other and the other two sets of donor atoms

Table 7.5
Crystal data and structure refinement for the compound

Empirical formula	$MnC_{28}H_{26}N_8S_2$
Formula weight	593.630
Temperature	183 (2) K
Wave length	0.71073 Å
Crystal system and space group	Monoclinic,C2 / c
Unit cell dimensions	a = 13.5897 (1) A $\alpha = 90^0$ degree
	b = 18.7968 (1) A $\beta = 96.427^0$ degree
	c = 10.9688 (1) A $\gamma = 90^0$ degree
Volume	2784.29 (4) $A^{0\ -3}$
Z , calculated density	4. 1431 Mgm^{-3}
Absorption coefficient	$0.660mm^{-1}$
F(000)	1244
Crystal size	0.24× 0.20 × 0.16 mm
Theta range for data collection	2.51 to 28.26 deg
Limiting indices	10 h 17 , -24 k 24, -14 1 14
Reflection collected / unique	8419 / 3381 [R (INT) = 0.0899]
Completeness to theta = 28.26	97.9 %
Absorption correction	Empirical
Maximum and minimum transmission	0.9017 and 0.8576
Refinement method	Full- method least square on F^2
Data / restraints / parameters	3381 / 0 / 178
Goodness of fit on F^2	0.986
R indices (all data)	RI = 0.0784, wR2 = 0. 1650
Final R indices	[1>2 σ (1)] RI = 0.0543, wR2 = 0.1474
Largest diff.peak and hole	0.772 and – 1.334 e. A^{-3}

Table 7.6
Selected bond lengths (Å) and angles (deg) for the compound

bond lengths (Å)		bond angles (deg)	
N1-Mn1	2.262	N1-C1-C2	122.59
N2-Mn1	2.252	N2-C6-C5	115.72
S1-Mn1	2.513	N2-C6-C7	123.30
Mn1-N2	2.252	C13-C8-N5	125.96
Mn1-N1	2.262	C1-N1-Mn1	123.78
Mn1-S1	2.513	C5-N1-Mn1	117.11
N2-N3	1.378	C6-N2-N3	115.63
N3-C8	1.315	C6-N2-Mn1	119.66
N3-N2	1.378	N3-N2-Mn1	124.30
N4-C8	1.378	N3-C8-S1	128.56
C8-N3	1.315	N2-Mn1-N2-2	170.40
S1-C8	1.739	N2-Mn-N1	71.62
C1-N1	1.332	N2-Mn1-N1-2	101.58
C4-C5	1.392	N2-Mn1-S1	110.19
C5-N1	1.362	N2-Mn1-S1	76.19
C6-N2	1.298	N1-Mn1-N1-2	93.46
C9-N4	1.404	N1-Mn1-S1	91.45
C9-C10	1.408	N1-Mn1-S1-2	147.77
N1-C1	1.332	S1-Mn1-S1-2	101.08

viz, thiolate sulphur (S1) and pyridine nitrogen (N1) are *cis* to each other [22]. In the crystal of the title complex, pairs of molecules are related by crystallographic inversion centers form dimmers, (Fig 7.7) which are held together by hydrogen bonds.

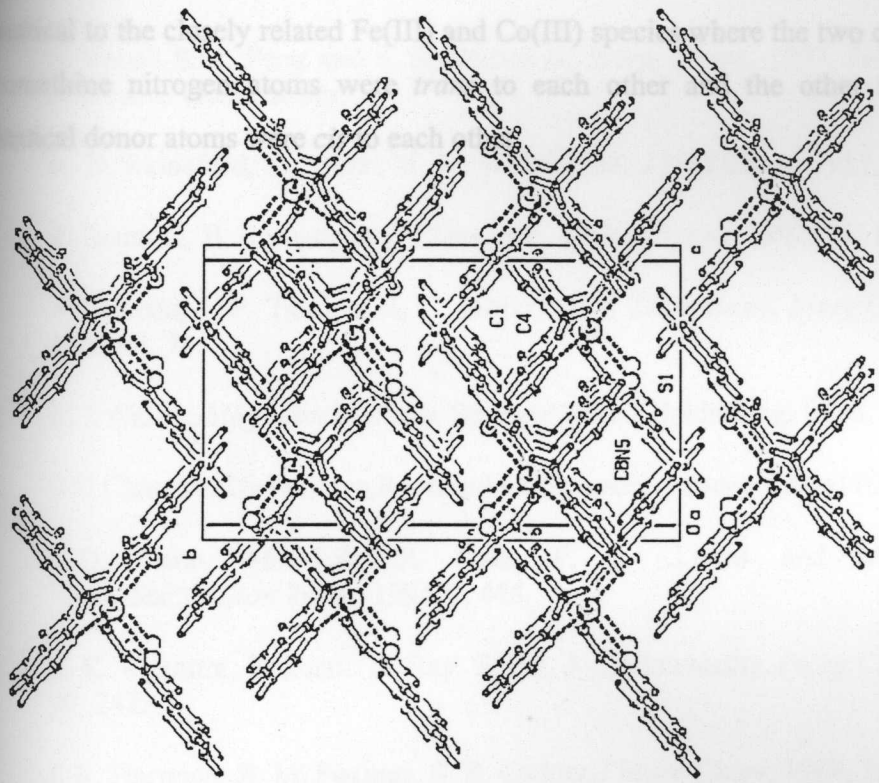

Fig 7.7 packing of the compound viewed along a axis

7.7 Concluding remarks

We synthesized four high spin manganese(II) complexes with monoanionic N-N-S and O-N-S donors. In Complexes with N-N-S donors, thiolate sulphur and with O-N-S donors thione sulphur were coordinated. From the electronic spectral data of complexes we , calculated Racah parameters and the values were in good agreement with reported results for similar types of ligands. From the EPR spectra of the complexes we calculated bonding and spin Hamiltonian parameters and the results

showed an octahedral EPR symmetry and considerable covalency in metal ligand bonding. The cyclic voltammetric studies opened the window for $Mn^{+3/+2}$ redox couple. The complexes were found to be moderately active against certain selected clinical pathogens. Single crystal studies of the six coordinate distorted octahedral high - spin Mn(II) complex containing two-deprotanated ligand had a structure, identical to the closely related Fe(III) and Co(III) species where the two coordinating azomethine nitrogen atoms were *trans* to each other and the other two sets of identical donor atoms were *cis* to each other.

References

1 D. Evans K. S. Hallwood C. H. Cashin H, Jackson, *J Med Chem* 1967, **10**, :4235.

2 F. Basuli S.M. Peng and S. Bhattacharya, *Inorg. Chem.* 1997, **36** 5645, and references cited therein.

3 K. D. Rainsford, K. Brune, M. W. Whitehouse, *J Med Chem*, 1981, **2**, 865.

4 B. Samiran, B. Ramgopal, *J. Chem. Soc., Dalton Trans.* 1992, **14**, 1357.

5 A. Saxena, J. P. Tandon, K. C. Molloy, J. J. Zuckerman, *Inorg.Chim. Acta*, 1982 **63**, 71.

6 R. L Carlin, *Magnetochemistry*, Springer,Berlin,Heidelberg, 1986, 346.

7 S.K.Chandra,KSrivastava,RainaandA.Chkravorthy,*Inorg.Chem*1992,**31**,760.

8 G.D. Cano, M. J.Sanz,R. Ruiz, F. L. .J.Faus and M. Julve,*J. Chem.Soc.,Dalton Trans,* 1994, **3**, 465.

9 S. K. Chandra, P. Basu.. D. Ray, S. Pal, A.Chakravorthy,.*Inorg.Chem*, 1990, **29**, 2423.

10 J. R. Hartman, B. M. Foxman, S. R. Cooper,*J Inorg Chem*, 1984, **23** 1381.

11 W. Linert,F. Renz and R. Boca, *J.Coord Chem*, 1996.vol **40** 293

12 S. Purohit, A.P. Koley, L.S. Prasad, P.T. Manoharan, S. Ghosh, *Inorg. Chem.* 1989, **28,** 3735.

13 B. A. Gingras, A. F. Sirianni, *Can. J. Chem.* 1964, **42,** 17.

14 J. E. Wertz and J. R. Bolton,*Electron spin resonance Elemental theory and practical applications*,Chapman and Hall, Ltd, 1986, W**47**, p 335.

15 F. Tisato, F. Refosco, G. Bandoli, *Coord. Chem. Rev.* 1984, 135:1363.

16 M. A. Ali, D. A. Chowdhury, I. M. Nazimuddin, *Polyhedron* 1984, **3**, 595.

17 C. A.Brown, W. Kaminsky and D. X. West, *JBraz.Chem.Soc,*2002, **113**,1,10

18 G.Blandin, R. Davyoda, M. F. Charlot, S. Strying and A. Boussac,*J.Chem. Soc,Dalton Trans.*, 1997, **34**, 4069.

19 N. I. Dodoff, M Kubiak, and J. K. Jaworska, Text book of *Molecular Biology* Bulgarian Academy of Sciences, 1976, 21,1113

20 M. R. P. Kurup, Original thesis, Dept. of Chemistry,University of Delhi,1988.

21 T. Nyokong,Z. Gasyna, M. Stillman, *J. Inorg.Chem*,1987, **26,** 1097.

22 F.J.Femia,X.Chen,J.W.Babich, J. Zubieta, *Inorg. Chim. Acta*, 2002, **307** 149.

Chapter

8

SPECTRAL, BIOLOGICAL (STRUCTURE – ACTIVITY RELATION) AND ELECTROCHEMICAL STUDIES OF Ni(11) COMPLEXES WITH STUDIES OF $[Ni(HL4A)_2](ClO_4)_2 . H_2O$

8.1 Introduction

Nickel with atomic number 28 and atomic weight 58.70 is discovered by Cronstedt in 1751 from mineral niccelite. Ni is found as a constituent in most meteorites and often serves as one criterion for distinguishing a mineral from other mineral from meteorites. Usually they contain 5 to 20% .of nickel. It is reported [1] to be a genotoxic carcinogen but exact mechanism for nickel toxicity is not known. Ni can serve as a weak substitute for Mg in some polymerases of biological importance.

Ni(II) complexes show a diamagnetic behavior consistent with square planar environment or a paramagnetic behavior consistent with an octahedral or square planar environment around the metal atom. Five coordinate geometry is quite unusual in Ni(II) complexes however, there are reports on such complexes [2]. Octahedral Ni(II) has an orbitally nondegenerate $^3A_2$ ground state and magnetic moments are in the range of 2.8-3.3 B.M which is very close to spin only value of 2.828 B.M. Tetrahedral Ni(II) has a $^3T_1$ ground state and magnetic moments are in the range of 4 to 4.3 B.M. Both octahedral and tetrahedral complexes have two unpaired electrons; the latter is having higher magnetic moments. Nyholm had suggested an inverse relation ship between the magnetic moments and the distortion from tetrahedral geometry. Though square planar Ni(II) complexes are diamagnetic, there are reports [3] on weakly paramagnetic Ni(II) complexes with low spin. To

explain this phenomenon equilibrium between spin free and spin paired configuration is suggested.

This Chapter describes the syntheses, spectral characterization and antimicrobial studies of four square planar and one octahedral complexes of Ni(II) with N_2S donor ligands along with X-ray diffraction studies of the latter, which is having unusual thione sulphur coordination.

8.2 Experimental

8.2.1 Materials and methods

The thiosemicarbazones HL4M, .HL4P and HL4M were prepared and characterized as described in Chapter 2. Various nickel salts (Reagent grade, E. Merck) were purified by standard methods. Nickel perchlorate prepared from corresponding carbonate was purified by recrystallisation. The solvents were purified by standard procedure before use.

8.2.2 Measurements

The details of elemental analysis, conductivity, magnetic moments IR UV-Visible and NMR spectral techniques are described in Chapter 2. The metal content was estimated by conventional gravimetric methods and atomic absorption spectroscopy in a Perkin –Elmer Analyst 700 spectrometer, after decomposing the compounds by standard methods. Details of antimicrobial studies are described in Chapter 3.

8.2.3 Preparation of the complexes.

The general method of synthesis of nickel(II) complexes is as described below.

To a hot methanolic solution (20 mL) of the thiosemicarbazone (1 mmol) was added 15 mL of methanolic solution of nickel(II) salt (1 mmol) with constant stirring. The solution after refluxing for 2 h was allowed to cool to room temperature, when micro crystals of the nickel(II) complexes were crystallized out. The separated crystalline complexes were separated by filtration, washed well with hot water,

methanol and ether and dried in *vacuo* over P_4O_{10}. The thiocyanato complex was prepared by taking nickel acetate, ligand and potassium thiocyanate in the proportion 1:1:1.3 by the same procedure. The perchlorate complex was prepared by taking 1:2 metal to ligand ratio by the same method.

The synthesized complexes are, [Ni(L4M)NO_3],**38**; [Ni(L4M)NCS].H_2O,**39**; [Ni(L4M)ClO_4]. H_2O, **40**; [Ni(L4P)Cl], **41** and [Ni(HL4A)$_2$]$(ClO_4)_2$. H_2O, **42**.

8.3 Results and discussion

The new compounds are stable at room temperature and non-hygroscopic. The colours, elemental analyses, stoichiometries, conductivities and magnetic moments of Ni(II) complexes with N-N-S donors are presented in Table 8.1. The N-N-S donors are pleasant yellow, while complexes prepared from them are light to deep brown. Analytical data show the presence of one nickel atom, one molecule of mono anionic thiosemicarbazone and one polyatomic anion in complexes **38** to **41** where as complex **42** contains one nickel atom, two molecules of thiosemicarbazones, two polyatomic monoanion and one molecule of water. These complexes are insoluble in most of the organic solvents, however soluble in dimethylformamide, dimethyl sulphoxide and chloroform. Molar conductivities in dimethylformamide solution (10^{-3} M) are much lower than that expected for uni-univalent electrolytes and the results indicate their nonelectrolytic nature. However, **42** shows very high molar conductivity and it corresponds to 1:2 electrolyte.

8.3.1 Magnetic susceptibility

The room temperature magnetic susceptibility of the complexes, **38** to **41** in the polycrystalline state shows diamagnetic nature and the results are in agreement with a square planar geometry for the complexes [4]. The perchlorate complex **42** has magnetic moment 3.11B.M, which is close to spin only value of 2.8 B.M. An octahedral geometry is most suitable for the complex because for a tetrahedral

complex, the magnetic moment will be ≈ 4 B.M. The proposed octahedral geometry for the complex is supported by IR spectral and X-ray diffraction studies.

8.3.2 Vibrational spectra.

The significant IR bands of N_2S ligands and their Ni(II) complexes along with their tentative assignments in the range 4000-200 cm^{-1} are presented in Table 8.2.

With monoanionic N_2S donors, coordination is expected *via* pyridine nitrogen, azomethine nitrogen and thiolate sulphur. On coordination of azomethine nitrogen ν(C=N) shifts to lower energy by 7 to 38 cm^{-1}. The band shifting from *ca* 1627 cm^{-1} in the uncomplexed thiosemicarbazones spectra to 1589 cm^{-1} in the spectra of the complexes and ν(N-N) shifts to higher frequency side in all, is a clear sign of enolisation and coordination *via* the azomethine nitrogen atom. A new band in the range 435 to 485 cm^{-1} is assigned for the ν(Ni-N) azomethine, confirms the involvement [5] of azomethine nitrogen coordination.

The mode of coordination *via* sulphur atom is expected upon de protonation of the ligand. The spectral band ν(N-H) of the thiosemicarbazones disappears in the complexes indicating the deprotonation of the ^{3}NH and coordination *via* the thiolate sulphur is shown by a decrease in the frequency by 14 to 42 cm^{-1} of the thioamide band which is partially ν(C=S) and found at 1371 and 892 cm^{-1} for HL4M. Another band which is considered to be sensitive to bonding of sulphur to metal ion is the ν(N-N); since there is increased double bond character for N=C-S; ν(N-N) is expected to shift to higher energies. But in **42** we expect a thione sulphur coordination because ν(N-H) band remained almost unshifted. The frequency of ν(C=S) vibration of the free ligand at 892 cm^{-1} is lowered by 74 cm^{-1}, clearly indicating the coordination of the thioamide group to the nickel(II). Parallel shift is seen for the δ(NH) vibration of the thiosemicarbazone moiety, the free ligand band at 1586 cm^{-1} shifting to 1558 cm^{-1} ,and it is an evidence of decrease of bond order of (C=S) [6]. A new band in the range 385 to 405 $cm^{-1}$is assigned for the ν(Ni-S) establishes the involvement of thione sulphur coordination.

Table 8.1.
Colours, Conductivity, Magnetic moment and partial elemental analyses of Ni(II) complexes with N-N-S donor ligands

Compound	Emperical formula	Colour	Mol.Condu Ctivity[a]	μ.BM [b]	Analytical data, Found (Calculated) %			
					C	H	N	Ni
Ni(L4M)NO_3, **38**	$C_{12}H_{15}N_5O_4SNi$	Brown	21	Dia	37.81 (37.53)	4.02 (3.94)	18.51 (18.24)	15.49 (15.28)
Ni(L4M)NCS.H_2O, **39**	$C_{13}H_{17}N_5O_2S_2Ni$	Brown	14	Dia	39.62 (39.22)	4.14 (4.30)	17.39 (17.59)	15.01 (14.74)
Ni(L4M)ClO_4.H_2O, **40**	$C_{12}H_{17}ClN_4O_6SNi$	Brown	18	Dia	33.02 (32.89)	4.13 (3.90)	12.98 (12.75)	13.51 (13.35)
Ni(L4P)Cl, **41**	$C_{12}H_{15}ClN_4SNi$	Brown	21	Dia	41.96 (42.21)	4.24 (4.43)	16.54 (16.41)	17.14 (17.19)
Ni(HL4A)2(ClO4)2.H2O, **42**	$C_{28}H_{40}C_{l2}N_8NiO_9S_2$	Reddish brown	91	3.21	40.46 (40.60)	5.11 (5.11)	11.63 (11.53	07.12 (07.09)

a= ca. 10^{-3}M DMF solution at 298 K. ;b= Magnetic moment (BM) at 298 K

Table 8.2
IR spectral assignments (cm^{-1}) of Ni(11) complexes with N-N-S donor ligands

Compound	$\nu(^6C=^2N)$	$\nu(^3N-^8C)$	$\nu(^2N-^3N)$	$\nu(^8C-^1S)$	$\delta(^8C-^1S)$	δ_{OP}	δ_{IP}	$\nu(^3N-H)$	ν(Ni-N)	ν(Ni-S)	$\nu(NiN)_{PY}$	ν(Ni-X)
HL4M	1627 s	1480 s	1010 m	1371 s	892 m	649 m	408 m	3280 s	---	----	---	---
Ni(L4M)NO_3	1607 s	1337 s	1020 m	1229 s	831 m	663 m	418 m	----	486 w	324 m	264 m	323 m
Ni(L4M)NCS.H_2O	1589 s	1317 m	1021 m	1243 s	844 m	656 m	417 m	----	478 w	322 w	243 m	353 w
Ni(L4M)ClO_4.H_2O	1600 s	1357 s	1027 m	1263 s	825 m	668 m	414 m	---	483 w	325 w	253 m	386 m
HL4P	1604 s	1493 s	998 m	1380 s	843 m	637 m	406 m	3309 s	----	----	----	----
Ni(L4P)Cl	1620 s	1338 m	1016 w	1283 m	790 s	664 m	419 m	----	471 m	317 w	275 w	332 m
HL4A	1601 s	1487 s	1003 m	1363 s	867 m	624 m	402 m	3291 s	---	---	---	---
Ni(HL4A)2(ClO4)2.H2	1627 s	1357 s	1020 m	1209 s	818 m	629 m	411 m		484 m	346 m	269 w	----

S=strong; m=medium; w=weak; sh=shoulder

Coordination *via* the pyridine nitrogen is indicated by the shifts to lower frequencies of ν(C-N) + ν(C-C) and shift to higher frequencies of the in- plane and out-of plane ring deformation bands. Thus, the shift in pyridine ring out-of plane and in-plane bending vibrations by 7 to 19 cm^{-1} with N_2S donor on complexation confirms the coordination of ligand to Ni(II) *via* pyridine nitrogen [7]. A new band in the range 243 to 270 $cm^{-1}$is assigned for the ν $(Ni-N)_{pyridine}$

The perchlorate complex **42** shows band absorption in the region 3600-3200 cm^{-1} characteristic of lattice water. Strong and broad absorption band which is characteristic of ν_3 of ionic perchlorate is observed in the spectrum at about 1072cm^{-1}. Also $\nu_4(ClO_4)$ is present as a sharp shoulder at 624 cm^{-1} and a weak band at 988 cm^{-1} is assigned to ionic perchlorate, and it is slightly distorted from T_d symmetry due to lattice effect or hydrogen bonding by the coordinated ligand's N-H function [8].

The thiocyanato complex shows band around 2072, 801 and 474 cm^{-1} which can be assigned to the ν(CN), ν(CS) and δ(NCS) modes of vibration respectively. The position and intensity of these bands indicate unidentate coordination of thiocyanate group through the nitrogen [9]. It also shows a broad band around 3350 cm^{-1}, which is assigned to crystallization of water.

The chloro compound shows bands in the region 340-315 cm^{-1}, which is assigned to ν(Ni-Cl). The nitrato complex shows three bands ν_1,1529 cm^{-1}, ν_5,1410 cm^{-1}, and ν_2,1010 cm^{1} The positions of $\nu_1$and ν_5 and wide separation of 119 cm^{-1} clearly indicates mono dentate coordination of nitrato group [10].

8.3.3 Electronic spectra

The results of diffuse reflectance (Fig 8.1) and solution (dimethylformamide) electronic spectra of all Ni(II) complexes are presented in Table 8.3.

The configuration d^8 is usually prone to form four coordinate diamagnetic planar derivatives, especially with stronger field ligands and are characterized by no absorption below 1000 nm [11]. Diamagnetism is a consequence of eight electrons being paired in the four lower lying d orbital. The upper orbitals is either d_{x2-y2}.(b_{1g}) or d_{xy} (b_{2g}) which depends on the chelating nature of ligands. The four lower orbitals

are often so close together in energy that individual transitions there from to the upper d orbitals, cannot be distinguished and hence single absorption band. Recognizing that a square planar complex has a_{2u}, b_{2u} and e_u skeletal vibrations, three spin allowed transitions may be vibronically induced [12].

The complexes **38** to **41** have a single broad band rich in shoulders at 416-600 nm which we assigned to $^1A_{1g} \rightarrow {}^1B_{1g}$, $^1A_{1g} \rightarrow {}^1A_{2g}$, $^1A_{1g} \rightarrow {}^1E_g$ transitions.[13]. Based on the average of these energies the order of the ligand field strength of the anion is NCS > Cl > NO_3 which is in good with spectrochemical series. A second band may be seen near 430-335 nm which is often charge transfer in origin. In addition to this the ligand's $n \rightarrow \pi^*$ and $\pi \rightarrow \pi^*$ bands are almost remained undisturbed but in solution they often blue shifted or red shifted upon coordination.

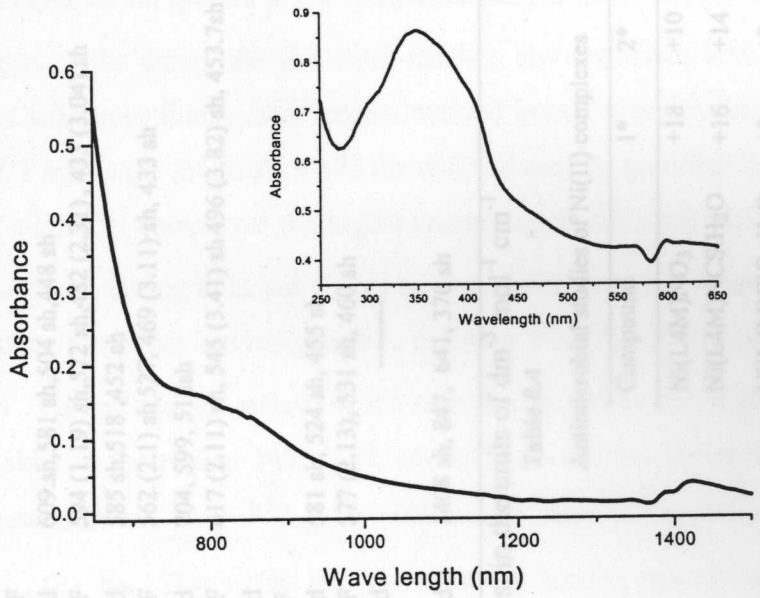

Fig 8.1 Electronic Spectrum of Compound $[Ni(L4A)_2](ClO_4)_2 \cdot H_2O$

The electronic spectrum of **42** is typical of pseudo octahedral Ni(II) complex. Three absorptions were observed in the UV-Visible region. Thiosemicarbazones

Table 8.3
Electronic spectral data (nm) of Ni(II) complexes with N-N-S donor ligands

Compound	Mode	d-d +CT	$n \rightarrow \pi^*$	$\pi \rightarrow \pi^*$
HL4M	Solid		335	324, 296
	DMF		331sh (4.01), 301 sh (4.14)	322, 292 sh
$Ni(L4M)NO_3$	Solid	609.sh,581 sh,504 sh,448 sh	338	316, 292 sh
	DMF	594 (1.19) sh,572 sh,482 (2.31), 433 (3.04) sh	335 (3.21)	300 (3.97) sh
$Ni(L4M)NCS.H_2O$	Solid	585 sh,518 ,452 sh	340	318, ,302 sh
	DMF	562 (2.1) sh,527, 469 (3.11) sh, 433 sh	337 (3.15), 329 (3.15) sh	312 (3.72) sh
$Ni(L4M)ClO_4.H_2O$	Solid	704, 599, 518sh	337	316 sh
	DMF	617 (2.11) sh, 545 (3.41) sh 496 (3.82) sh, 453.7sh	332 (3.89) sh, 334 sh	311.(3.90) sh
HL4P	Solid		334 sh	294 sh
	SMF		331 sh (4.01), 301 sh (4.14)	292 sh.321 sh
Ni(L4P)Cl	Solid	581 sh, 524 sh, 455 sh	333, 345	295 sh
	DMF	577 (2.13), 531 sh, 460 sh	338, 349 sh	295 sh
HL4A	Solid	--------	334 sh, 311	294 , 298
			330 sh (4.01), 310 sh (3.99)	291 sh (4.10), 300 sh
Ni(HL4A)2(ClO4)2.H2O	Solid	1408 sh, 847, 641, 370 sh	314,323 sh	244, 298 sh

Log ε in parentheses, in the units of $dm^{-3}\ mol^{-1}\ cm^{-1}$

Table 8.4

Antimicrobial studies of Ni(II) complexes

Compound	1*	2*	3*	4*
$Ni(L4M)NO_3$	+18	+10	+20	---
$Ni(L4M)NCS.H_2O$	+16	+14	+19	---
$Ni(L4M)ClO_4.H_2O$	+9	+9	+12	---
Ni(L4P)Cl	+11	+14	+16	+15

1*,*Staphylococcus aureus*, 2* *Bacillus sp*, 3*,*Shigella sp*, 4* *Salmonella typhi*

ligand and Ni complex have $\pi \rightarrow \pi^*$ at *ca* 244 nm and an $n \rightarrow \pi^*$ band at *ca* 314 nm. There is a slight shift in the energy of these bands on complexation. A second $n \rightarrow \pi^*$ band which is found below at *ca* 333 nm in the spectrum of uncomplexed thiosemicarbazones was found at ca 323 nm. The $n \rightarrow \pi^*$ transition associated with the pyridine ring at *ca* 333 nm in the solid state spectra of the thiosemicarbazones is often shifted in energy in solution, which is probably due to hydrogen bonding taking place between the thiosemicarbazones moiety and the solvent molecule [14]. The molar absorptivities are more than 10^4 which are consistent with previous studied heterocyclic thiosemicarbazones. Below 330 nm most of the thiosemicarbazones spectra show one or more $n \rightarrow \pi^*$ bands with the thiosemicarbazones moiety. On complexation the thiosemicarbazones moiety's $n \rightarrow \pi^*$ bands shifted to *ca* 357 nm and for some compounds combines with the pyridine $n \rightarrow \pi^*$. Absorption in the 430- to 370 nm range in the spectra of the complexes are due to $S \rightarrow$ Ni(II) CT bands [15]. The energies of the composite d-d band maxima are consistent with the nickel(II) complex of analogous thiosemicarbazones derived from 2-acetylpyridine. Two metal to ligand CT bands are found at *ca* 370 nm and 434 nm. In accordance with previous studies of nickel(II) complexes the higher energy bands are assignable to $S \rightarrow$ Ni(II) LMCT transition, tailing in to the visible region. Additional bands are present in the 500 to 370 nm range that are assignable to pyridine $\rightarrow$ Ni(II) CT transition.

UV .Vis and near IR spectra of the complex **42** shows two strong bands and a weak shoulder in the region 1408, 847, and 641 nm which may be assigned to the following transitions . $^3A_{2g} \rightarrow {}^3T_{2g}$, E $\approx$10Dq (ν_1); $^3A_{2g} \rightarrow {}^3T_{1g}$ (F), E $\approx$ 18Dq (ν_2); $^3A_{2g} \rightarrow {}^3T_{1g}$ (P), E$\approx$ 12Dq +15B. (ν_3) The third d-d band is less intense and actually obscured by $S \rightarrow$ Ni(II) LMCT. From these transition the value of B is calculated using the expression , $B=[E(\nu_2) + E(\nu_3) - 3E(\nu_1] / 15$ and taking $B_0 = 1030\ cm^{-1}$,we calculated β and β^0 which offered a convenient way to predict the nature of covalent bond. The calculated Dq (718.2 cm^{-1}), B (466 cm^{-1}), β (0.45) and β^0 (B/B_0 =55%)

indicated the presence of strong covalence [16]. Values of Dq, and β extracted from the spectra exhibits the anticipated reduction in the Nephelauxtic ratio β as the coordination sphere is enriched in sulphur donors. It has been suggested that a low β in complex **42** may be connected with the possibility of stabilizing its low oxidation state as the significant mixing of ligands and metal orbitals implies that any added electron charge could be more efficiously delocalized.

8.3.4 NMR spectra

As a representative of square planar complexes we recorded the ^{1}H NMR spectrum of [Ni(L4M)NO_3]. The spectrum is in conformity with a square planar geometry [17]. The absence of peak corresponding to the imino proton in it shows that the ligand is present in the deprotonated form. It shows a doublet at 11.06 ppm, a triplet at 8.93 ppm, a doublet at 8.56 ppm and a triplet at 8.95 ppm corresponding to four protons of pyridine moiety. An envelop at 3.82 ppm corresponds to protons of morpholino moiety. The methyl group appears as a singlet at 3 ppm. A substantial difference in the chemical shift of the proton alpha to pyridinyl nitrogen is observed in the complex. The difference in the chemical shift values is indicative of the difference in the electron density at that position [18]. It clearly indicates pyridine nitrogen coordination to nickel. Based on our studies we proposed following structures (Fig.8.2) for the complexes.

8.4 Electrochemical studies

The electrochemical study of **42** alone was undertaken. The profile of its voltammogram is presented in the Fig. 8.4 shows that the complex undergoes an electrochemically reversible one electron oxidation process at E = + 1010 mV, such a value is typical of $Ni^{3+/2+}$ redox couple where Ni is in mixed nitrogen, sulphur environment. The electrochemical characteristics support a one-electron assignment for the process.

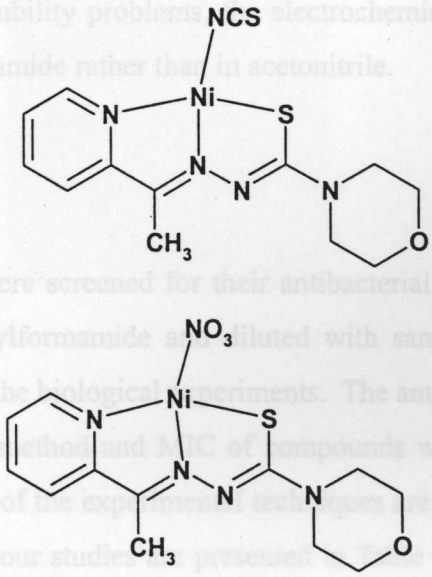

Fig. 8.2 Proposed structures for square planar Ni(II) complexes

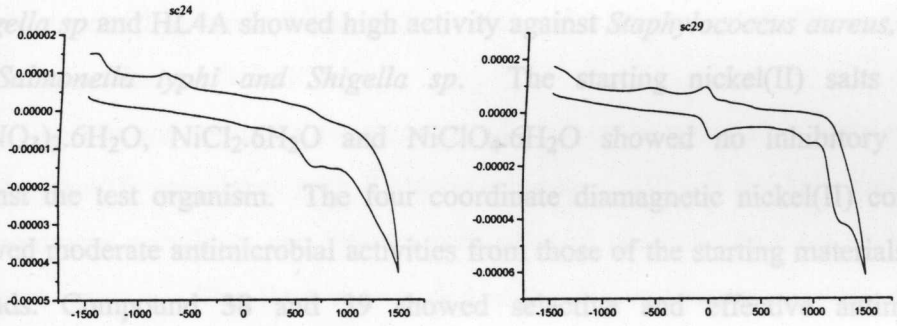

Fig 8.3Cyclic voltammogram of representative Ni complex

The reversibility of the redox couple is presumably a result of the maintains of the same six coordination in both oxidation states. At negative potential, the complex shows an exaggerated cathodic peak at -1530 mV with an anodic counter peak at + 64 mV, indicating a two-electron reduction with the deposition of metallic Ni [12].

Mainly because of the solubility problems, the electrochemical behavior of **42** was examined in dimethylformamide rather than in acetonitrile.

8.5 Antimicrobial studies

All the five compounds were screened for their antibacterial activity. The samples were dissolved in dimethylformamide and diluted with same solvent to have the desired concentrations for the biological experiments. The antimicrobial studies were done using disc diffusion method and MIC of compounds was done by using agar diffusion method. Details of the experimental techniques are described at lengths in Chapter 3. The results of our studies are presented in Table 8.4. The antimicrobial activities of ligands differ from each other. From the data available, it is clear that all the compounds expect **42** are biologically active. The free ligand HL4M showed no or a little activity against any Gram positive and Gram negative bacteria but HL4P showed high activity against *Staphylococcus aureus*, *Bacillus sp*, *Proteus Sp* and *Shigella sp* and HL4A showed high activity against *Staphylococcus aureus, Bacillus sp Salmonella typhi and Shigella sp.* The starting nickel(II) salts such as $Ni(NO_3)_2.6H_2O$, $NiCl_2.6H_2O$ and $NiClO_4.6H_2O$ showed no inhibitory activity against the test organism. The four coordinate diamagnetic nickel(II) complexes showed moderate antimicrobial activities from those of the starting materials or free ligands. Compound **38** and **39** showed selective and effective antimicrobial antimicrobial activities against *Staphylococcus aureus, Bacillus sp and Shigella sp.* Compounds **40** and **41** showed moderate activity against *Staphylococcus aureus, Bacillus sp Salmonella typhi and Shigella sp.*

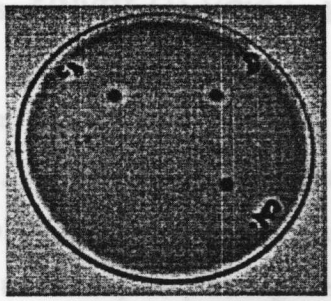

Fig 8.4 Antimicrobial studies (zone of inhibition)of Ni(II)complex

The chloro compounds showed only moderate activity at the studied concentration against three bacteria *viz Staphylococcus aureus, Bacillus sp and Shigella sp* and others showed very high activity against the above mentioned organisms at higher concentration The activity of these compounds are lower than corresponding copper(II) compounds. Among the nickel complexes, the most antimicrobial activity is shown by the nitrato compound, **38**. The MIC values of compounds are far below than that of copper compounds and contain nearly hundred fold of compound per disc. None of the compound is active against *Vibrio cholerae* and *Vibrio paraheaemolyticus*.

These results are useful to interpret and explain the structure activity relation ship of nickel(II) complexes with thiosemicarbazones [19]. It is likely that labile four-coordinate complexes can interact with selected bacteria while six coordinate complexes cannot. The four coordinated nickel(II) complexes consists of one tridentate ligand and one replaceable gegenion such as chloride, nitrate or thiocyanate. The six coordinate complex with two tridentate ligand does not undergo ligand replacement easily [20]. We assume that in this series of nickel(II) complexes the antimicrobial activity against the organism tested would correlate with their ligand replacement abilities rather than with lipophilicity, solubility or hydrophobicity of the complexes [21].

8.6 X-ray diffraction studies of $[Ni(HL4A)_2](ClO_4)_2 . H_2O$

8.6.1 Synthesis of the complex

To $Ni(ClO_4)_2$ $6H_2O$ (2 m.mol,0.73 g)in 70% aqueous methanol (25 mL) was added 4 mmol of HL4A in methanol and the resulting mixture was refluxed for 2h and filtered. Cooling the solution and slowly evaporating the solvent led to reddish brown crystalline products with yield approximately 68%.X-ray quality crystals for the compound **42** is grown by slow diffusion of ethyl ether into a solution of the compound dissolved in minimum amount of dimethylformamide to give well defined reddish brown crystals.

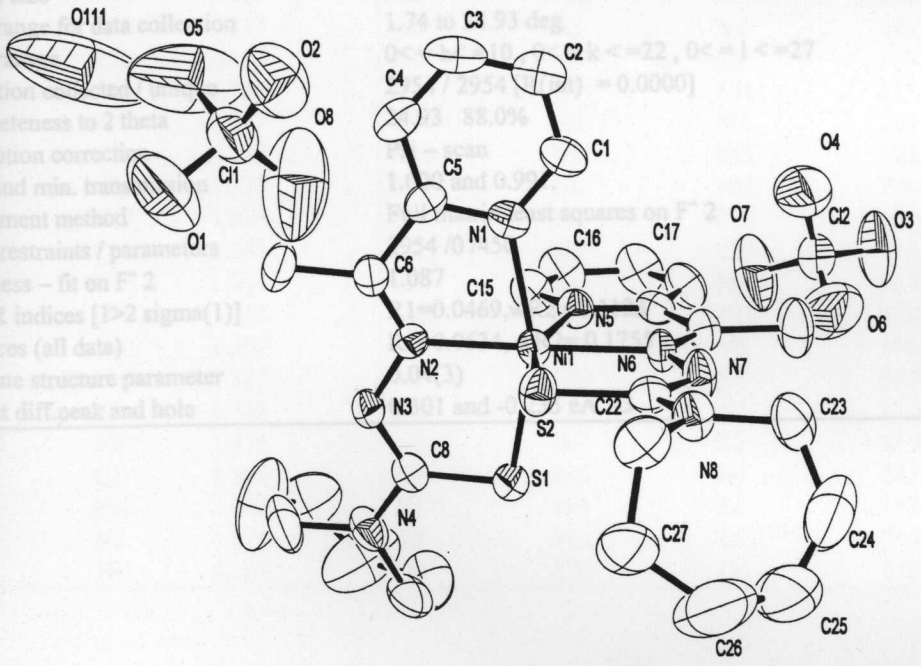

Fig 8.5. ORTEP diagram for compound 4 $[Ni(apatsc)_2](ClO_4)_2 . H_2O$, Displacement ellipsoids are drawn at the 54% probability level and hydrogen atoms are omitted for clarity.

Table 8.5

Crystal data and structure refinement for $[Ni(HL4A)_2]ClO_4 \cdot H_2O$

Empirical formula	$C_{28}H_{40}C_{12}N_8O_9S_2$
Formula weight	826.41
Temperature	293(2)K
Wave length	0.70930 Å
Crystal system, space group	Orthorhombic, p b c 21
Unit cell dimensions	a = 8.5440(9) A^0 α = 90.000(7) deg
b = 18.5970(16)A^0 β = 90.000(8) deg	
c = 23.416(2) A^0 γ = 90.000(8) deg	
Volume	3720.6(6) Aˆ 3
Z , Calculated density	4.1475 Mg / mˆ 3
Absorption coefficient	0.837mm ˆ ˆ1
F(000)	1720
Crystal size	0.30× 0.25× 0.20 mm
Theta range for data collection	1.74 to 24.93 deg
Index ranges	0< = h< =10 , 0< = k < =22 , 0< = l < =27
Reflection collected / unique	2954 / 2954 [R(int) = 0.0000]
Completeness to 2 theta	24.93 88.0%
Absorption correction	Psi – scan
Max. and min. transmission	1.000 and 0.991.
Refinement method	Full matrix least squares on Fˆ 2
Data / restraints / parameters	2954 /0 /450
Goodness – fit on Fˆ 2	1.087
Final R indices [1>2 sigma(1)]	R1=0.0469,wR2 =0.1123
R indices (all data)	R1=0.0634, wR2= 0.1255
Absolute structure parameter	0.04(3)
Largest diff.peak and hole	0.301 and -0.235 eAˆ -3

Table 8.6

Selected bond lengths(Å) and Bond angles(^{0})

Bond length(A^0)			Bond angles (^{0})			
C1	N1	1.334	N1	C1	C2	122.32
C1	C2	1.374	C3	C2	C1	119.81
C2	C3	1.346	N1	C5	C4	120.30
C3	C4	1.388	N2	C6	C5	113.46
C4	C5	1.381	N4	C8	N3	116.60
C5	N1	1.354	N5	C15	C16	123.21
C5	C6	1.488	N5	C19	C20	114.41
C6	N2	1.273	N6	C20	C19	114.00
C6	C7	1.502	N6	C20	C21	125.75
C8	N3	1.351	N8	C28	C27	112.16
C8	S1	1.691	C1	N1	C5	119.26
C9	N4	1.458	C1	N1	Ni1	128.03
C9	C10	1.484	C5	N1	Ni1	112.64
C10	C11	1.527	N3	N2	Ni1	120.40
C11	C12	1.417	C8	N3	N2	118.70
C12	C13	1.457	C14	N4	C9	115.29
C13	C14	1.384	C19	N5	Ni1	115.13
C14	N4	1.457	C20	N6	N7	120.94
C15	N5	1.329	C20	N6	Ni1	120.04
C15	C16	1.373	N7	N6	Ni1	I19.03
C16	C17	1.379	C22	N8	C23	122.02
C17	C18	1.368	C23	N8	C28	116.80
C18	C19	1.366	C8	S1	Ni1	96.89
C19	N5	1.350	C22	S2	Ni1	97.62
C20	N6	1.260	N2	Ni1	N5	104.80
C22	N8	1.327	N2	Ni1	S2	96.51
C22	S2	1.702	N6	Ni1	N5	76.37
C23	N8	1.476	N6	Ni1	S2	82.22
N1	C1	1.334	N5	Ni1	N1	88.69
N1	Ni1	2.103	N1	Ni1	S1	158.60
N2	N3	1.376	S2	Ni1	S1	95.98
N2	Ni1	2.006	O8	C11	O5	110.88

The selected crystals of compound **42** were measured with a Siemens P4 diffractometer equipped with the SMARTCCD system and using graphite-monochromatic Mo Kα radiation (0.70930 Å). The data collection was carried out at 293 (2) K. The data were corrected for Lorentz and polarization effects, and absorption corrections were made using SADABS. Neutral atom scattering factors were taken from Cromer and Waber. Anomalous dispersion corrections were taken from those of Creagh and McCauley All calculations were performed using SHELXL [22, 23]. The structure was solved by direct methods and all of the non-hydrogen atoms were refined with anisotropic displacement parameter. No anomalies were encountered in the refinements. The relevant parameters for crystal data, data collection, structure solution and refinement are summarized in Table 8.5, and important bond lengths and angles in Table 8.5 Crystallographic data (excluding structure factoress) for the structure reported here have been deposited with the Cambridge crystallographic data center. CCDC No.199130.

8 6.2 Description of the structure

A perspective view of the title compound is shown in the Fig. 8.5 and molecular packing in Fig.8.5. (Thermal ellipsoids are drawn at 54% probability level and hydrogen atoms are not included for clarity). Selected bond angles and bond lengths are presented in Table 8.5.

The single crystal X-diffraction studies reveals the occurrence of a hexa coordinated cationic complex of distorted octahedral geometry. The title complex crystallizes as di perchlorate monohydrate salt (with out ligand deprotonation).

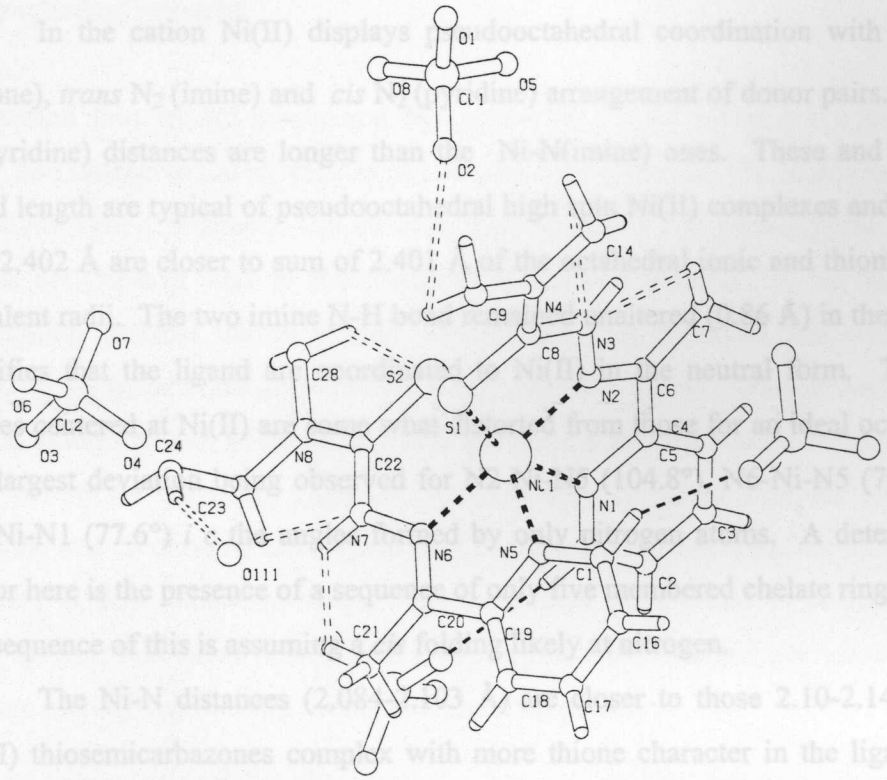

Fig 8.6. PLATON diagram of Compound 4, $[Ni(apatsc)_2](ClO_4)_2 .H_2O$ indicating H- bonding interactions between the molecules. Some carbon atoms in the hexamethyleneimine ring of the compound has been removed for clarity.

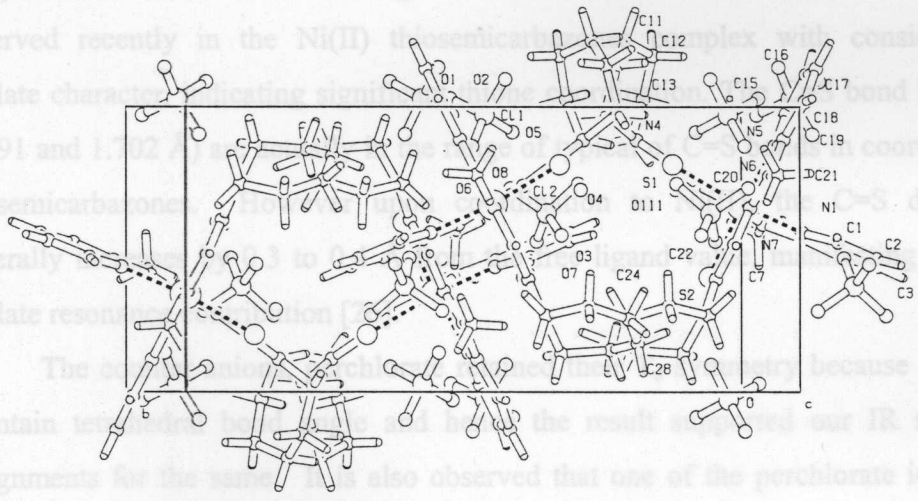

Fig 8.7 Packing diagram for compound **42** *$[Ni(apatsc)_2](ClO_4)_2 .H_2O$, viewed along b axis.*

In the cation Ni(II) displays pseudooctahedral coordination with a *cis* S_2 (thione), *trans* N_2 (imine) and *cis* N_2 (pyridine) arrangement of donor pairs. The Ni-N(pyridine) distances are longer than the Ni-N(imine) ones. These and the Ni-S bond length are typical of pseudooctahedral high spin Ni(II) complexes and at 2.400 and 2.402 Å are closer to sum of 2.401 Å of the octahedral ionic and thione sulphur covalent radii. The two imine N-H bond remained unaltered (0.86 Å) in the complex signifies that the ligand are coordinated to Ni(II) in the neutral form. The bond angles centered at Ni(II) are some what distorted from those for an ideal octahedron, the largest deviation being observed for N2-Ni-N5 (104.8°), N6-Ni-N5 (76.4°) and N2-Ni-N1 (77.6°) *i c* the angles formed by only nitrogen atoms. A determinative factor here is the presence of a sequence of only five membered chelate rings [24]. A consequence of this is assuming a *cis* folding likely at nitrogen.

The Ni-N distances (2.084-2.103 Å) are closer to those 2.10-2.14 Å for a Ni(II) thiosemicarbazones complex with more thione character in the ligand. [25]. The Ni-S (thione) bonds 2.4 and 2.402 A°are within the range of (2.36 -2.39 Å) observed recently [26] in the Ni(II) pseudo octahedral high spin thiosemicarbazones complex. The Ni –S bonds are longer than (2.4 Å) the Ni –S bonds (2.36 -2.39 Å) observed recently in the Ni(II) thiosemicarbazones complex with considerable thiolate character, indicating significant thione coordination. The C=S bond lengths (1.691 and 1.702 Å) are actually in the range of typical of C=S bonds in coordinated thiosemicarbazones. However upon coordination to Ni(II), the C=S distance generally increases by 0.3 to 0.4 Å from the free ligand value, manifesting a little thiolate resonance contribution [26].

The counter anions, perchlorate retained their T_d symmetry because of they maintain tetrahedral bond angle and hence the result supported our IR spectral assignments for the same. It is also observed that one of the perchlorate ions has engaged in intermolecular hydrogen bonding with water.

8.7 Concluding remarks

Synthesized four square planar and one octahedral Ni(II) complexes with N-N-S donor and characterized by various physicochemical methods. The four coordinated complexes were diamagnetic and six coordinated complex was paramagnetic. The IR spectral assignments were in accordance to N-N-S coordination. In the octahedral coordination unusual thione sulphur coordination was observed and which was proved by IR spectral assignments and X-ray analysis. The UV-Visible and near IR spectral studies helped to calculate Racah parameters and the results suggest strong covalence in the complex. The CV study of the octahedral complex showed a reversible one electron transfer which may be attributed to the retention of the same geometry in both oxidation states. The complexes were found to be moderately active against both Gram positive and Gram negative bacteria and also established a structure activity relationship for the antimicrobial activity.

References

1 M. A. Halcrow and G. Christou, *Chem. Rev.*, 1994, **94**, 2421;

2 E. Bermejo, A. Castineiras, L.M. Fostiak, I. Garcia, A.L. Llamas, J.K. Swearingen and D.X. West, *J. Brazilian Chem. Soc*, 2001, **56b**, 1297

3 M. Mathew, G. J. Palenik and G. R. Clark,*J Inorg. Chem.*, 1973, **12**, 346.

4 C. A. Brown, W. Kaminsky, K. A. Claborn, K. I. Goldberg and D. X. West, *J. Brazilian Chem. Soc.*, 2002.**13**, 10-18

5 M. R. McDevitt and A. W. Addison, *Inorg. Chim. Act*a, 1993, **204,** 679.

6 S.M.Hart, J.C.A. Boeyens and R. A. Hancock,*J Inorg. Chem.*, 1983, **22**, 982.

7 D. R. Kelman, K. A. Claborn, W. Kaminsky, K. I. Goldberg, and D. X. West, *J. Brazilian Chem. Soc.*, 2000.**17**, 107

8 C. R. Lucas and S. Liu, *J. Chem. Soc., Dalton Trans.*, 1994, **185,** 347.

9 A. W. Addison, B. Watts and M. Wicholas, *J Inorg. Chem,* 1984, **23**,813.

10 V. V. Pavlishchuk and A. W. Addison,*J. Inorg. Chim. Act*a, 2000, **298**, 97.

11 W. Kaminsky, J. P. Jasinski, R. Woudenberg, K. I. Goldberg and D. X. West, *J. Mol. Struct.*, 2002, **608**, 135.

12 K. Nag and A. Chakravorty, *Coord. Chem. Rev.*, 1980, **33**, 87.

13 L. Sacconi, F. Mani and A. Bencini, in *Comprehensive Coordination Chemistr*y, , Pergamon Press, Oxford, 1987, vol. **5**, p. 1.

14 A. B. P. Lever, *Inorganic Electronic Spectroscop*y,., Elsevier, New York, 1984, **2**nd edn.

15 K. A. Ketcham, I. Garcia, E. Bermejo, J. K. Swearingen, A. Castiñeiras and D. X. West, *Z. Transition Met. Chem,* 2002, **628**, 409-415.

16 S. R. Cooper, S. C. Rawle, J. A. R.Hartman, E. J. Hintsa and G. A. Adman, *Inorg. Chem.*, 1988, **27**, 1209.

17 J. K. Swearingen, W. Kaminsky and D. X. West, *Transition Met. Chem.*, 2002, **27**, 724.

18 F. L. Urbach and D. H. Busch, *Inorg. Chem.*, 1973, **12**, 408.

19 M. A. Halcrow and G. Christou, *Chem. Rev.*, 1994, **94**, 2421.

20 Y. W. Lee, C. Pons, D. M. Tummolo, C. B. Klein, T. G. Rossman and N. T. Christie, *Environ. Mol. Mutagen.*, 1993, **21**, 365.

21 a) G. G. Fletcher, F. E. Rossetto, J. D. Turnbull and E. Nieboer, *Environ. Health Perspect. Suppl.*, 1994, **102**, 69.
b) F. E. Rossetto, J. D. Turnbull and E. Nieboer, *Sci. Total Environ.*, 1994, **148**, 201.

22 SHELXTL, Version 5.030, Siemens Analytical X-Ray Instruments, W. I. Madison, and J. A. Ibers, *Inorg. Chem.*, 1994, **6**, 197.

23 a) T. X Houston, D. T. Cromer and J. T. Waber, in *International Tables for X-Ray Crystallography*, Kynoch Press, Birmingham, 1974, vol. **4**, Table 2.2A.
b) C. K. Johnson, ORTEP II, Report ORNL-5138, Oak Ridge National Laboratory, Oak Ridge, TN, 1976.

24 R. Restivo and G. J. Palenik, *Acta Crystallogr., Sect.* B, 1971, **27**, 59.

25 D. X. West, M. A. Lockwood, A. E. Liberta, X. Chen and R. D.Willett, *Transition Met. Chem. (Weinheim)*, 1993, **18**, 221.

26 R. P. John, A. Sreekanth, M. R. P. Kurup, A. Usman, A. R. Ibrahim, , H. K. Fun, *Spectrochemica Acta*, 2003, 1, 1349.

Chapter 9

Zn(II) COMPLEXES WITH TRIDENTATE N_2S LIGAND; SYNTHESES, SPECTROSCOPIC AND ANTIMICROBIAL PROPERTIES.

9.1 Introduction

Zinc with atomic number 30, atomic weight 65.39 and oxidation state (II) is an essential element in all living systems and plays a structural role in many proteins and enzymes. It is recognized that transcription factors regulate gene expression and the essential feature is binding to a regulatory protein in the recognition sequence of the gene. Many proteins have been found to have a zinc-containing motif that serves to bind DNA embedded in their structure. In the relevance of zinc to DM, zinc is known to be present in insulin, coordinated by three nitrogen atoms from histidines and three water molecules in an irregular octahedral environment, which is also believed to have a functional structure [1]. Surprisingly, zinc was found to have important physiological and pharmaceutical functions involving insulin-mimetic activity. In 1980, Coulston and Dandona first reported the insulin-mimetic activity of zinc ion. Although zinc(II) ion has been revealed to have an insulin-mimetic activity, zinc complexes have never been examined. Glucose normalizing effects of zinc complexes are reported [2].

Zn is regarded as one of the main healing minerals, and is found concentrated in hair, nails, nervous system, skin, liver, bones, blood and pancreas. There is an increasing amount of interest in the role of zinc in appetite control since patients with anorexia nervosa often have a low serum zinc level [3]. It is also a constituent of at least 100 enzymes in the body (25 of which specifically for food digestion) e.g. Zn forms part of the enzyme *carbonic anhydrase* which is required for the utilization and transport of

carbon dioxide in the body functions as an anti-oxidant, maintains normal taste and smell, essential for health of the prostate gland in males, aids wound healing and burns, boosts immunity aids, normal absorption of vitamins in the formation of insulin (component of insulin and the pancreatic enzyme), assists in the maintenance of the body's acid / alkaline balance, important for brain tissue formation, vital role in protein synthesis and promotes cell division. Deficiencies of zinc are usually the result of dietary insufficiency and deficiency causes excessive sweating, mal absorption of food, loss of taste and smell, baldness, glossitis (inflammation of tongue) stomatitis (inflammation of mouth), blepharitis (inflammation of eyelids), paronchyia (inflammation of nail/nailbed), sterility, low sperm count, dwarfism, delayed wound healing, Splenomegaly / hepatomegaly (enlarged spleen and liver) retarded growth delayed sexual maturity and white spots on nails [4]

The thiosemicarbazones of 2-acetylpyridine as well as their complexes with metals are biologically and pharmacologically active and have been the object of a considerable amount of research. There have nevertheless been relatively few studies of the coordination of thiosemicarbazones to non-transition metals, and of the biological activity of the resulting coordination compounds. The complexes of thiosemicarbazones with zinc metals constitute an especially attractive topic in view of marked differences among group 12 metals as regards both chemical behaviour and biological activity [5].

A growing number of reviews and publications have highlighted the utility of organometallic complexes in which organic chromophores are bound to metal centers for second harmonic generation. Molecular polarizabilities are frequently larger for the metallic complex than for the free chromophore because of metal-to ligand or ligand to metal charge transfer and because of the involvement of the orbitals on metals and these metal centers may act as anchors in the engineering of three-dimensional geometries giving rise to octupolar molecules. Moreover, the combination of organic and inorganic elements affords materials of relatively high mechanical and thermal stability, as is also observed for organic chromophores in inorganic host matrixes [6].

This Chapter describes the syntheses, of three Zn(II) complexes with tridentate N-N-S donor thiosemicarbazone, characterization of them by various spectral techniques and their antimicrobial activities.

9.2 Experimental

9.2.1 Materials and method

The synthesis of HL4M and its characterizations are described in Chapter 2. Various Zn salts (S. D. Fine, G. R Grade) were used as received. Zinc perchlorate heptahydrate was prepared by treating Zn(II) carbonate with 1:1 perchloric acid, followed by filtration concentrating the filtrate and recrystallisation. The solvents were purified by standard procedures before use.

9.2.2 Measurements

Details of various physical measurements and characterization techniques are given in Chapter.2. Details of antibacterial studies are reported in Chapter.3. The complexes were analyzed for their metal content by EDTA titration after decomposition with a mixture of perchloric acid and hydrochloric acid followed by Conc. hydrochloric acid alone.

9.2.3 Syntheses of complexes

The general method of syntheses of the Zn(II) complexes is as described below.

To a hot solution of (25 mL) of HL4M (0.05 mmol) in hot methanol was added an equimolar amount of the appropriate metal salt dissolved or suspended in methanol. The mixture was stirred for about 1 week. The yellow coloured solid so formed was filtered out, washed with methanol, ether and vacuum dried and kept over P_4O_{10}.

The complexes that we synthesized are [Zn(L4M)Cl], **43**; [Zn(L4M)OAc].H_2O,**44** and [Zn(L4M)ClO_4],**45**.

9.3 Results and discussion

The colours yields, partial elemental analyses, stoichiometries of complexes are presented in Table 9.1.

The complexes are diamagnetic and yellow in colour, insoluble in most of polar solvents but soluble in organic solvents such as dimethylformamide, dimethyl sulphoxide. The complexes are mono ligated with a 1:1:1 ratio of metal ion, ligand and gegenions. The colour of complexes indicates that the thiosemicarbazones functional group determines the colour of the solid. The analytical data indicates that the complexes present one monoanionic tridentate ligand per metal ion and fourth coordination position is occupied by mono or polyatomic anion. The molar conductivities in dimethylformamide, suggest that the complexes are non-electrolytes.

9.3.1 IR spectral investigation

Table 9.2 lists the main IR bands of HL4M and their complexes in the 4000-200 cm^{-1} region.

The spectra of the ligand shows a band of maximum intensity at 3280 cm^{-1} which is assigned to ν(N-H). Absence of any broad band around 2400-2600 cm^{-1} confirms that the ligand exists in thioketo form. The ^1H NMR further confirms this, which shows no signal for the S-H group. The sharp band at 1627 cm^{-1} which was assigned to ν(C=N) in the ligand has shifted to lower energy and ν(N-N) to higher energy in complexes suggesting coordination of azomethine nitrogen to Zn.

In the complexes ν(N-H) band disappears and there appears a weak band at 674 cm^{-1} assigned to ν(C-S) stretching. Vibrational coupling among thioamide groups are distributed at *ca* 1535, 1422, 1371 and 892 cm^{-1} identified as thioamide bands I.II, III and IV. Bands at 1371 and 892 cm^{-1} which have major contribution from ν(C=S) are shifted to lower energies with reduced intensity suggesting coordination of thiolate sulphur. In the complexes coordination *via* the pyridine nitrogen is indicated by the shifts to higher frequencies of ν(CN) + ν(CC) and of the

Table 9.1
Analytical data, conductivity, magnetic moments, colours and yields of complexes of Zn(II) with HL4M

Compound	Emp.formula [b]	Yield (%)	Colour	μ [c](BM)	ΛM [d]	Analytical data Found, (Calculated), %			
						C	H	N	Zn
ZnL4MCl, **43**	$C_{12}H_{15}ClN_4OSZn$	69	Yellow	Dia	12	39.37 (39.58)	4.20 (4.15)	15.29 (15.38)	18.01 (17.96)
ZnL4MOAc.H_20, **44**	$C_{14}H_{21}N_40_4SZn$	71	Yellow	Dia	10	41.34 (41.44)	4.72 (4.97)	13.69 (13.81)	16.20 (16.11)
ZnL4MClO_4, **45**	$C_{12}H_{15}ClN_4O_5SZn$	64	Yellow	Dia	10	33.45 (33.66)	3.61 (3.53)	13.13 (13.08)	15.31 (15.27)

. [b] Empirical formula. [c] Magnetic moment [d] Molar conductivity, 10^{-3} M solution (DMF) at 298 K.

Table 9.2
IR spectral assignments (cm^{-1}) of Zn(II)complexes with HL4M

Compound	ν(C=N)+ ν(C=C)	ν(N-N)	ν(C-S)	δ(C-S)	δ_{OP}	δ_{IP}	$\nu(ZnN_{AZ})$	$\nu(ZnN_{PY})$	ν(ZnS)	ν(ZnX)	ν(N-C)
HL4M	1627 s	1010 m	1371 m	892 m	649 m	408 m	----	----	----	----	----
ZnL4MCl	1615 s	1024 m	1303 m	840 m	654 m	430 m	387 w	344 s	278 m	317 m	1590 m
ZnL4MOAc.H_20	1602 s	1030 m	1315 m	838 m	661 m	434 m	391 sh	347 s	269 m	298 sh	1586 m
ZnL4MClO_4	1611 s	1028 m	1310 m	844 m	657 m	432 m	391 sh	341s	279 m	308 m	1591 m

s =strong; m = medium; w = weak; sh = shoulder.

Table 9.3
Electronic spectral assignments(nm) and antimicrobial activities of Zn(II) complexes withHL4M

compound	CT	π—π*	n $\rightarrow \pi$*	Con/disc	1*	2*	3*	4*	5*
HL4M	----	292	301, 331, 390						
ZnL4MCl	386, 415	291	302, 334, 398	50 µg	+10	---	+11	---	---
ZnL4MOAc.H_20	398. 425	288	302, 334, 396	50 µg	+12	+11	+16	+10	---
ZnL4MClO_4	350, 417	290	302, 332, 392	50 µg	+9	---	+10	---	+11

1*-*Staphylococcus aureus*;2*-*Salmonella typhi*;3*-*Shigella sp;* 4**Bacillus sp* ; 5*-*Vibrio cholera.*

increase in shift of pyridine ring, out-of plane and in-plane bending vibrations at 649 and 408 cm^{-1} assigned for HL4M by 12 to 25 cm^{-1} on complexation

The compound **43** shows a medium intensity band at 289 cm^{-1} indicating terminal rather than bridging chlorine. Asymmetric and symmetric stretching vibrations of the acetate grouping in **44** appear at 1585 and 1441 cm^{-1} respectively. The difference between $\nu_{asym}(COO)$ and $\nu_{sym}(COO)$ is 142 cm^{-1}, which reflects the unidentate coordination mode of acetate group [7]. A medium intensity band at 3325 cm^{-1} indicates presence of non-coordinated water. The compound **45** shows broad bands at 1150, 1028 and 920 cm^{-1}, suggesting mono coordinated [8] perchlorate group.

9.3.2. Electronic spectra

The electronic spectral data of complexes are listed in Table 9.3

The principal ligand HL4M has a band at 292 nm due to $\pi \rightarrow \pi^*$ transition. This band is almost unchanged in the spectra of complexes. The ligands also shows broad bands at 301nm and a shoulder at lower energy (331 nm) due to $n \rightarrow \pi^*$ transitions associated with the azomethine linkage. This band in the complex has shown a bathochromic shift due to the donation of a lone pair of electrons to metal and hence the coordination of azomethine. The broad shoulder centered at 390 nm in the ligand was assigned to $\pi \rightarrow \pi^*$ of the thioamide chromophore which suffers a blue shift in the complex due to thio enolisation. The moderately intense band for the complexes in the region 350-425 nm is assigned to $S \rightarrow Zn(II)$ LMCT. The LMCT maxima of the complexes show line broadening with a tale running in to the visible part of the spectra. Except this the complexes show no appreciable absorption in the region above 450 nm in dimethylformamide solution and also in polycrystalline state. The results are in consistent with the d^{10} electronic configuration of Zn(II) ion [9].

9.3.3 ^1H *NMR spectra*

The ^1H NMR signals of the ligand and complexes are listed in Table 9.4.

The ligand HL4M has a signal at δ 8.77 ppm due to N-H proton, which disappears on D_2O exchange. Protons of $C\text{-}CH_3$ are observed at δ 3.35 ppm. A multiplet around δ 3.81 ppm is due to protons of morpholine ring. Protons of

aromatic ring are found between δ 7.46 to 8.25 ppm. In complexes signals due to N-H is absent, supporting thio enolisation. Deprotonation of ^{3}NH in complexes is reflected by the lack of N^{3}H signal (singlet) that appears at δ 8.77 ppm in the spectrum of HL4M. The coordination *via* pyridine nitrogen causes their pyridine protons signals to shift much more with respect to their positions in the free ligand spectrum. The signals due to protons of pyridine ring show splitting. This may be due to the dissymmetry caused by the non planarity of the ligand on complexation [10]. The down field shift in **44** of the acetate resonance (δ, 1.99) compared with that of the ionic acetate suggests interaction of the acetate with the metal centers in solution [11].

9.3.4 ^{13}C NMR spectra

Coordination of the ligand *via* the azomethine nitrogen is indicated in the spectra of all the complexes by the down field shift of the methyl carbon signal. Coordination *via* the sulphur atom is indicated by the up field shift of the ^{8}C signals. Among the pyridine carbon signals, by far the most affected by complexation is that of ^{3}C, which shifts up field in all those spectra in complexes, this may be attributed to coordination *via* the pyridine nitrogen. The methyl and morpholine ring carbon signals lie at practically the same position as in free ligands.

9.3.5 Two-dimensional NMR techniques

Two dimensional correlation spectroscopy assist in determining the connectivity of a molecule showing proton-proton (COSY) as well as carbon-proton coupling (HMQC)

Chemists can now readily glean information about spin-spin coupling and the exact connectivity of atoms in molecules through techniques called multidimensional NMR spectroscopy. The most common multidimensional techniques utilize two-dimensional NMR (2D NMR) and go by acronyms such as COSY, HETCOR, and a variety of others. The two-dimensional sense of 2D NMR spectra does not refer to the way they appear on paper but instead reflects the fact that the data are accumulated using two radio frequency pulses with a varying time delay between them. The result is an NMR spectrum with the usual one-dimensional spectrum along the horizontal

and vertical axes, and a set of correlation peaks that appear in the x-y field of the graph.

When 2D NMR is applied to ^{1}H NMR it is called ^{1}H-^{1}H correlation spectroscopy (COSY). COSY spectra are exceptionally useful for deducing proton-proton coupling relationships. 2D NMR spectra indicate coupling between hydrogens and the carbons to which they are attached. In this case, it is called heteronuclear correlation spectroscopy (HETCOR, or C-H HETCOR). When ambiguities are present in the one-dimensional ^{1}H and ^{13}C NMR spectra, a HETCOR spectrum can be very useful for assigning precisely which hydrogens and carbons are producing their respective peaks.

In a COSY spectrum, the ordinary one-dimensional ^{1}H spectrum is shown along both the horizontal and the vertical axes. Meanwhile, the x-y field of a COSY spectrum is similar to a topographic map and can be thought of as looking down on the contour lines of a map of a mountain range. Along the diagonal of the COSY spectrum is a view that corresponds to looking down on the ordinary one-dimensional spectrum of compound though each peak were a mountain. The one-dimensional counterpart of a given peak on the diagonal lies directly below that peak on each axis. The peaks on the diagonal provide no new information relative to that obtained from the one-dimensional spectrum along each axis. The important and new information from the COSY spectrum, however, comes from the correlation peaks ("mountains") that appear off the diagonal (called "cross peaks"). If one starts at a given cross peak and imagines two perpendicular lines (i.e., parallel to each spectrum axis) leading back to the diagonal, the peaks intersected on the diagonal by these lines are coupled to each other. Hence, the peaks on the one-dimensional spectrum directly below the coupled diagonal peaks are coupled to each other. The cross peaks above the diagonal are mirror reflections of those below the diagonal; thus the information is redundant and only cross peaks on one side of the diagonal need be interpreted. The x-y field cross-peak correlations are the result of instrumental parameters used to obtain the COSY spectrum. First, one chooses a starting point in the COSY spectrum [Fig.9.1] from which to begin tracing the coupling relationships [12]. A peak whose

Table 9.4
^{1}H NMR assignments of N-N-S donor and its zinc(II) complexes. (All absorptions are in (δ) ppm

Compound	^{3}NH	^{1}CH	^{2}CH	^{3}CH	^{4}CH	^{8}CH	$^{9\text{-}12}CH$
HL4M	8.77	7.89	7.27	7.34	7.34	2.62	3.72-3.84
ZnL4MCl	---	7.81	7.25	7.10	7.23	2.61	3.72-3.82
ZnL4MOAc. H_20	---	7.80	7.24	7.00	7.21	2.59	3.72-3.86
$ZnL4MClO_4$	---	7.81	7.26	7.12	7.20	2.61	3.72-3.82

Table 9.5
^{13}C NMR spectral assignments of HL4M and it's zinc(II) complexes (All absorptions are in ppm)

Compound	C1	C2	C3	C4	C5	C6	C7	C8	C9	C10	C11	C12
HL4M	137.82	120.78	124.51	119.80	148.77	185.51	13.86	150.24	52.25	52.25	66.66	66.66
ZnL4MCl	131.58	129.05	149.01	122.56	138.07	156.22	17.66	168.27	48.99	48.98	65.28	65.28
ZnL4MOAc.H_20	135.84	129.17	150.35	122.69	142.33	172.62	17.05	159.89	48.99	48.99	65.28	65.28
$ZnL4MClO_4$	136.93	131.28	149.40	124.79	143.42	176.48	17.61	166.87	48.99	48.99	65.28	65.28

assignment is relatively apparent in the one-dimensional spectrum is a good point of reference. For the compound, **45** the singlet from the alpha hydrogen at 7.99 ppm is quite obvious and readily assigned. If we find the peak on the diagonal that corresponds to this, an imaginary line can be drawn parallel to the vertical axis that intersects a correlation peak in the x-y field off the diagonal. From here a perpendicular imaginary line can be drawn back to its intersection with the diagonal peaks. At its intersection we see that this diagonal peak is directly above the one-dimensional spectrum peak at δ 7.2 ppm. Thus, the alpha hydrogen is coupled to the hydrogen whose signal appears at δ 7.2 ppm. It is now clear that the peak at δ 7.2 ppm is due to the hydrogen on the ^{3}C of pyridine ring. Moving back up to the diagonal from each of these cross peaks indicates that the hydrogen whose signal appears at δ 7.8 ppm is coupled to the hydrogens whose signals appear at δ7.2 ppm. The hydrogen at δ 7.4 ppm is coupled with hydrogen atδ 7.2 ppm.

The hydrogens at δ 3.8 ppm and δ 3.6 ppm are therefore the two hydrogens on the carbon of morpholine moiety. Thus, from the COSY spectrum we can quickly see which hydrogens are coupled to each other. Furthermore, from the reference starting point, we can "walk around" a molecule, tracing the neighbouring coupling relationships along the molecule's carbon skeleton as we go through the COSY spectrum [13]

COSY spectrum of the compound **45** is consistent to an AMX spin system. Aromatic protons of the pyridine ring appear at δ 7.4 (d, J=7.5 Hz; 7.22(t, J= 7.2 Hz) 7.28(dd,J=7.4 &2.4 Hz) and 7.3(d , J= 8.1 Hz) respectively. Aliphatic protons of the ^{7}C were observed as singlet and protons of morpholino moiety are observed as multiplet.

HETCOR or *HMQC cross-peak correlations*

In a HETCOR spectrum a ^{13}C spectrum is presented along one axis and a ^{1}H spectrum is shown along the other. Cross peaks relating the two types of spectra to each other are found in the x-y field. Specifically, the cross peaks in a HETCOR spectrum indicates which hydrogens are attached to which carbons in a molecule, or

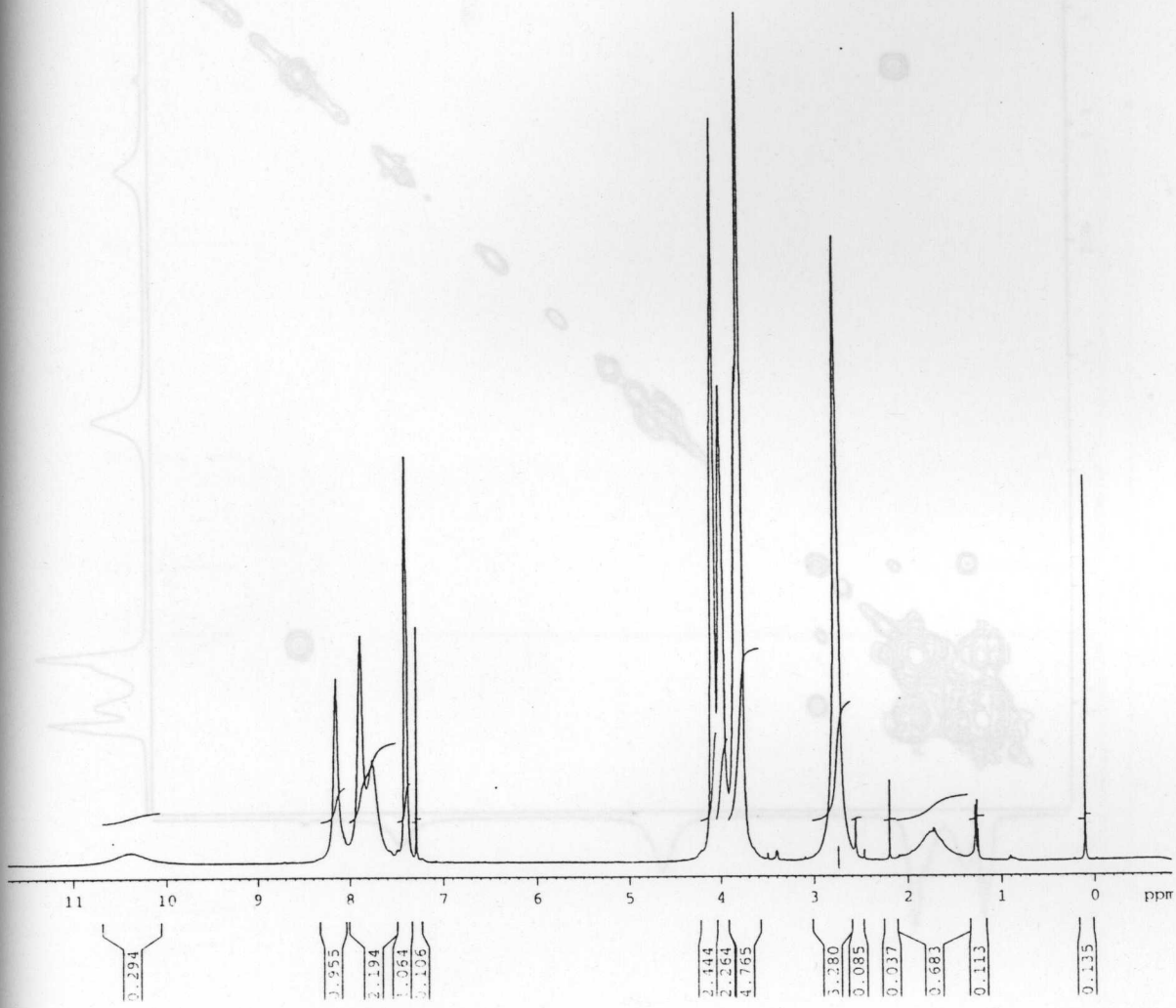

*Fig. 9.1 ^{1}H-NMR spectrum of the zinc complex **45***

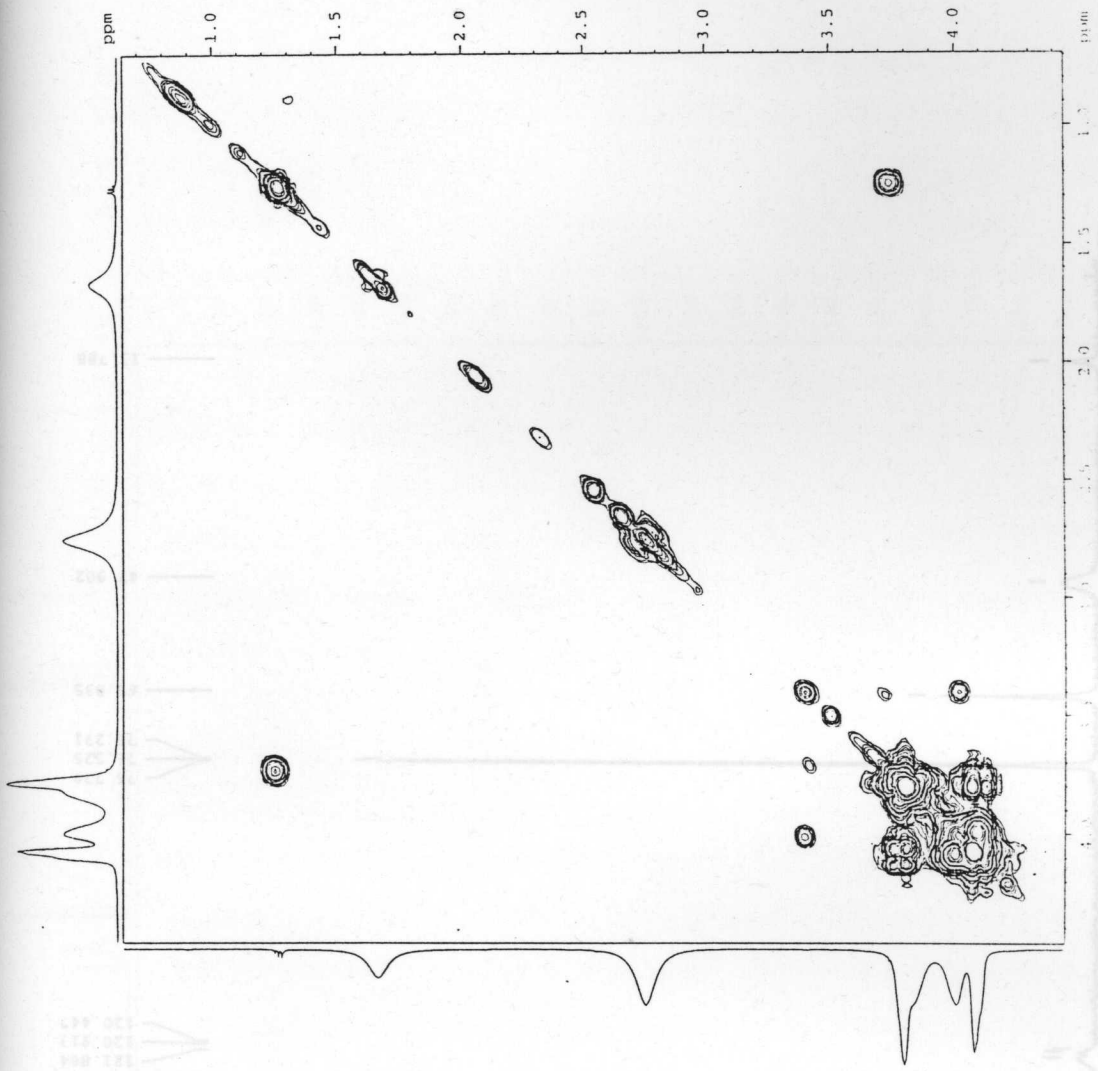

Fig. 9.1 COSY spectrum of the zinc complex **45**

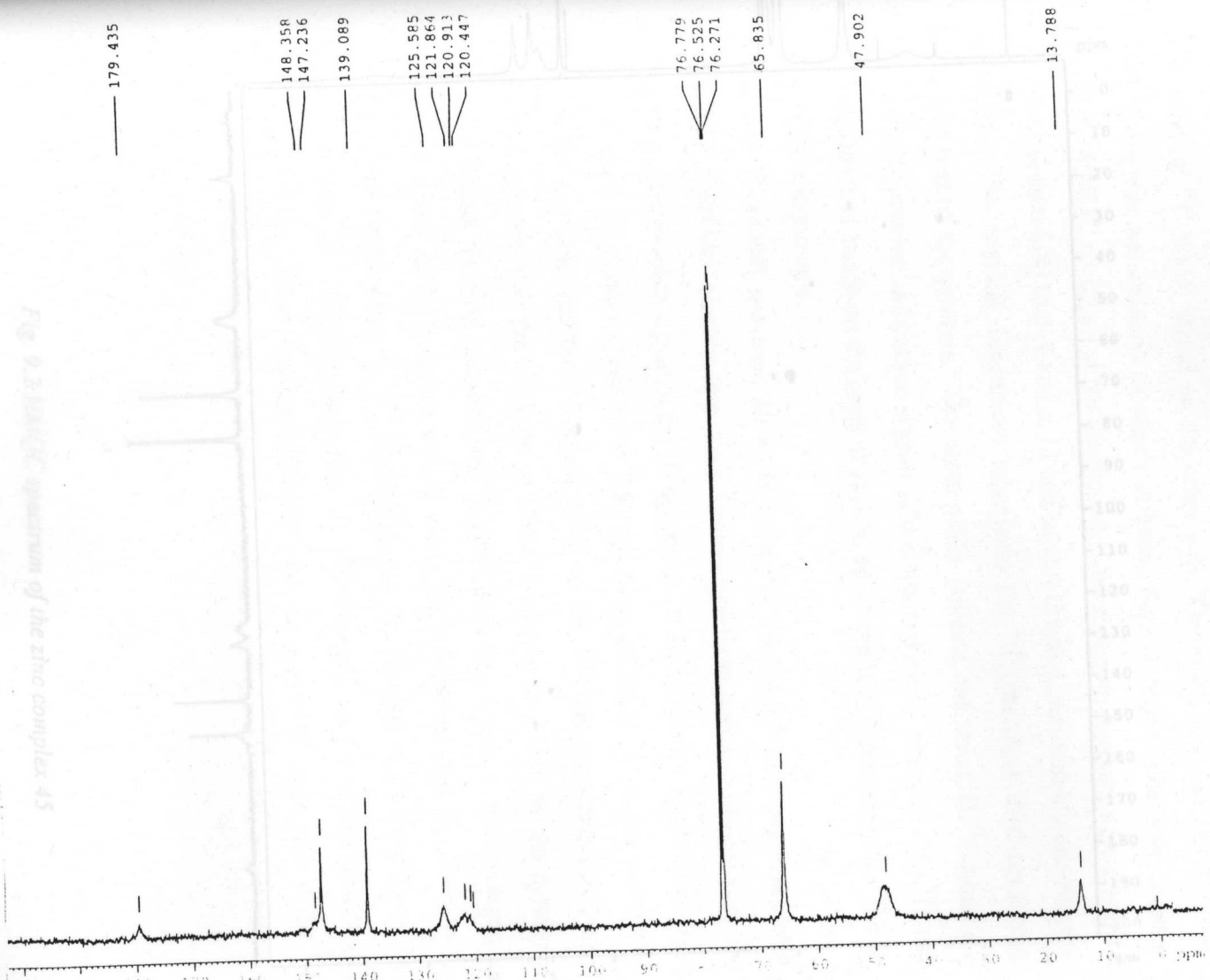

Fig. 9.2 ^{13}C-NMR spectrum of the zinc complex 45

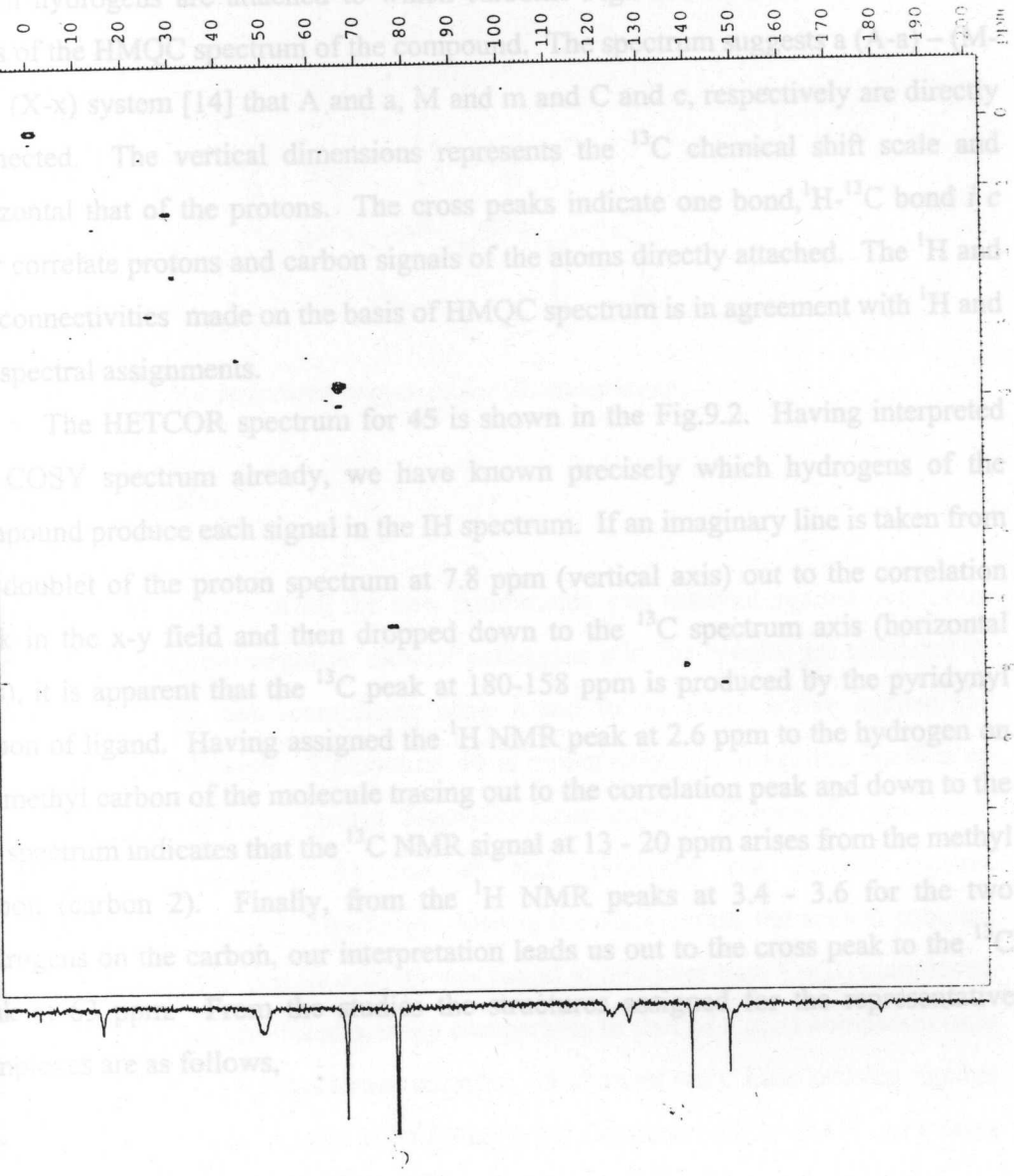

Fig. 9.2 HMQC spectrum of the zinc complex 45

vice versa. There is no diagonal spectrum in the x-y field like that found in the COSY. If imaginary lines are drawn from a given cross peak in the x-y field to each respective axis, the cross peak indicates that the hydrogen giving rise to the ^{1}H NMR signal on one axis is coupled (and attached) to the carbon that gives rise to the corresponding ^{13}C NMR signal on the other axis. Therefore, it is readily apparent which hydrogens are attached to which carbons. Fig.9.2 shows schematic counter plots of the HMQC spectrum of the compound. The spectrum suggests a (A-a) – (M-m) - (X-x) system [14] that A and a, M and m and C and c, respectively are directly connected. The vertical dimensions represents the ^{13}C chemical shift scale and horizontal that of the protons. The cross peaks indicate one bond,^{1}H-^{13}C bond *i c* they correlate protons and carbon signals of the atoms directly attached. The ^{1}H and ^{13}C connectivities made on the basis of HMQC spectrum is in agreement with ^{1}H and ^{13}C spectral assignments.

The HETCOR spectrum for **45** is shown in the Fig.9.2. Having interpreted the COSY spectrum already, we have known precisely which hydrogens of the compound produce each signal in the IH spectrum. If an imaginary line is taken from the doublet of the proton spectrum at 7.8 ppm (vertical axis) out to the correlation peak in the x-y field and then dropped down to the ^{13}C spectrum axis (horizontal axis), it is apparent that the ^{13}C peak at 180-158 ppm is produced by the pyridynyl carbon of ligand. Having assigned the ^{1}H NMR peak at 2.6 ppm to the hydrogen on the methyl carbon of the molecule tracing out to the correlation peak and down to the ^{13}C spectrum indicates that the ^{13}C NMR signal at 13 - 20 ppm arises from the methyl carbon (carbon 2). Finally, from the ^{1}H NMR peaks at 3.4 - 3.6 for the two hydrogens on the carbon, our interpretation leads us out to the cross peak to the ^{13}C peak at 63 ppm. From the studies the structures assigned for the representative complexes are as follows,

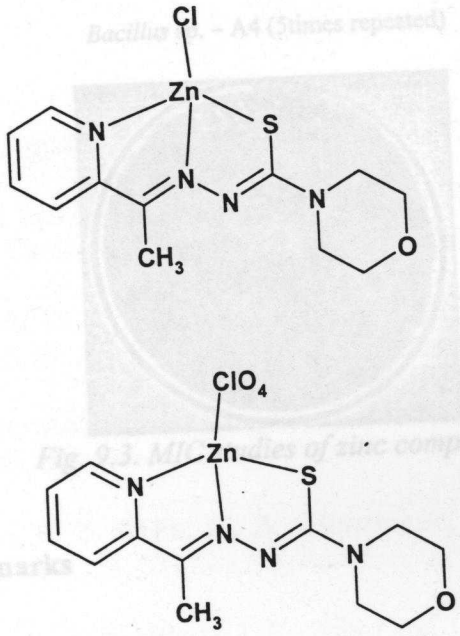

Fig.9.3 strictures proposed for Zn complexes.

9. 4 Biological studies

The antibacterial activity of all the new compounds was assayed against two Gram positive and nine Gram negative clinical pathogens and the results are tabulated in Table 9.3. All the new complexes were found to be more active against the pathogens than the ligands. Compound **44** is moderately active against *Bacillus sp* and showed high activity against *Staphylococcus aureus, Salmonella typhi and Shigella sp.* Compounds **43** and **45** had relatively low activity against *Staphylococcus aureus and shigella sp.* Among the compounds, the acetate complex **44** is the most reactive. But its activity was found to be lower than Cu(II) complexes. The Zn(II) complexes exhibited activity comparable to that of Cu(II) complexes only at high concentrations. Perchlorate complex **45** showed very little activity against *Vibrio cholera.* The MIC values were found to be almost similar to Cu(II) complexes showing their importance in antimicrobial uses.

Bacillus sp. – A4 (5times repeated)

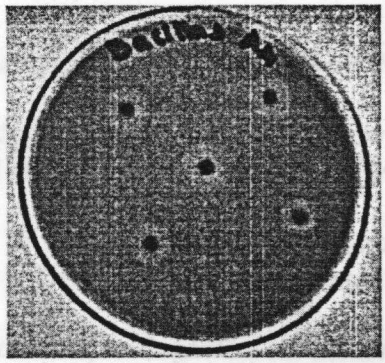

Fig. 9.3. MIC studies of zinc complexes

9.5 Concluding remarks

In this Chapter an attempt was made to elucidate the structure of three zinc complexes of a thiocarbonyl morpholino moiety which provides a backbone for the N-N-S donor ligand. The structure proposed tentatively for the complexes was tetrahedral. By synthesizing these compounds, we were heading towards the designing of synthetic models of sulphur-rich zinc complexes. Enhancement of antimicrobial behaviour upon complexation could be utilized for pharmacological applications.

References

1 H. Sakurai, Y. Kojima ,K. Kawabe. *Coord. Chem. Rrev.*, 2002, **226,** 187.

2 T. Walsh, H H. Sandstead, A, S. Prasad, P, M. Newberne, and Pamela J. *Zinc: Health Effects* Carol Boston University School of Medicine, Boston,1990.

3 a) H. P. Berends, D. W. Stephen, *Inorg. Chem. Acta*, 1984, **93**, 173.,
b) E. Bouwman, W. L. Driessen, *Synth. Commun.* 1988, **18**, 1581.

4 H. Sakiyama R. Mochizuki, A. Sugawara M. Sakamoto *J. Chem. Soc.,Dalton Trans.* 1999, **23**, 997.

5 M. Bochmann, K. J. Webb, M. B. Hursthouse, M. Mazid *J. Chem. Soc., Dalton Trans.* 1991, **15**, 2317.

6. E. W. Ainssough A. M. Brodie J. Rangford and J. M. Waters *J. Chem Soc., Dalton Trans.* 1997.**32**,546.

7 R. H. Prince, G. Wilkinson, *Comprehensive Coordination Chemistry*, Pergamon Press: Oxford, 1987; 925.

8 P. K. Choudhary S. N. Yadav, H. N. Tiwari. and G. Mishra *J. Indian Chem. Soc.* 1998, **75** 392.

9 P. Guerriero U. Casellato U, Ajo, Sitran S and P. A. Vigato *Inorg. Chim. Acta* 1988 , **42** 305.

10 M. Bochmann, G. C. Bwembya, R. Grinter, A. K. Powell, K. J. Webb,*Inorg. Chem.* 1994, **33**, 2290.

11 N. K. Singh A. Srivastava A. Sodhi and P. Ranjan , *Transition Metal Chem.* 2000 **25** 133.

12 R. M. Silverstein, G. C. Bassler, T. C. Morril, *Spectrometric identification of organic compounds*, J. W. and Sons,1991, Ed.**5.**

13 S. A. Koch and E. S. Gruff, *J. Am. Chem. Soc.* 1989, **111**, 8762.

14 S. P. McGlynn, J. K. Smith, *J. Molec.Spectrosc*,1961,**6**,164.

SUMMARY OF THE WORK

The work embodied in the thesis was divided in to nine chapters.

Chapter1 It describes a brief report on thiosemicarbazones, their transition metal complexes and objectives of the present study. Thiosemicarbazones belong to a group of thiourea derivatives; have been studied at lengths due to their wide range of potential biological uses, wide application in industry and analytical determination of various metal ions. Considerable numbers of thiosemicarbazones derivatives have been reported as antibacterial antiviral and antiproliferative. The broad spectrum of medicinal properties of this class of compounds has been studied for activity against tuberculosis, leprosy, psoriasis, rheumatism, trypanosomiasis and coccidiosis. Certain thiosemicarbazones in particular showed a selective inhibition of HSV and HIV. The stereochemistry assumed by the thiosemicarbazones during coordination with transition metal ions depends on the factors such as preparative conditions and availability of additional bonding site in the ligand moiety and charge of the ligand. Metal complexes of thiosemicarbazones are proved to have improved pharmacological and therapeutic effects. Motivated by the proliferate functionality of thiosemicarbazones, we prepared two O-N-S and three N-N-S donor ligands and synthesized forty-five metal complexes of first transition series with the donors. The studies were conducted to bring about a fair understanding of the structure activity relationship and to develop certain effective and economical metal-based antimicrobial agents.

Chapter.2 It deals with syntheses and characterization of three N-N-S and two O-N-S donor ligands. The ligands were prepared according to the reported procedure by John. P. Scovill. The N-N-S donors are 1) 2-acetylpyridine ^{4}N – morpholino thiosemicarbazone, 2) 2-acetylpyridine^{4}N -pyrrolidine thiosemicarbazone, 3) 2-acetylpyridine ^{4}N –hexahydroazipine thiosemicarbazone. The O-N-S donor ligands are

4) salicylaldehyde ^{4}N –pyrrolidine thiosemicarbazone, 5) 2-hydroxy acetopheone ^{4}N –pyrrolidine thiosemicarbazone

They were characterized by partial elemental analysis and spectral studies such as IR, electronic, and ^{1}H and ^{13}C NMR. Single crystal X-ray diffraction studies of HL4M and HL4A were also performed and found that both were crystallized with monoclinic. space group. Both N-N-S and O-N-S donors existed in solution in mono anionic state.

Chapter.3. It describes the spectral characterization, cyclic voltammetric and biological studies of twelve square planar Cu(II) complexes having the general formula [Cu(NNS)X], were X is a mono or poly atomic anion. The complexes were characterized by partial elemental analyses, magnetic susceptibility, molar conductivity, IR spectra, electronic spectra (both DRS and solution), and EPR spectra (polycrystalline at RT, solution at RT and LNT). Spectral simulations of EPR spectra were also conducted and calculated various spin Hamiltonian and bonding parameters. Cyclic voltammetric studies showed quasireversible one electron transfer in addition to the redox responses of principal ligands. The biological activity of them were screened against two gram positive and nine gram negative bacteria and found most of them were more active against gram negative bacteria particularly *Vibrio cholera O1* and *Vibrio parahaemolyticus*. We successfully isolated two complexes having antibacterial activity equal or more than commercial antibiotics against *Vibrio cholera O.1*. The MIC of them was found to be far less than certain commercially available antibiotics. We observed that antibacterial activity of complexes increases with increase in, $g_{\|}$ value, covalency of M-L bond and distortion from planarity.

Chapter4. It deals with spectral characterization, cyclic voltammetric and biological studies of thirteen square planar Cu(II) complexes having the general formula [Cu(HONS)X], were X is a mono or poly atomic anion and HONS is mono anionic principal ligand. The complexes were characterized by partial elemental

analyses, magnetic susceptibility, molar conductivity, IR spectra, electronic spectra (both DRS and solution), and EPR spectra (polycrystalline at RT, solution at RT and LNT). Spectral simulations of EPR spectra were also conducted and calculated various spin Hamiltonian and bonding parameters. Cyclic voltammetric studies showed quasireversible one electron transfer. The biological activity of them were screened against two gram positive and nine gram negative bacteria and found most of them were more active against the clinical pathogens. The activity of the complexes were found to be lower than N-N-S donor Cu(II) complexes.

Chapter 5. It deals with syntheses, spectral characterization of two vanadyl(IV) and two vanadate(V) complexes having distorted square pyramidal geometry and single crystal X-ray diffraction studies of a vanadate complex. Vanadyl complexes were formed on stirring the equmolar solutions of ligands and metal salt under nitrogen atmosphere and vanadate complexes were formed under ordinary reflux conditions. Vanadyl complexes were magnetically dilute and found to be EPR active where as vanadate complexes were diamagnetic. The complexes were characterized by various spectral methods such as IR, electronic, and EPR. The cyclic voltammetric studies showed that the number of electrons involved in the reaction was one. The quasireversible peaks were due to the successive $V^{(IV / III)}$ and $V^{(III / II)}$ redox couples. The irreversible peak in the reverse scan was assigned to $V^{(IV/ V)}$ oxidation. All the new complexes were found to be biologically inactive. The cyclic voltammograms of the vanadate complexes displayed irreversible peaks indicating the degradation of the formal vanadium species. The compound $[VO_2L4M]$ was crystallized in the monoclinic space group P 2_1 /n. The unit cell is comprised of eight molecules. The vanadium atom in each molecule is five coordinate, existing in a distorted square pyramidal geometry, derived from the tridentate ligand and one of the oxygen atoms of the dioxo vanadium moiety. The two oxo groups are *cis* to each other.

Chapter 6. It deals with, spectral, electrochemical and biological studies of four distorted octahedral or capped octahedral iron(III) complexes with HL4M. All new complexes prepared were either black or olive green. They were characterized by partial elemental analyses. The magnetic moments of two complexes were low and therefore existed as low spin iron(III). The magnetic moment of nitrate complex was 3.816 BM and the value is slightly lower than the spin only value for iron(III) with $^4A_2$ ground state. The slightly low value is suggestive of spin equilibrium $^6A_1$ $^2T_2$. The compounds had molar conductivity values slightly below the expected range for 1:1 electrolytes. They were characterized by IR, electronic, Mössbauer and EPR spectroscopy. The Mössbauer spectrum of the complex showed the presence of two types of iron atoms. The values for the isomer shift (δ) and the quadruple split (ΔE_q) of the high spin iron(III) atom inFeCl4 $^-$ anion are found to be 0.8 and 3.2 mm s^{-1} respectively, indicating that Fe(III) to be in high spin state supporting magnetic moment data and the small quadruple splitting indicates distortion from Td symmetry. The isomer shift and the quadruple split (ΔE_q) for the low spin iron(III) atom was found to be 0.49 mm s^{-1} and 0.22 mm s^{-1} with respect to nitroprusside. The complexes gave almost similar voltammograms. The poorly resolved $Fe^{III/II}$ reduction peak was observed in the potential range -150 mV and the counter peak was observed in the potential range -86 mV, were due to a non Nerstian one electron transfer process. The successive peaks corresponding to + 260 mV and + 516 mV in the reverse scan were supposed to be the due to reduction of Fe^{2+} to Fe^0. All iron(III) complexes were inactive against *Vibrio cholerae O1* and *Vibrio parahaemolyticus*. All the complexes were moderately active against *Staphylococcus aureus, Bacillus sp, Shigella and Proteus sp.*

Chapter 7 . It deals with syntheses, spectral, biological and electrochemical studies of four Mn(II) complexes with N-N-S and O-N-S donors and single crystal X-ray diffraction studies of bis(2-acetylpyridine -$_k$N-phenyl thiosemicarbazonato K^2N^1,S) manganese(II). They were characterized by partial elemental analyses and

various spectral techniques such as IR, UV-Visible and EPR. They were having the general formula $Mn(L4M)_2$, $Mn(L4P)_2$, $Mn(HSAP)_2$ and $Mn(HAPP)_2$. The room temperature magnetic moments of the complexes in the polycrystalline state fall in the 5.3-6.01 B.M range, which were very close to spin only value of 5.91 B.M. for d^5. There was no magnetic evidence for any manganese –manganese interaction. The electronic spectra of all manganese(II) complexes had high intensity charge transfer. The X band EPR spectra were measured in dimethyl formamide at 77 K. The spectra of complexes were almost similar and exhibited six line manganese hyperfine pattern centered at g =2.001 and coupling constant A_0, = 95 G. Compounds showed only a single wave in the anodic region at *ca* + 0.89V corresponding to the quasireversible reversible couple $Mn^{(+3/+2)}$. The results of biological screening reflelected that complexes at higher concentrations had more antibacterial activities than ligands. Complexes of N-N-S donors were more active than O-N-S donors. The six coordinate distorted octahedral high -spin Mn(II) complex containing two-deprotonated ligands had a structure, identical to the closely related Fe(III) and Co(III) species where the two coordinating azomethine nitrogen atoms are trans to each other and the other two sets of identical donor atoms are cis to each other. The title compound crystallized in to a monoclinic C2 /c space group symmetry.

Chapter 8. It deals with, spectral, biological and electrochemical studies of five Ni(II) complexes with N-N-S donor ligands and single crystal X-ray diffraction studies of bis (2-acetylpyridine -$_k$n-hexa hydro azepinyl thiosemicarbazonato $_k$ ^{2}n^{1}s) nickel(II). Of the five complexes four of them were four coordinated square planar monohydrate complexes and last one is an octahedral complex. The square planar complexes had the general formula $[Ni(NNS)X]\cdot H_2O$ and the octahedral complex had $Ni(HL4A)_2(ClO_4)_2\cdot H_2O$. In this new complex an unusual thione sulphur coordination was observed and had a magnetic moment 3.11B.M, which was nearer to spin only value. The electronic spectrum of octahedral complex was typical of pseudo octahedral Ni(II) complex. Three absorptions were observed in the UV-Visible

region. The profile of its voltammogram showed that the complex underwent an electrochemically reversible one electron oxidation process at E = + 1010 mV, such a value is typical of $Ni^{3+/2+}$ redox couple where Ni is in a mixed nitrogen, sulphur environment. The electrochemical characteristics support a one-electron assignment for the process. The four coordinate diamagnetic nickel(II) complexes showed moderate antimicrobial activities from those of the starting materials or free ligands. These results were useful to explain the structure activity relation ship of nickel(II) complexes with thiosemicarbazones. It was assumed that labile four-coordinate complexes could interact with selected bacteria while six coordinate complexes could not. The four coordinated nickel(II) complexes consisted of one tridentate ligand and one replaceable ligand such as Cl^-, NO_3^- and NCS^- where as six coordinate complex with two tridentate ligand did not undergo ligand replacement easily. The single crystal X-diffraction studies revealed the occurrence of a hexa coordinated cationic complex of distorted octahedral geometry.

Chapter 9. It deals with syntheses, spectral characterisation and antimicrobial studies of three tetrahedral complexes of Zn(II) with HL4M. The new complexes were non-electrolytes and prepared by stirring an equimolar amount of the appropriate metal salt dissolved or suspended in methanol and ligand in methanol for about 1 week. The complexes were diamagnetic and yellow in colour and insoluble in most of polar solvents The moderately intense band for the complexes in the region 350-425 nm was assigned to S Zn(II) LMCT. The IR and NMR spectral studies were consistent with N-N-S coordination. The complexes showed no appreciable absorption in the region above 450 nm which was in accordance with the d^{10} electronic configuration of Zn(II) ion. For deducing proton-proton and carbon - proton coupling relationships 2D NMR spectra were used. The complexes were found to be moderately active against *Staphylococcus aureus, Salmonella typhi and Shigella sp.*

ABBREVIATIONS

SOD	Superoxide dismutase
shf	Superhyperfine (EPR)
m	medium(IR spectra)
s	strong (IR spectra)
sh	shoulder (electronic spectra)
sp	species(biological studies)
mm	millimeter(biological studies)
tbp	trigonal bipyramidal
sp	square pyramidal
ε	molar absorptivities
δ	isomer shift
MIC	minimum inhibitory concentration
BM	Bohr magneton
CT/ ct	charge transfer
α^2	in-plane sigma bonding parameter
β^2	in-plane pie bonding parameter
MOL	metal-oxo-ligand